EVALUATION OF THE SUPERPAVE GYRATORY COMPACTOR FOR ASSESSING THE RUTTING RESISTANCE OF ASPHALT MIXTURES

By

DANIEL DUAQUAYE DARKU

A DISSERTATION PRESENTED TO THE GRADUATE SCHOOL
OF THE UNIVERSITY OF FLORIDA IN PARTIAL FULFILLMENT
OF THE REQUIREMENTS FOR THE DEGREE OF
DOCTOR OF PHILOSOPHY

UNIVERSITY OF FLORIDA

2003

This document is dedicated to the memory of the Discovery crew.

ACKNOWLEDGMENTS

I extend my sincere appreciation to my advisor and chairman of my supervisory committee, Dr. Bjorn Birgisson, for his invaluable professional and personal assistance throughout my studies. He was a pillar of support. This dissertation was made possible through his guidance and understanding. I would also like to thank Dr. Reynaldo Roque (the co-chair of my committee). His patience and time led to an understanding of this work. Special thanks go to the other members of my advisory committee (Dr. Byron E. Ruth, Dr. Mang Tia, and Dr. Randolph Carter).

I thank the Florida Department of Transportation (FDOT) for providing the financial support for this project. The support offered by the personnel of the FDOT state materials laboratory, (especially Mr. Frank Suarez and Suzanne Andrew) was greatly appreciated. Special thanks go to Mr. George Lopp for procuring materials and ensuring the proper functioning of the equipment. I appreciate the friendship of the students of the Civil Engineering Infrastructure Materials and Pavements group, (especially, Bensa Nukunya, Sylvester Asiamah, Eric Otoo, Franklin Twumasi, Claude Villiers, Jagannatha Katuri, Tipakorn Samarnrak and Boonchai Sangpetgngam. The support and understanding of my family and the Lovatt-Donkor family throughout my studies cannot be overlooked and I give my heartfelt thanks to all of them.

To God be the glory, for he has done great things and I give praise and thanks to him for strengthening me throughout my stay in Gainesville.

TABLE OF CONTENTS

Page

LIST OF TABLES

LIST OF FIGURES

Abstract of Dissertation Presented to the Graduate School
of the University of Florida in Partial Fulfillment of the
Requirements for the Degree of Doctor of Philosophy

EVALUATION OF THE SUPERPAVE GYRATORY COMPACTOR FOR ASSESSING THE RUTTING RESISTANCE OF ASPHALT MIXTURES

By

Daniel Duaquaye Darku

May 2003

Chair: Bjorn Birgisson
Cochair: Reynaldo Roque
Major Department: Civil and Coastal Engineering

Premature rutting of asphalt pavements remains a concern to pavement engineers. In the last decade, several state and federal agencies have performed research projects and developed specifications to address rutting. Design and production of asphaltic mixtures that are resistant to rutting continues to be a top priority in pavement design. Asphalt mixture rutting is generally a costly failure that poses a considerable safety problem in terms of potential hydroplaning.

This research focuses on evaluating simple equipment that simulates field conditions for evaluating mixture resistance to permanent deformation during the mixture design process. A review of the literature showed that a Superpave gyratory compactor with shear resistance measurements as obtained in the Servopac is a promising device. The equipment simulates field compaction and traffic densification. It also can measure shear resistance, which may provide an insight into the resistance of mixtures to shear deformation.

We prepared laboratory and field mixtures with known performance and tested them with the Servopac Superpave gyratory Compactor. Supplementary tests on these mixtures were made with the Asphalt Pavement Analyzer (APA) and the Superpave Indirect Tension Tester (IDT) to allow comparison of the results.

Results of the analysis showed that the gyratory compactor with the shear measurement device can be used as a screening tool for asphalt paving mixtures. Substandard mixtures were identified and specification limits were set for the mixtures tested using the slope of the gyratory shear and the strain to the minimum gyratory shear resistance of a proposed modified procedure of compaction to simulate pavement critical loading conditions. Based on the analysis, mixtures were prepared and Marshall stability and flow tests were performed at he FDOT to set specification limits for using the equipment as a simple tool for evaluating asphalt mixtures during design.

As an addendum, the proposed Superpave™ tests were performed on some of the mixtures and simple parameters were derived for further evaluation for the evaluation of the rutting performance of hot mix asphalt (HMA) mixtures.

CHAPTER 1
INTRODUCTION

1.1 Background

One prevalent sign of pavement distress is rutting, which manifests itself as longitudinal depressions that form under traffic in the wheel path. Asphalt mixture rutting is generally a costly failure, which poses a considerable safety problem in terms of potential hydroplaning. Motorist comfort is also compromised. There are basically three different types of pavement ruts (Dawley, et al. 1990). The first one is wear rutting, which is due to progressive loss of coated aggregate particles from the pavement surface. The second one is structural rutting, which is due to the permanent deformation of the pavement structure under repeated traffic loads, and may be a reflection of permanent deformation within the subgrade or inadequate compaction of the base layer. The third type of rutting is instability rutting within the wheel paths, which is due to lateral displacement of material within the asphalt concrete layer. Instability rutting occurs when the strength and/or stiffness properties of the compacted pavement are inadequate to resist the applied wheel loads. This thesis presents the development of a simple index test for instability rutting. The equipment used for obtaining the necessary parameters to evaluate the likelihood of rutting are obtained from Superpave™ gyratory compactor measurements with gyratory shear measurements.

Although the Superpave volumetric mixture design procedure has resulted in some significant improvements over the Marshall method of mixture design, it essentially remains a volumetric design procedure, except that a different compaction method is used

to produce the laboratory specimens. Superpave Level I does not require any physical performance test on the asphaltic mixture to determine whether or not the volumetric design would actually result in a mixture with suitable resistance to rutting or cracking.

It is widely recognized among the pavement engineering community that a physical index test to evaluate rutting potential of asphalt mixtures is needed to verify results of volumetric designs. Furthermore, physical index tests that can be used to evaluate the rutting potential of mixtures may serve many other useful and necessary purposes (e.g., optimizing rutting resistance during mixture design). Therefore, the identification of an appropriate simple laboratory testing system that can be used to provide an index of the rutting potential of asphalt mixtures is crucial for successful design and production of rut-resistance asphalt mixtures. Ideally, the simple index test should allow testing during compaction/mix design to provide a history of responses under conditions representative of the field.

Current Superpave™ gyratory compactors operate on a "shear compaction" principle, meaning that compaction occurs under not only vertical pressure, but also shear displacement. These two elements allow for a closer simulation of mechanisms of field compaction. The Superpave™ gyratory compactor was developed only to densify mixtures. No attempts were made to measure resistance to compaction or gyratory shear strength during compaction, or to use the device to gauge mixture stability or sensitivity.

However, because of the implied relationship between compaction and mixture strength, numerous attempts have been made to develop compaction parameters that relate to the evolution of mixture strength. A number of gyratory compactors have now been developed that not only measure the change in height during compaction, but also

the resistance to compaction through a parameter called the 'gyratory shear strength.' These include the Finnish Intensive Compaction Tester (ICT) gyratory compactor, the Superpave™ compatible Australian Servopac gyratory compactor, and the Gyratory Testing Machine (GTM). These compactors all were developed under the basic assumption that likely field performance of asphalt mixtures could be inferred by measuring the gyratory shear strength. These gyratory compactors have the advantages of simplicity of testing and the ability to obtain the gyratory shear for the range of void conditions experienced during compaction.

The gyratory compactor has been proved over the years to provide responses representative of the field during compaction. It provides densities in the laboratory specimen that closely approximate the ultimate densities of the asphalt concrete pavement when subjected to in-service traffic loads and climatic conditions and is likely to be a versatile tool when adapted with shear measurements for the evaluation of the shear resistance of paving mixtures which is indicative of their rutting resistance.

Various researchers, have proposed methods of analysis of the compaction curve obtained from the Superpave gyratory compactor to evaluate the resistance to permanent deformation of asphalt mixtures (Anderson 1997, Langlois 1998, McGennis 1997, and Tarn et al. 1999) proposed the use of the compaction slope. Mallick (1999) suggested the use of parameters such as the Gyratory Ratio (N_{98} / N_{95}), Vavrik (2000), introduced the locking point concept, and Bahia (1998) proposed the use of the terminal densification energy ($TDI_{92\text{-}98}$) which is the area bounded by the compaction curve from 8% air voids to 2% air voids.

Butcher (1998) and Guler (2000), presented procedures for measuring shear resistance of asphalt mixtures during compaction in the Servopac Superpave™ compatible gyratory compactor. Butcher (1998) discussed the use of the maximum shear stress with the Servopac compactor, and noted that mixtures using softer asphalt binders appear to have lower maximum shear stresses than mixtures with harder asphalt binders. Guler (2000) discussed the development of a shear measuring device to be used in conjunction with Superpave compatible compactors. Mixtures with higher asphalt binder contents experience drastic drops in shear resistance when compacted beyond the maximum shear. Anderson (2002), using the Superpave compactor with shear measurements proposed the parameter of cycles at maximum stress ratio ($N\text{-}SR_{max}$) as a measure of the permanent deformation resistance of mixtures.

The above developments are however not conclusive, with no single method capable of consistently identifying the true rutting potential of mixtures. Critical field conditions that may trigger rutting instability in the field are not captured in the present Superpave mode of compaction, which is used for mixture design purposes only. The Australian Servopac Superpave gyratory compactor allows for the change in gyratory angle during compaction. Thus, it is possible to compact at 1.25 degree gyratory angle up to a density level that corresponds to field compaction, and then increase the gyratory angle to 2.5 degrees to induce a shear failure in the mixture, which may be more consistent with observed rutting instability shear failures in the field.

1.2 Research Hypothesis

Instability rutting occurs when the mixture fails under a state of high shear stresses at low confinement. Using the Superpave gyratory compactor, it is possible to compact hot mix asphalt mixtures to a density that is consistent with the density of field

pavements immediately after construction. The subsequent application of high shear stresses by increasing the gyratory angle to 2.5 degrees will result in material states at which parameters can be measured that are relevant to instability rutting and rutting resistance.

1.3 Objectives

The primary objective of this research is to develop a new testing procedure for evaluating the rutting potential of mixtures using the Superpave gyratory compactor with shear measurements. A secondary objective is to quantify the various parts of the typical compaction curve obtained from the Superpave gyratory compactor with shear measurements. In particular, three main parts of compaction curves are of interest, namely the compaction part of the curve (air voids higher than 7 %), the densification part of the curve (air voids between 7 and 4 %), and the post peak part of the curve (air voids typically lower than 4 %).

Results from our study showed that the Superpave gyratory compactor using gyratory shear measurements and a modified compaction procedure can be used to evaluate the rutting potential of mixtures. A set of simple evaluation charts are developed and presented for evaluating the rutting resistance of mixtures. The results also show that the compaction curve can be broken down into three separate parts, which have distinct characteristics. Importantly, the post-peak part of the compaction curve is shown to be unsuitable for evaluating the stability of mixtures, due to the high degree of material degradation associated with a fixed gyration angle and low air voids.

1.4 Scope

Goals of our research were as follows:

- To conduct a thorough literature review of the state of practice of the use of the Superpave gyratory compactor with and without shear measurements for evaluating the rutting potential of asphalt mixtures and its comparison to other potentially suitable laboratory based testing systems.

- To obtain data on Florida mixtures of known relative rutting performance with emphasis on gradation effects, aggregate type, and fine aggregate type.

- To test mixtures using the Servopac gyratory compactor with gyratory shear measurements. Two replicates were tested per each mixture. The compaction curves from the Servopac are analyzed so as to delineate the compaction, densification, as well as instability zones of asphalt paving mixtures.

- To perform Asphalt Pavement Analyzer (APA) and Superpave Indirect Tension (IDT) tests to independently evaluate the rutting and creep behavior of these mixtures.

A total of 32 different mixtures, consisting of 10 mixes in which the aggregate type in the fine portion of the gradation (defined as material passing the No. 4 Sieve) is varied, 8 limestone mixtures consisting of the same aggregate type, but different gradations, 6 granite mixtures consisting of the same aggregate type, but different gradations, 6 field mixtures of known field performance, and finally 2 mixtures from accelerated pavement testing using the Heavy Vehicle Simulator. 1 of the field mixtures, project number 8, was obtained from the plant, however, there was not enough for all the tests.

CHAPTER 2
LITERATURE REVIEW

2.1 Introduction

The purpose of this chapter is to review the evolution of the Superpave gyratory compaction equipment (SGC) and its predecessor gyratory compactors with regards to their capability for use as an indicator test to check for problematic mixtures. In doing this, attention will be focused on the ability to evaluate the rutting resistance of dense graded HMA mixtures. The review of Asphalt Pavement Analyzer (APA) and the Superpave™ Indirect Tension Test (IDT) will be made, as results from these tests will be used for comparison with measurements from the SGC. Finally, a review of the proposed Superpave™ simple performance test will be made limited testing will be done to evaluate and confirm the properties of the mixtures in this work.

The use of the Superpave gyratory compactor for compacting mixtures at high compaction temperatures, around 275°F (135°C) means that compaction is done when asphalt binder viscosities are very low. In this compaction mode, the influence of the asphalt binder viscosity on the measured parameters is minimal. Attempting to evaluate the effects of asphalt binder viscosity on HMA rutting performance using parameters from this equipment may therefore be erroneous.

According to the Superpave mixture design, gyratory specimens are compacted at equiviscous binder temperatures corresponding to a viscosity of 0.28 Pa.s (Asphalt Institute Superpave Design (MP-2) Manual), 1996). This protocol makes it near impossible to use parameters from the SGC for the comparison of the performance of

mixtures with different types of asphalts. Anderson, (2002), found that various proposed analysis methods on measurements from the SGC could not differentiate between mixture performance with regards to the properties of asphalt binder type used in the mixtures. The main material effects that can be obtained from compaction with the SGC using the current Superpave compaction temperatures will therefore be those of the aggregate, i.e. aggregate type, gradation, filler content and aggregate particle properties such as fine aggregate angularity, surface texture, and gyratory shear strength, when the Superpave gyratory compactor is equipped with a gyratory shear measurement system. As a prelude to the review of the SGC, a thorough review of the aggregate properties that affect the performance of HMA mixtures was therefore made.

2.2 Aggregate Properties that Affect Mixture Rut Resistance

According to Ahlrich (1998) and Ruth et al.(1989), and, the properties of the fine and coarse aggregates used in an asphalt concrete mixtures play a dominant role in the rutting performance of the mix. The size, shape and texture of the individual aggregate particles are all factors that affect the stiffness of the mix and the resistance to permanent deformation (Ahlrich (1998), Park et al. (2001) and Ruth et al. (1989). The ratio of crushed particles to uncrushed particles is also a factor. Further, the absorption of asphalt cement by the aggregates affects the film thickness of the binder on the surface of the aggregate particles and thus the stiffness of the mix (Ruth et al.1989). Any dust or dirt coating on the aggregate particles can affect the degree of rutting that occurs by stripping of the binder from the surface of the aggregates. The gradation of the aggregates, including the uniformity of the grading from coarse to fine and the amount and

characteristics of the #200 sieve, have a significant effect on the properties of the mix and the susceptibility to rutting (Ruth et al., (1989).

2.2.1. Aggregate Shape, Crushed Content and Surface Texture

The shape of the aggregates used in the mix has a very important effect on the tendency of that mix to rut (Cross and Brown 1992, Huber 1998, Park et al. (2001) Ruth et al. 1989 and Sanders 1992). Coarse aggregates which are rounded have no interlocking ability and can easily slide over each other when subjected to shear loads of heavy vehicles. In the same regard, fine aggregates which consist of rounded natural sand particles do not possess the stability needed in asphalt concrete mixes.

Increasing the crushed content of the fine and coarse aggregates may significantly increase the resistance of the mixture to rutting (Ahlrich 1998). The coarse aggregates can be crushed so that the material contains at least one or two fractured faces. Further, the use of manufactured sand or screenings increases the angularity of the fine aggregate particles, thereby increasing the interlock between the sand particles and reducing the susceptibility of the mix to rutting (Park et al. 2001)).

The texture or smoothness of the individual aggregate particles also plays a part in the ability of the mix to resist permanent deformation. Aggregates, which have smooth surfaces, such as gravels, have a tendency to rut much more readily than crushed aggregates (Park et al. 2001, Sanders and Dukatz 1992). Moreover, the asphalt cement film around the aggregate particles will bond more tenaciously to rougher textured surfaces.

2.2.2 Aggregate Asphalt Absorption

An aggregate which has high asphalt binder absorption can provide a rut resistant mixture (Bouchard 1992), or it can have the opposite effect and can cause an increase in the tendency of the mix to rut. When properly designed to take into consideration the absorbed asphalt to arrive at an effective asphalt content, such mixtures have good rutting performance (Ruth et al 1989). However, lack of the understanding of the absorptive capacity of the aggregates may lead to mixtures, which may have deficient film coating, which can increase the susceptibility of the mix to permanent deformation (Ruth et al, 1989). There is also the tendency of some residual moisture left in the pores of the aggregates after heating. Excess moisture can lead to bleeding due to water vapor forcing asphalt to the surface of a newly laid pavement. Also this moisture can increase the stripping potential of the mixture. A mix that is susceptible to moisture damage is also susceptible to rutting. (Ruth et al., (1989))

2.2.3 Aggregate Gradation

Aggregate gradation is probably the single most important factor affecting the probability of the mix to rut. The aggregates should be relatively uniformly graded from coarse to fine. They should not be so well graded, however, that there is not enough room in the mix for the asphalt cement which affects the long-term durability of the pavement (Ahlrich 1998, Huber and Schuler 1992 and Ruth et al. 1989). There should be enough space in the mix between the aggregate particles to allow room for an adequate amount of asphalt binder to obtain the proper film thickness on the individual pieces of aggregates and to accommodate traffic densification without degrading the aggregate particles. For

similar mix characteristics and properties, the coarser aggregate blends will require less asphalt cement in the mix to achieve adequate coating and mix properties. In general, one would expect the coarser mixes to be more resistant to permanent deformation.

2.2.4 Aggregate Passing #200 Sieve

The amount of material which passes the #200 sieve (mineral filler) is one of the criteria to be considered in minimizing the potential for permanent deformation. (Ruth et al. 1989, and Tayebali et al. 1996). Tayebali et al. 1996, observed that increased amount of mineral filler can be accommodated in asphalt mixtures without adversely affecting its rutting resistance. However, it should be noted that although rutting performance is enhanced, the effective asphalt content is reduced at higher mineral filler content. This may have detrimental effects on other performance such as fatigue, cracking and raveling.). Generally, if too little mineral filler is incorporated in the mix, the air void content of the mix will be high and the mix will require a relatively high asphalt content. If too much mineral filler is incorporated, the asphalt content of the mix will still be high in order to coat the surface of the filler particles, but the air void content and the VMA of the mix will typically be very low. Therefore, mixtures which contain small amounts of mineral filler can be susceptible to rutting as well as mixtures which contain very high volumes of mineral filler (Al-Suhaibani et al. 1992).

To prevent the effect of mineral filler content, the Superpave protocol specifies limits within which the filler/Asphalt ratio should lie (AASHT MP-2 and AASHTO PP-28).

2.3 The Need for a Simple Rutting Performance Test

Although the Superpave volumetric mixture design procedure has resulted in significant improvements over Marshall method of mixture design, it essentially remains a volumetric design procedure, except that a different compaction method is used to produce the laboratory specimens. Superpave Level I does not require any physical testing of the asphaltic mixture to determine whether or not the volumetric design would actually result in a mixture with suitable resistance to rutting or cracking.

The traditional Marshall test for flow and stability and the Hveem stabilometer tests were the most popular tests available before the advent of the Superpave system of mixture design and analysis. These tests however are empirical in nature, the results of which have little correlation with field rutting performance (Ford 1985, and Ford 1988). It is widely recognized among the pavement engineering community that a physical index test is needed to evaluate rutting potential of asphalt mixtures. The identification of an appropriate simple laboratory testing system that can be used to provide an index of the rutting potential of asphalt mixtures is crucial for successful design and production of rut-resistance asphalt mixtures.

Ideally, the simple index test should allow testing during compaction/mix design to provide a history of responses under conditions representative of the field. This research seeks to evaluate the use of the Superpave gyratory compactor with gyratory shear strength measurements as a simple testing equipment for the identification of the rutting potential of asphalt paving mixtures during the design stage.

2.4 Background of the Gyratory Compactor

In 1939, the Texas Highway Department initiated an investigation to compare different compaction procedures (Phillipi 1952, and Ortolani and Sandber 1952). Nine different methods were evaluated on the basis of the following criteria (Ortolani and Sandber 1952):

- The method must be equally adaptable to the field control of the mix as to the design.).
- The method should yield essentially the same density, or void ratio, as that obtained in the finished pavement after some time period, which would allow for the increased density due to traffic.
- The molding method should approximate, as nearly as possible, the aggregate degradation obtained under field conditions.

As a result of this investigation, the gyratory method of molding asphalt concrete test specimens was used as a tentative method from 1940 to 1946 when it was made a standard of the Texas Highway Department (Phillipi 1952, and Phillipi 1957). Subsequently, the U.S. Corps of Engineers became interested in the gyratory because airfield pavement densities exceeded mixture densities obtained by other methods. Experimentation and development of the Gyratory Testing Machine (GTM) proceeded up to about 1961 when the Model 4-C TM became available form the Engineering Developments Company, Inc. (MacRae and Foster(1959), U.S. Army and Waterway Atation (1962)). Concurrently, the Ohio Department of Highways designed and built a gyratory compactor with an entirely different mechanism than the Corps of Engineers. Their investigations indicated that maximum resistance occurred at approximately 30 revolutions with a 2-degree angle and a 690-kPa ram pressure. Also, it tended to

correspond to the range in field densities for different mixtures (Kimble and Gibboney 1961). Shortly afterwards a GTM study conducted by the Asphalt Institute indicated that the design asphalt content could be selected as 1 percent below that identified by a 14-minute increase in the angle of gyration (Kallas 1964).

Laboratory and field investigations conducted in the 1960's resulted in the development of procedures to simulate field compaction (Ruth and Schaub 1966) and to design asphalt concrete mixtures (Ruth and Schaub 1968) using the GTM equipped with an air-roller. Minor changes in the machine settings were implemented in 1990 to make the testing procedure more user-friendly (Sirgurjonsson and Ruth 1990)). A schematic of the GTM is shown in Figure 2-1. The machine settings used for compaction and testing were as follows:

initial angle of gyration	3 degrees
ram pressure	690 kPa
air-roller pressure: (Model 4C)	103 kPa
Model 4C, 100 mm diameter x 65 mm,	69 kPa
Model 6B-4C, 150 mm diameter x 100 mm,	290 kPa (approx.)

The testing procedure involved compaction at 150 °C for 18 revolutions to simulate vibratory roller compaction and 200 revolutions at 60 °C or some other representative temperature to select the design asphalt content based on a Gyratory Shear (Gs) of 372 kPa at 200 revolutions or 386 kPa for very heavy traffic. (Ruth et al., 1989 and Moseley (1999)) The Gs value, which is the shear moment per unit volume of mix, was computed based on the air-roller pressure and the dimensional characteristics of the Model 6G-4C GTM for the 100 mm diameter molds as follows:

$$Gs = 183.45(P/h) \quad (2\text{-}1)$$

where Gs = gyratory shear strength, kPa

p = air-roller pressure, kPa

h = specimen height, mm

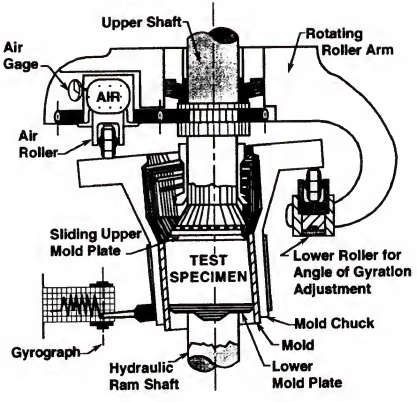

Figure 2-1 The Gyratory Testing Machine

Ruth and Schaub (1966) reported that the gyratory testing machine has been used to simulate both field and laboratory mixture compaction. They also showed that the GTM

Because of the implied relationship between compaction and mixture strength, attempts have been made to develop compaction parameters that relate to the evolution of mixture strength using Superpave gyratory compactors. Currently, Superpave gyratory compactors with shear measuring devices exist. Butcher (1998) and Guler (2000), presented procedures for measuring shear resistance of asphalt mixtures during compaction. Butcher (1998) discussed the use of the maximum shear stress with the Servopac compactor, and noted that mixtures using softer asphalt binders appear to have lower maximum shear stresses than mixtures with harder asphalt binders. Guler (2000), discussed the development of a shear measuring device to be used in conjunction with Superpave compatible compactors. Mixtures with higher asphalt binder contents experiences drastic drops in shear resistance when compacted beyond the maximum shear. Anderson (2001), using the Superpave compactor with shear measurements proposed the parameter of cycles at maximum stress ratio ($N\text{-}Sr_{max}$) as a measure of the permanent deformation resistance of mixtures.

Butcher (1998), comparing the Australian Servopac with the SHRP Gyratory compactor, observed the following:

- The percentage voids achieved by compacting to a specified number of cycles decreases linearly with increasing vertical stress. However the number of cycles required to achieve a specified air void percentage decreases exponentially with increasing vertical stress.
- Rate of rotation has a minimal effect on gyratory characteristics.
- Maximum gyratory shear increases logarithmically with increasing angle of gyration but increases linearly with increasing vertical stress.
- The maximum shear stress is achieved within a tight percentage void band for all dense mixes and independent of angle and vertical stress.

provides aggregate particle orientation comparable with that of roller compaction in the field.

Sigurjonsson and Ruth (1990) evaluated the combined effect of aggregate particle size, surface texture and gradation using the Gyratory Testing Machine procedure of mixture design. Field compaction simulation was achieved with the air roller mode at between 12 and 18 revolutions. The percent air voids achieved by compacting to a specified cycle value or the cycles required decreases exponentially with increasing angle of gyrations. Similar to the GTM and the Texas Gyratory Compactor, current Superpave™ gyratory compactors operate on a "shear compaction" principle, meaning that compaction occurs under not only vertical pressure, but also shear displacement. These two elements allow for a closer simulation of the mechanism of field compaction. The Superpave™ gyratory compactor was developed only to densify mixtures. No attempts were made to measure resistance to compaction or gyratory shear strength during compaction, or to use the device to gauge mixture stability or sensitivity.

Various researchers, have proposed methods of analysis of the compaction curve obtained from the Superpave gyratory compactor to evaluate the resistance to permanent deformation of asphalt mixtures for example the use of the compaction slope by Anderson (1997) Langlois (1998) McGennis (1997), and Tarn et al. (1999). Mallick (1999) suggested the use of parameters such as the Gyratory Ratio (N_{98} / N_{95}) Malick (1999). Vavrik (2000) introduced the concept of the locking point. Finally, Bahia (1998) introduced the concept of terminal densification energy ($TDI_{92\text{-}98}$), which is the area bounded by the compaction curve from 8% air voids to 2% air voids.

- The rate of change of percentage voids at the maximum shear stress position is a characteristic of the mix gradation and is independent of angle and vertical stress.
- Compaction is highly sensitive to gyratory angle below 1degree and to a lesser extent between 1 and 2 degrees.

These compactors all were developed under the basic assumption that likely field performance of asphalt mixtures could be inferred by measuring the gyratory shear strength. These gyratory compactors have the advantages of simplicity of testing and the ability to obtain the gyratory shear for the range of void conditions experienced during compaction.

2.5 The Servopac Superpave™ Gyratory Compactor

The gyratory compaction device used in this study was the Australian Servopac gyratory compactor (Butcher, 1998). The Servopac gyratory compactor is a servo-controlled gyratory compactor designed to apply a static compressive vertical force to an asphalt specimen while simultaneously applying a gyratory motion to a cylindrical mold containing the asphalt.

The Servopac gyratory compactor has been found (Hanson (1998)) to meet the AASHTO TP 35-98 standard protocol test for comparability to the SuperpaveTM gyratory compactors. In addition to recording change in height of specimens during compaction, the Servopac is also capable of measuring shear resistance, which is achieved by the installation of pressure transducers in the pressure lines of the three gyratory actuators (Butcher (1998)). Another distinguishing feature of the Servopac gyratory compactor is the ability to perform compaction at fixed angles of up to 3 degrees. The equipment can be used to compact both 4 and 6 inches diameter samples.

The gyratory shear resistance Gs of a mixture at any given cycle is recorded during the compaction process (Butcher, 1998):

$$GS = 2PL/(Ah) \quad (2\text{-}2)$$

where,

P = Average pressure measured in the gyratory actuators.

L = The distance from the center of the specimen to the midpoint of the gyratory actuators.

A = Cross sectional area of the specimen, and

H = Height of specimen at the specified cycle for which the shear is measured

The Servopac gyratory compactor used in this research has additional capability for compacting 4 inches samples. However, this research is done on 6 inches samples alone.

2.6 Review of Current SGC Analysis Methods

2.6.1 Compaction Slope

Therefore a measure of the compactability can be determined directly by computing the slope of this part of the curve. This slope is generally considered to be a function of the strength of the aggregate skeleton, as noted by Anderson et al. (1997). Corté and Serfass (2000) observed that the change in air voids content, Va with the number of gyrations, n_g, applied with the SGC is shown in equation 2-3:

$$100\text{-}Va = C_1 + K_1 \log(n_g) \quad (2\text{-}3)$$

where,

Va = Air voids

C1 = intercept

K1 = Slope

ng = Number of cycles

The slope of the densification curve between the Nini and Ndes gyrations is generally linear, when plotted on a semi-log graph as illustrated in Figure 2-2.

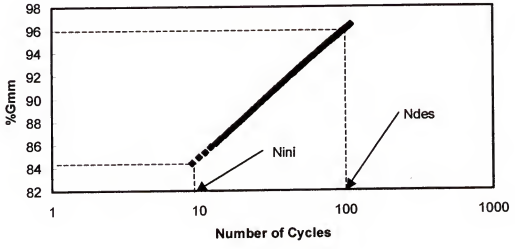

Figure 2-2. Plot of%Gmm between Nini and Ndes

Mixes which have an aggregate skeleton which tend to be unstable during compaction and sensitive to rutting show relatively high C1 and lower K1 values. Their void content decreases rapidly during the first few gyrations.

2.6.2 Energy indices

Bahia et al. (1998) presented the idea of the use of energy indices for the evaluation of the rutting potential of asphalt mixtures. This involves the calculation of the energy required to change the volume of asphalt during compaction with the SGC. The vertical deformation of the mixture during compaction is assumed to be resulting from the applied ram pressure. A strong aggregate skeleton, with a high angle of internal friction , will require more energy to tilt the mold to the required angle during each cycle of gyration. A weak aggregate skeleton, on the other hand, will require less energy (or force) to tilt the mold.

The work input can be used to either overcome the frictional resistance, or in moving the applied vertical load a certain distance. The part that is effectively reducing the volume is equal to the product of the load applied and the distance the ram has moved. Since the load is kept constant, the deflection measured during compaction is proportional to the work used effectively in compacting the mixture. Based on this analysis, a strong aggregate skeleton will dissipate more energy in friction, and therefore, less energy will be available for densification during each cycle. The strong skeleton will be more resistant to densification and thus less deflection will be measured by the SGC during each cycle. More cycles will be required to achieve density. A weak aggregate skeleton will dissipate less energy in shear, and therefore, more energy will be available for vertical densification. More vertical densification will be seen for each cycle, compared to the strong skeleton.

If the number of cycles is plotted versus the amount of volume reduction, the area under the curve will represent the amount of work that is required to achieve the change in density as illustrated in Figures 2-3 and 2-4. For the same reduction in density, a stronger aggregate skeleton will require more gyrations because the reduction in volume per gyration is small. Because the number of gyrations is larger, the area under the curve to achieve the same change in percent Gmm is larger. For a weak aggregate skeleton, a lower number of gyrations will be required, and thus smaller area for the same change in percent Gmm is determined under the densification curve. Based on the above reasoning, two indices, the "Compaction Energy Index" and the "Densification Energy Index" were proposed for evaluation of mixture resistance to construction compaction and traffic densification respectively.

2.6.2.1 The compaction energy index (CEI)

The CEI effort was considered to be the work applied by the paver and/or rollers to compact the mix to the required density during construction. In the analysis, it was assumed that the typical paver compaction effort is represented by a constant applied energy equivalent to eight gyrations in the SGC. The energy that the contractor expends in compacting the mix from its initial behind the paver density, to the required density at end of rolling (8 % air voids) is estimated by the area under the compaction curve between these two points and this is referred to as the CEI. Mixes that require lower compaction energy in this range (lower CEI) are more desirable. Figure 3-4 shows the compaction energy index (CEI).

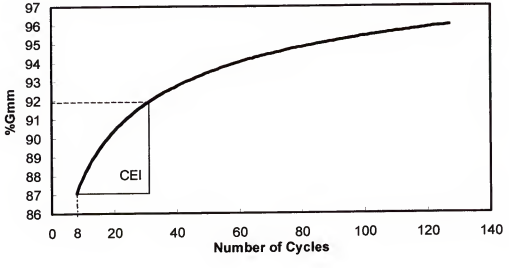

Figure 2-3. Compaction energy index (CEI)

2.6.2.2 Traffic densification index (TDI)

This index represents the total effort required to compact the mixture to 4% air voids, which is the density the mixture is expected to reach under traffic in the early life of the pavement. The use of the TDI to 2% air voids was recommended by Bahia et al (1998) which is considered as a terminal density ($TDI_{Terminal}$). This index represents the total effort required to compact the mixture to a terminal density of 98% of Gmm. Figure 3-4 illustrates the energy method of analysis.

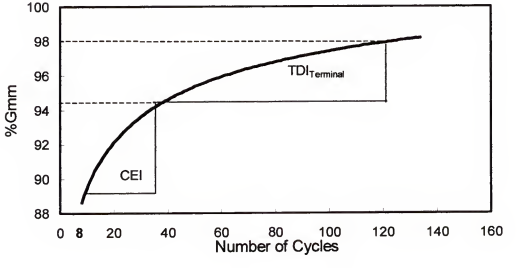

Figure 2-4. Energy indices.

2.6.3 Number of gyrations to the maximum stress ratio (N-SRmax)

Evaluation of the results from the NCHRP 9-16 laboratory experiment indicated that a promising compaction parameter related to asphalt mixture shear stiffness and rutting potential appeared to be $N\text{-}SR_{max}$ as determined using a modified Pine AFG1 SGC.

The N-SR_{max} parameter is the number of gyrations at which the stress ratio (shear stress divided by vertical stress) reaches a maximum value. The N-SR_{max} parameter appears to lend itself easily to mix design or quality control testing. Threshold values were identified separating mixtures with good and poor expected performance. Unlike other parameters, the N-SR_{max} value for an asphalt mixture specimen can be determined immediately following the compaction process. Initial laboratory mix design validation of two mixes confirms the potential utility of the N-SR_{max} parameter as a mixture performance screening tool.

Based on the findings of the experiment, it appears that the N-SR_{max} determined during SGC compaction provides a general indication of expected mixture rutting performance.

In an effort to improve the repeatability of the N-SR_{max} values within a set of three specimens for each mixture and eliminate false peaks caused by identifying absolute maximum values, the Stress Ratio curve was plotted from 10 gyrations to the maximum (160 gyrations) on a normal, arithmetic scale. A second-order polynomial was then fit to the data. Identifying the N-SR_{max} was then a matter of taking the derivative of the equation (dSR/dN) and setting it equal zero.

Although the use of regressed (or calculated) N-SR_{max} values improves the correlation with mechanical properties, the predictive relationship is still weak. In other words, the regression equations cannot be used to accurately predict the high temperature shear stiffness or estimated rut depth of a mixture from the N-SR_{max} values obtained during the SGC compaction process. However, while the relationship between N-SR_{max} values and mixture mechanical properties may not be good enough to get an accurate

estimate of the rut depth of an asphalt mixture, it may be good enough to identify gross mixture instability, thus serving as a screening test for further mechanical property tests. Based on the findings from the experiment (PG 64-22 asphalt mixtures), the following procedure was developed to serve as a performance-screening tool for asphalt mixtures.

- Compact three specimens to $N_{maximum}$ using an SGC with the capability to measure shear stress during compaction. This may involve the use of the Servopac, Pine Modified AFG1, or other gyratory compactor with a shear plate or other shear stress measurement capability. The stress ratio is determined at each gyration as the measured shear stress divided by the applied normal stress (nominally 600 kPa).

- Plot the stress ratio as a function of gyrations on a normal arithmetic scale from 10gyrations to $N_{maximum}$.

- Fit a second-order polynomial curve to the stress ratio data ($SR = aN^2 + bN + c$), and determine the regression equation and correlation (R^2).

- If the R^2 of the regression is less than 0.75, then examine the data. If the low correlation is due to data scatter, then the specimen should be discarded and a replacement specimen made (if necessary). If the low correlation is due to the inability of the regression equation to account for the initial curvature (below 20 gyrations), then keep the specimen and make a note of the reason for the low correlation.

- Determine the number of gyrations where the slope of the curve is zero. This value of N is the number of gyrations at which the maximum stress ratio occurs. It is identified as $N\text{-}SR_{max}$.

The concept is illustrated in Figure 3-6 below. Generally, mixtures that have high asphalt effective content will nave low number of gyrations to the maximum shear strength when compared with a one of the same aggregate characteristics. Correlation of the N-SRmax value with rutting was not high, but an analysis was presented for the use of this parameter for screening mixtures..

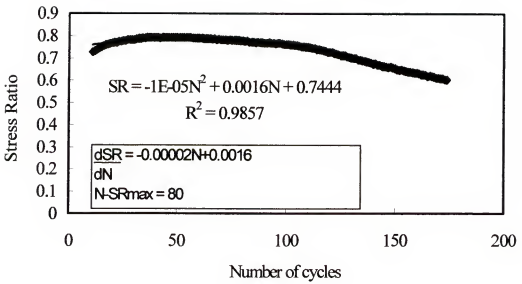

Figure 2-5. N-SRmax concept

- If the ratio of the log of N-SR_{max} to the log of $N_{maximum}$ is greater than or equal to 0.95, the specimen is likely to have good high temperature performance properties.

- If N-SR_{max} is less than N_{design}, the specimen is likely to have poor high temperature performance properties. High temperature performance testing is recommended before the mixture can be used.

- If N-SR_{max} is between N_{design} and the value for $N_{critical}$ in the previous table, the specimen is likely to have fair high temperature performance properties. The user should evaluate the mixture application before deciding if further high temperature performance testing is required.
- If in a set of three specimens any single "Poor" result is obtained (N-SR_{max} less than N_{design} for any single specimen), further high temperature performance testing of the mixture is recommended.

2.7 The Asphalt Pavement Analyzer (APA)

The Georgia Department of Transportation (GDOT), began the development of a loaded wheel tester (GLWT) in 1985 to better evaluate the rutting susceptibility of

asphalt concrete mixtures through a cooperative research study between the Georgia Department of Transportation and the Georgia Institute of Technology (Lai, 1986). Development of the GLWT consisted of modifying a wheel tracking device originally designed by C.R. Benedict of Benedict Slurry Seals, Inc. to test slurry seals (Collins et al, 1995). The primary purpose for developing the GLWT was to perform efficient, effective, and routine laboratory rut proof testing and field production quality control of asphalt mixtures (Lai, 1989).

The GLWT is capable of testing asphalt beam or cylindrical specimens. Beam dimensions are generally 125 mm wide, 300 mm long, and 75 mm high (5 in x 12 in x 3 in). Compaction of beam specimens for testing in the GLWT has varied greatly according to the literature. The original work by Lai (1986) utilized a "loaded foot" kneading compactor. Heated asphalt mixture was "spooned" into a mold as a loaded foot assembly compacted the mixture. A sliding rack, onto which the mold was placed, was employed as the kneading compactor was stationary. West et al. (1991) utilized a static compressive load to compact specimens. Heated asphalt mixture was placed into a mold and a compressive force of 267 kN (60,000 lbs) was applied across the top of the sample and then released. This load sequence was performed a total of four times. In 1995, Lai and Shami (1995) described a new method of compacting beam samples. This method utilized a rolling wheel to compact beam specimens.

Laboratory prepared cylindrical specimens are generally 150 mm in diameter and 75 mm high. Compaction methods for cylindrical specimens have included the "loaded foot" kneading compactor, Lai (1985) and a Superpave gyratory compactor, Hanson and Cooley (1999).

Both specimen types are most commonly compacted to either four or seven percent air void content. However, some work has been accomplished in the GLWT at air void contents as low as two percent, Collins et al (1996). Testing of samples within the GLWT generally consists of applying a 445 N (100 lb) load onto a pneumatic linear hose pressurized to 690 kPa (100 psi). The load is applied through an aluminum wheel onto the linear hose, which resides on the sample. Test specimens are tracked back and forth under the applied stationary loading. Testing is typically accomplished for a total of 8,000 loading cycles (one cycle is defined as the backward and forward movement over samples by the wheel). However, West et al (1991) have suggested fewer loading cycles may suffice.

Test temperatures for the GLWT have ranged from 35 to 60 C (95 to 140 F). Initial work by Lai (1985) was conducted at 35 C (95 F). This temperature was selected because it was Georgia's mean summer air temperature (Collins et al, 1995). Test temperatures within the literature subsequently tended to increase to 40.6 C (105 F) (Collins et al (1995), West et al (1991), Lai (1988), Lai (1993 and Miller et al (1995)), 46.1 C (115 F) (Miller et al (1995)), 50 C (122 F) (Collins et al (1995), Collins et al (1996),), and 60 C (140 F) (Collins et al (1996),).

At the conclusion of the 8,000 cycle loadings, permanent deformation (rutting) is measured. Rut depths are obtained by determining the average difference in specimen surface profile before and after testing. A template with seven slots that fits over the sample mold and a micrometer are typically used to measure rut depth (Lai, 1986).

The Asphalt Pavement Analyzer (APA), shown in Figure 2-3, is a modification of the GLWT and was first manufactured in 1996 by Pavement Technology, Inc. The APA has been used to evaluate the rutting, fatigue, and moisture resistance of HMA mixtures.

Since the APA is the second generation of the GLWT, it follows the same rut testing procedure. A wheel is loaded onto a pressurized linear hose and tracked back and forth over a testing sample to induce rutting. Similar to the GLWT, most testing is carried out to 8,000 cycles. Unlike the GLWT, samples can also be tested while submerged in water. Testing specimens for the APA can be either beam or cylindrical. Currently, the most common method of compacting beam specimens is by the Asphalt Vibratory Compactor (Kandhal and Cooley, 1999). However, some have used a linear kneading compactor for beams (Neiderhauser, 1999). The most common compactor for cylindrical specimens is the Superpave gyratory compactor (Khandall and Mallick, 1999). Both specimen types are most commonly compacted to four or seven percent air voids (Khandall and Mallick, 1999). Tests can also be performed on cores or slabs taken from an actual pavement. Test temperatures for the APA have ranged from 40.6 to 64 C (105 to 147 F). The most recent work has been conducted at or slightly above expected high pavement temperatures (Khandall and Mallick, 1999,Williams and Powell,1999). Wheel load and hose pressure have basically stayed the same as for the GLWT, 445 N and 690 kPa (100 lb and 100 psi), respectively. However, two recent research studies (Williams and Powell,1999. Khandall and Mallick, 1999) did use a wheel load of 533 N (120 lb) and hose pressure of 830 kPa (120 psi) with good success.

Several states, including Georgia, Florida, and Virginia, have used the APA successfully in ranking a limited number of different asphalt mixtures for their potential for rutting. However, the correlation between APA rut depths and field rut depths of ten WesTrack test pavements subjected to the same traffic was attempted for the first time by

Williams and Prowell (1999). The R^2 value of 82.3 percent obtained in this correlation was encouraging.

Currently, Kandhal and Cooley (2002), in a preliminary report of NCHRP 9-17, found good correlation between the APA and the repeated load confined creep test and recommended the use of the APA as a proof-test for rutting performance for Superpave mixtures until a simple performance test based on fundamental engineering principles is developed. The researchers further recommended a critical value of rut depth of 8.0 mm when mixtures are tested at the high temperature of the standard PG grade for a location at an air void content of 6.0 ± 0.5%.

The cost of the APA equipment makes it difficult for all the stakeholders in the pavement fraternity to acquire it for the evaluation of mixtures during the design stage. Moreover, even though the test is intuitive in nature, the test results are not fundamental engineering properties. The search for a simple test to provide fundamental properties for the evaluation of the rutting potential of asphalt paving mixtures is still of concern. In view of the intuitiveness of the APA and the fact that rut depths measured with it correlate with field performance, the gyratory compactor was evaluated based on a comparison with output from the APA using the protocol recommended by Kandhal and Cooley (2002).

2.8 The Superpave™ Indirect Tension Test (IDT)

Under the Strategic Highway Research Program (SHRP), indirect tensile creep testing and analysis system in obtaining fundamental properties of asphalt mixtures at low temperatures was developed (Butler and Roque (1994), Roque and Butler(1992)). The procedures for the test are described in AASTO TP-9. Zhang et al. (1997), described viscoelasticity based interpretation of data obtained with constant load creep on diametral

compression of short cylinders. Nukunya et al. (2002), used the creep result from the indirect tension test to evaluate mixtures with respect to their rutting resistance. In this research, the testing procedure and data reduction was done according to the IDT procedures by Roque et al. (1997). The test procedures and material preparations are specified in AASHTO TP9 and LTPP protocol P07.

2.9 Simple Performance Tests

It has been shown in the previous sections that parameters derived from the gyratory compactor, can be used for the inference of the rutting behavior of HMA mixtures. The gyratory compactor measurements are however, not fundamental engineering properties. They can not be used in a mechanics of materials model to predict response to load. It will be ideal if a performance related property can be obtained to infer the behavior of HMA pavements. Generally, a performance-related property is an engineering property that is connected to performance, but is not directly used to predict performance. Such a property may not be used to predict material response directly, but can be used, knowing that there is a fundamental relationship between the property measured and performance in the field.

2.9.1 Superpave Simple Performance Tests

The Federal Highway Administration (FHWA) has since 1996 (NCHRP 1-37A through NCHRP 9-19), been making efforts to identify and evaluate a simple strength test that could provide reliable information on the probable performance of HMA mixtures during the Superpave mixture design process. The form of the test was to measure a fundamental engineering property, which accurately and reliably measures a mixture response characteristics or parameter that is highly correlated to the occurrence of

pavement distress (eg rutting and cracking) over a diverse range of traffic and climatic conditions.

Efforts were commenced under NCHRP project 1-37A (Witzac et al) at the University of Maryland to identify and validate simple performance tests for permanent deformation, fatigue cracking and low temperature cracking.

NCHRP project 9-19 (Witzac et al 2002), a continuation of the University of Maryland project, evaluated and recommended simple performance tests for use during Superpave mix design. Two of the test methods which produced results having the highest correlation with the rutting resistance of HMA paving mixtures (Witzak et al 2002) are the triaxial dynamic modulus and the unconfined creep tests. A review of these two tests is presented below.

2.9.2 The Dynamic Modulus Test

The The stress and strain on the specimen are as shown in Figure 2-6.

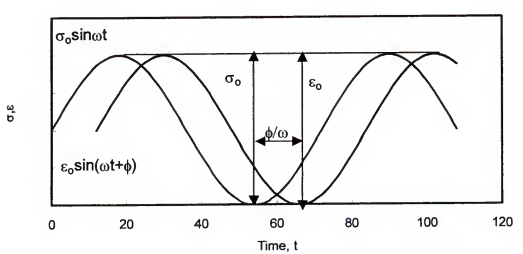

Figure 2-6. Stress strain responses under sinusoidal loading

The dynamic modulus test is performed in accordance with ASTM D3497, "Standard Test Method for the Dynamic Modulus of Asphalt Concrete Mixtures." The test is performed by applying a uniaxial, sinusoidal compressive stress to an unconfined or confined HMA cylindrical specimen.

. Various researchers have used and derived material relationships from the complex modulus testing on HMA (Daniel and Kim 1998, Swan 2002, Witczak et al. 2000, and Witczak et al. 2002).

The strain response to the externally applied sinusoidal stress will be an oscillation of the same form and frequency as the stress, but lagging by a phase angle ϕ.

The phase angle, is often called the loss angle, and is a function of the internal friction of the material (Findley et al (1989)).

2.9.3 Relating Dynamic Modulus Test Results to Material Properties

The viscoelastic nature of asphalt calls for the expression of the separation of load responses into elastic and viscous components. The dynamic modulus is mathematically defied as the maximum dynamic stress divided by the peak recoverable axial strain.

$|E^*| = \sigma_o/\varepsilon_o$

The real and imaginary portions of the complex modulus E*, is presented as

$$E^* = E' + E'' \qquad (2\text{-}3)$$

E' is generally referred to as the storage or elastic modulus and E" is referred to as the loss or viscous modulus. The phase angle ϕ, the angle by which the train (ε_o) lags the stress (σ_o), is an indication of the viscous property of the material being investigated (Yodder and Witczak (1985), Ullidtz (1987)). As a material becomes more viscous, the

phase angle increases. A phase angle of 90° indicates purely viscous behavior while a phase angle of 0° indicates a purely elastic material.

Ullidtz (1987) mathematically showed that for a simple Maxwell model, the complex modulus can be expressed in terms of an elastic stiffness, $E = E^*/\cos(\phi)$ and a viscous stiffness, $V = E^*/(\omega\sin(\phi))$. Ullidtz however observed that the Maxwell model is much too simple to imitate the rheological properties of asphalt. However, with the current proposal of the viscous parameter in the Superpave simple performance tests, there is the need to evaluate this parameter alongside others..

2.9.4 Energy Concept from Dynamic Test

The storage modulus E' as defined above is associated with energy storage and release during periodic deformation. On the other hand, the loss modulus E" is associated with dissipation of energy and its transformation into heat. The ratio $E'/E'' = \tan\phi$ is widely used as the damping capacity of viscoelastic materials (Finley et al(1987)). Damping is the dissipation of energy in an oscillating system.

Finley et al (1989), mathematically showed that the damping energy of a viscoelastic material, defined as $\Delta W/W$, where ΔW is the energy loss per cycle of vibration of a given amplitude and W is the maximum energy which the system can store for a given amplitude, can be expressed as:

$$\Delta W/W = 2\pi\sin\phi \qquad (2\text{–}4)$$

This equation shows that the damping ability of a linearly viscoelastic material is only dependent on the phase angle. Which is a function of frequency and is a measure of a physical property of the material, but is independent of the stress and strain. It may be possible to infer the relative rutting resistance of asphalt mixtures using its damping

energy. There will be no energy loss if the stress and the strain are in phase, and hence ϕ=0.

2.9.5 Dynamic Creep Compliance

Mathematical relationship have been determined for the inter-conversion of the complex modulus in a dynamic test to a dynamic creep compliance or complex compliance, which is frequency dependent, Findley et al (1989). The relationship between the two is given by equation 2-4:

$$D^* = 1/E^* \quad (2\text{-}4)$$

D^* is the complex creep compliance

Algorithms for this inter-conversion was presented by Kim et al. (1997), and Zhang et al. (1997).

2.9.6 Other Rutting Parameters from the Dynamic Test

Shenoy and Romero (2002), presented an analysis method for the characterization of asphalt mixtures with respect to their rutting resistance. The method consisted of fitting a unified curve for the dynamic modulus from which model parameters are developed. The slope B1 in the low frequency region of the unified curve (log-log plot), divided by a specification temperature, Ts (Temperature at which the mixture has attain a standardized complex modulus at a loading frequency of 1 Hz.). The lower the parameter B1, the greater will be the resistance of the mixture to rutting. Similarly the higher the value of Ts, the greater is the resistance of the mixture to rutting. Tests were conducted at 5Hz. at three different temperatures for the rutting analysis.

2.9.7 The Uniaxial Static Creep Test

The creep test is conducted by applying a static load to a HMA specimen and measuring the resulting permanent deformation with time. Figure 7-2 shows the variation with time on loading and unloading of the specimen. With the unconfined compression test, the applied pressure cannot usually exceed 30 psi (206.9 kPa) (Roberts et al 1996) to ensure that the sample will not fail. Test temperatures are also low, up to 40°C. Figure 2-7 shows a typical relationship between the calculated creep compliance D(t) and loading time, t, where

$$D(t) = \varepsilon(\tau)/\sigma \qquad (2\text{–}5)$$

Many attempts have been made to use the uniaxial static creep test for characterizing HMA mixtures, however, this test has not yet been specified by either the AASTO or the ASTM. The Texas Department of Transportation uses a form of the test for mixture characterization. In view of the fact that the test is one of the candidate Superpave simple performance tests, there is the need for its evaluation in addition to other known tests. 2.9.8 Creep parameters for HMA characterization

Generally, power models are used to model the linear portion of the creep compliance curve as illustrated in Figure2-9.

$$D' = D(t) - D_o = D_1 t^m \qquad (2\text{-}6)$$

Where

D' = viscoelastic compliance component at any time,

D(t) = total compliance at any time

D_o = instantaneous compliance,

t = loading time, and

D_1 and m = materials regression coefficients.

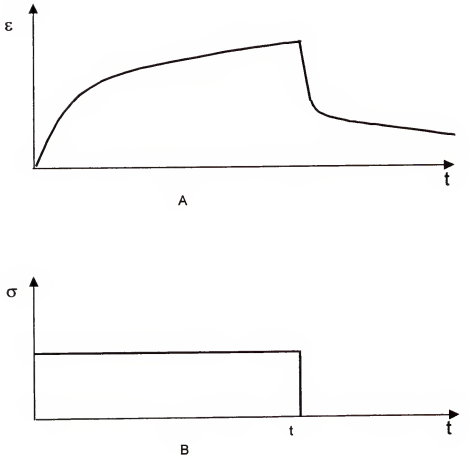

Figure 2-7. Strain response (A) to a static load σ (B) for a loading time t.

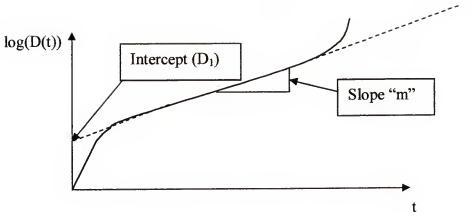

Figure 2-8. Regression constants of the creep compliance plot.

The regression coefficients D_1 and "m" are generally referred to as compliance parameters. These parameters are general indicators of permanent deformation behavior of the material. The larger the value of D_1, the larger the compliance value, the lower the modulus and the larger the permanent deformation. For a constant Di value, an increase in the slope parameter "m" implies higher permanent deformation (Witczak et al. (2002)).

CHAPTER 3
MATRIALS AND METHODOLOGY

3.1 Introduction

This chapter provides information on the materials and research methodology used. The physical properties of materials used are discussed, such as their aggregate gradation, aggregate physical properties, mixture design procedure, material preparation, as well as testing equipment and testing protocol. The data analysis procedures and research methodology are also explained.

3.2 Materials

3.2.1 Overview of Mixtures Used

The mixtures used in this study can be divided into five distinct groups: 1) ten mixtures (entitled "Fine Aggregate Angularity (FAA) Mixtures") with different fine aggregates (defined as material passing the no. 4 Sieve) and the coarse portion of the aggregates consisting of oolitic limestone (Whiterock) from South Florida, 2) eight mixtures of varying gradations with oolitic limestone (Whiterock) from South Florida, entitled "Limestone Gradation Study Mixtures," 3) six mixtures of varying gradations with Georgia granite (GA185), entitled "Granite Gradation Study Mixtures," 4) six field mixtures of varying gradations and aggregate types from Superpave monitoring test sites in Florida, entitled "Superpave Field Monitoring Mixtures," and 5) two mixtures with the same gradation, aggregate type and aggregate structure, but with and without a SBS modified binder (PG 76-22) used in an experiment at the Heavy Vehicle Simulator (HVS) test site in Florida and entitled "HVS Mixtures". In the following the binders

used in these mixtures will be discussed, followed by a discussion of the aggregate characteristics and gradations for each of the mixtures used.

3.2.2 Asphalt Binder

The grade of the asphalt cement used in an asphalt concrete mixture is one factor that can have an effect on the amount of rutting that occurs in the mix. All other things being equal, the stiffer the asphalt cement, the less the rutting that is expected in the mix under a given weight and volume of truck. In this research, only one type of unmodified asphalt cement, AC 30 (PG67-22), which is commonly used in Florida was used for all mixtures tested, except in one of the HVS mixtures, in which SBS modified asphalt (PG 76-22) binder was used.

3.2.3 Aggregates

This section describes the type of aggregates, aggregate gradations and combination of various aggregates in this research.

3.2.3.1 Fine aggregate angularity (FAA) mixtures

The first part of the research was performed using gradations of coarse and fine Whiterock limestone mixtures (C1 and F1) provided by FDOT for use as the reference mixtures. The nominal maximum aggregate size for these mixtures is 12.5 mm (1/2-in). These Superpave mixtures were selected because they are commonly used FDOT gradations and they are known to perform well in the field. Figure 3-1 shows the gradation curves for the C1 and F1 mixtures. The fine aggregate portions of these mixtures were volumetrically replaced by the four other fine aggregates (passing the No. 4 Sieve) to obtain five fine graded and five coarse graded mixtures. This helps to minimize the effects of gradation for the purposes of this portion of the research.

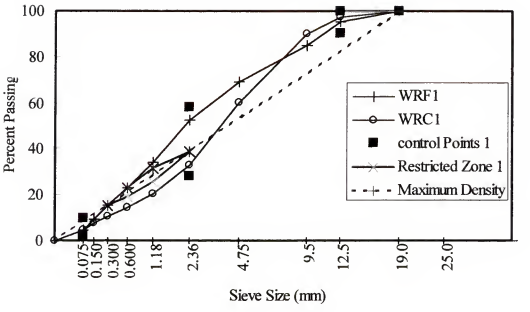

Figure 3-1. Gradation curves for C1 and F1

All materials were washed in accordance with ASTM C-117 and a washed sieve analyses were performed according to ASTM C-136. The fine aggregates used were selected to be of varying angularity, texture, toughness, and historical rutting performance. The designations for the fine aggregates used are as follows:

- Limestone
  - Whiterock (baseline aggregate)
  - Cabbage Grove (FL)
  - Calera (AL)
- Granite
  - Ruby (GA)
- Gravel
  - Chattahoochee FC-3 (TN)

The aggregates are designated in this project as follows:

- Calera-CAL
- White Rock-WR
- Cabbage Grove-CG

- Ruby-RB
- Chattahoochee FC-3 – CH

Nova Scotia – NS

Tables 3-1 and 3-2 show the resulting coarse and fine gradations respectively.

Table 3-1. Coarse Gradations for Fine Aggregate Effects

	Mixture				
Sieve Size (mm)	WRC	CGC	RBC	CHC	CALC
25(1")	100.0	100.0	100.0	100.0	100.0
19(3/4")	100.0	100.0	100.0	100.0	100.0
12.5(1/2")	97.4	97.4	97.5	97.5	97.5
9.5(3/8")	90.0	88.8	89.5	89.4	89.3
4.75(#4)	60.2	54.8	57.6	56.9	56.5
2.36 (#8)	33.1	30.4	31.6	31.3	31.2
1.18(#16)	20.3	20.5	21.1	20.9	20.9
0.6(#30)	14.7	14.8	15.1	15.0	15.0
0.3(#50)	10.8	11.0	11.0	11.0	11.0
0.15(#100)	7.6	7.2	7.0	7.1	7.1
0.075(#200)	4.8	5.5	5.2	5.2	5.3

Table 3-2. Fine Gradations for Fine Aggregate Effects

	Mixture				
Sieve Size (mm)	WRF	CGF	RBF	CHF	CALF
25(1")	100.0	100.0	100.0	100.0	100.0
19(3/4")	100.0	100.0	100.0	100.0	100.0
12.5(1/2")	95.5	97.4	95.1	95.0	94.9
9.5(3/8")	85.1	83.8	85.0	84.7	84.6
4.75(#4)	69.3	66.0	68.5	67.9	67.6
2.36 (#8)	52.7	49.4	51.2	50.8	50.6
1.18(#16)	34.0	33.3	34.2	34.0	34.0
0.6(#30)	22.9	21.9	22.4	22.2	22.2
0.3(#50)	15.3	13.9	14.0	14.0	14.0
0.15(#100)	9.6	7.0	6.9	6.9	6.9
0.075(#200)	4.8	4.5	4.3	4.3	4.3

Table 3-3 shows the Bulk Specific Gravity and toughness, as well as the surface texture, particle shape, direct shear strength (DST) from a geotechnical direct shear box test, and Fine Aggregate Angularity (FAA) values of the five fine-graded aggregates used.

Table 3-3: physical properties of fine aggregates

Material	Bulk Specific Gravity	Los Angeles Abrasion[a]	Tough-ness[b]	Surface Texture[c]	Particle Shape[d]	FAA	DST (psi)
White Rock	2.48	34%	Mediu m	3.3	3.0	43.4	134.4
Calera	2.56	25%	High	1.7	3.5	42.7	140.8
Cabbage Grove	2.56	41%	Low	4.6	2.4	53.1	106.7
Ruby	2.68	20%	High	2.7	4.3	46.3	120.5
Chattahoo-chee FC-3	2.60	42%	Low	2.3	3.5	44.0	106.9

[a]Los Angeles Abrasion Test performed on the parent rock. Values provided by the Florida DOT Materials Office.
[b]Definition of toughness based on L.A. Abrasion: High: <30; Medium: 30-40; Low: >40
[c]Average of 8 evaluations, where 1 = smooth and 5 = rough.
[d]Average of 8 evaluations, where 1 = rounded and 5 = angular.

Bulk Specific Gravity ranged from 2.27 for relatively porous limestone to 2.68 for very non-porous granite. Toughness of the parent rock varied from 18% as the lowest value to 42 % as the highest value of the L.A. Abrasion test. Average surface texture values ranged from 1.7 to 4.6, while average particle shape values ranged from 2.4 to 4.3.

Bulk Specific Gravities for each material were determined in accordance with ASTM C-128. The Florida Department of Transportation (FDOT) provided L.A. Abrasion values. The FAA values were calculated using the Uncompacted Void Content of Fine Aggregate Test (ASTM C-1252 and AASHTO TP33), and the Direct Shear Test (DST, ASTM Standard Method D 3080) was used to determine the shear strength of each

fine aggregate. Both FAA and DST values were provided by previous research done by Casanova (2000).

3.2.3.2 Determination of fine aggregate batch weights

To volumetrically replace the fine aggregates in the FDOT Whiterock limestone C1 and F1 mixtures with the other aggregate types, the weight of Whiterock aggregate retained on each sieve (from #8 Sieve to # 200 Sieve) was replaced with an equivalent volume of fine aggregate of the replacement material during the batching process using the following formula:

$$W_r = \frac{Gmb_r * W_L}{Gmb_L} \quad (3\text{-}1)$$

W_L : Weight of Whiterock limestone retained on a specified sieve

W_r : Weight of replacement fine aggregate retained on the specified sive size

Gmb_L : Bulk specific gravity of Whiterock Limestone

Gmb_r : Bulk specific gravity of replacement aggregate

3.2.3.3 Limestone gradation study mixture gradations

The second part of the research was done with an oolitic limestone aggregate, entitled "Whiterock" aggregate, which is commonly used in mixtures in Florida. This aggregate was made up of three components: coarse aggregates (S1A), fine aggregates (S1B) and screenings. These were blended together in different proportions to produce ten (10) HMA mixtures consisting of five coarse and five fine gradations, two of which are the same gradations as in the Fine Aggregate study, namely WRC and WRF. Georgia granite (GA 185) mineral filler was used in all the above gradations. These gradations were produced and extensively studied in a previous research at UF (Nukunya, 2000). Tables

3-4 and 3-5 show the gradations for the coarse and fine blends respectively. These are also displayed in Figures 3-2 and 3-3.

Table 3-4. Gradations for Whiterock Coarse Graded Mixtures

	Mixture				
Sieve Size (mm)	WRC1	WRC2	WRC3	WRC4	WRC5
25(1")	100.0	100.0	100.0	100.0	100.0
19(3/4")	100.0	100.0	100.0	100.0	100.0
12.5(1/2")	97.4	91.1	97.6	94.5	97.4
9.5(3/8")	90.0	73.5	89.3	84.9	89.9
4.75(#4)	60.2	47.1	57.4	66.5	47.1
2.36 (#8)	33.1	29.6	36.4	36.6	33.1
1.18(#16)	20.3	20.2	24.0	26.1	20.3
0.6(#30)	14.7	14.4	17.7	20.5	14.7
0.3(#50)	10.8	10.4	12.9	13.6	10.8
0.15(#100)	7.6	6.7	9.0	8.3	7.6
0.075(#200)	4.8	4.8	6.3	5.8	4.8

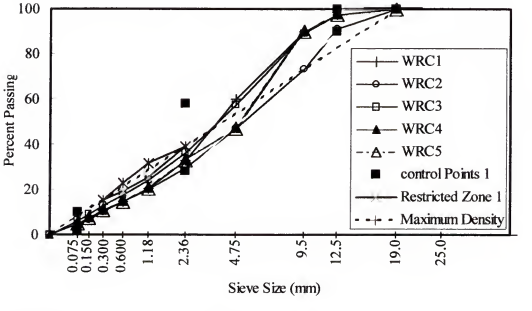

Figure 3-2 Coarse gradations for limestone gradation effects

Table 3-5. Gradations for Whiterock Fine Graded Mixtures

Sieve Size (mm)	Mixture WRF1	WRF2	WRF4	WRF5	WRF6
25(1")	100.0	100.0	100.0	100.0	100.0
19(3/4")	100.0	100.0	100.0	100.0	100.0
12.5(1/2")	95.5	90.8	95.5	95.5	95.5
9.5(3/8")	85.1	78.0	85.1	85.1	85.1
4.75(#4)	69.3	61.3	69.3	61.3	69.3
2.36 (#8)	52.7	44.1	52.7	52.7	44.1
1.18(#16)	34.0	34.7	40.0	34.0	34.7
0.6(#30)	22.9	23.6	29.0	22.9	23.6
0.3(#50)	15.3	15.7	20.0	15.3	15.7
0.15(#100)	9.6	8.9	12.0	9.6	9.1
0.075(#200)	4.8	6.3	6.3	4.8	6.3

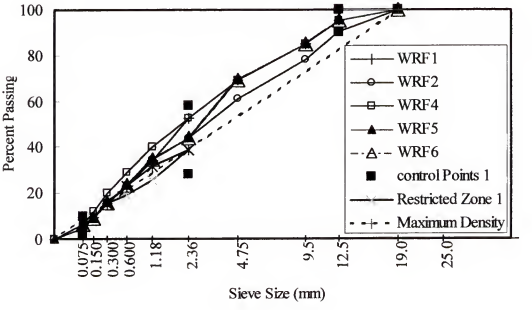

Figure 3-3 Fine gradations for gradation effects studies

3.2.3.4 Granite gradation to study mixture gradations

Six mixtures were prepared by volumetrically replacing the aggregate particles in the WRC1, WRC2, WRC3, WRC4, WRF1 and WRF2 limestone mixtures with the appropriate sizes of Georgia granite (GA185) aggregates from pit #185 (code #7 for 12.5 and 9.5 mm sieves, code #89 for 4.75mm (#4) sieve and code #W10 for sieves less than #4). Table 3-6 to 3-8 show the gradations, which are also displayed in Figures 3-4 to 3-7.

Table 3-6: Granite based mixture gradations

	Mixture					
Sieve Size (mm)	GAC1	GAC2	GAC3	GAF1	GAF2	GAF3/C4
25(1")	100.0	100.0	100.0	100.0	100.0	100.0
19(3/4")	100.0	100.0	100.0	100.0	100.0	100.0
12.5(1/2")	97.4	90.9	97.3	94.7	90.5	94.6
9.5(3/8")	89.0	72.9	89.5	84.0	77.4	85.1
4.75(#4)	55.4	45.9	55.4	66.4	60.3	65.1
2.36 (#8)	29.6	28.1	33.9	49.2	43.2	34.8
1.18(#16)	19.2	18.9	23.0	32.7	34.0	26.0
0.6(#30)	13.2	13.2	16.0	21.0	23.0	18.1
0.3(#50)	9.2	9.2	11.2	12.9	15.3	12.5
0.15(#100)	5.3	5.6	6.8	5.9	8.7	7.7
0.075(#200)	3.4	3.9	4.7	3.3	5.4	5.8

The mineral filler used in this gradation is from the same source as the filler used in the Whiterock gradations. These granite gradations have been studied under a moisture damage project at the University of Florida. Georgia granite (GA 185) is extensively used for the paving of highways in the sate of Florida, the study of the behavior of various gradations with this aggregate is likely to provide results which will help in evaluating tis aggregate. Moreover, the aggregates could be obtained readily from local suppliers close to the research laboratory.

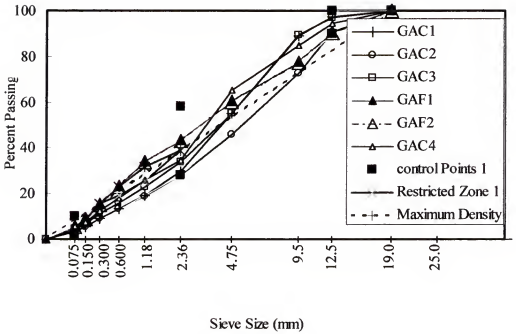

Figure 3-4 Granite aggregate gradations

3.2.3.5 Superpave field monitoring mixture gradations

Six Superpave mixtures from Florida, and tested for performance at the University of Florida (Asiamah 2001) were also evaluated. Table 3-5 and Figures 3-5 and 3.7 display the gradations of these mixtures.

Table 3-7: Gradations for field projects

	Mixture				
Sieve Size (mm)	P1	P2	P3	P5	P7
25(1")	100.0	100.0	100.0	100.0	100.0
19(3/4")	100.0	100.0	100.0	100.0	100.0
12.5(1/2")	100.0	98.0	93.6	100.0	95.3
9.5(3/8")	100.0	88.5	90.4	94.8	88.7
4.75(#4)	65.4	44.7	70.3	65.8	69.2
2.36 (#8)	40.6	27.7	35.8	39.7	54.6
1.18(#16)	27.9	21.6	24.8	29.6	37.4
0.6(#30)	19.5	17.3	16.8	21.3	24.6
0.3(#50)	12.9	12.4	11.8	14.9	14.6
0.15(#100)	8.3	7.2	5.5	7.3	6.2
0.075(#200)	5.2	4.9	3.5	3.1	3.3

Project 1 (P1) and Project 5 (P5) are 9.5 mm nominal gradations while all the other projects are of 12.5 mm nominal size. With the exception of project number 7, all the field mixtures are coarse-graded (i.e. the gradations pass below the Superpave Restricted Zone). Project numbers 1 and 2 are made up of granite aggregates while project numbers 3, 5, 7, and 8 are made up of limestone aggregates. Samples for project number 8 were obtained directly from the field, the gradation is therefore not showed in Table 3-7.

It is worth noting that all the Superpave project mixtures contained reclaimed asphalt pavement (RAP) materials. However, the laboratory produced mixtures did not include RAP because the original material was not available.

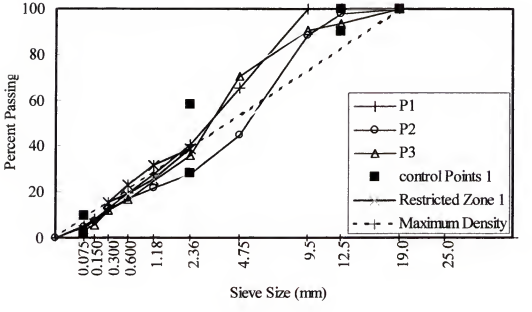

Figure 3-5: Gradations for field projects 1, 2 and 3

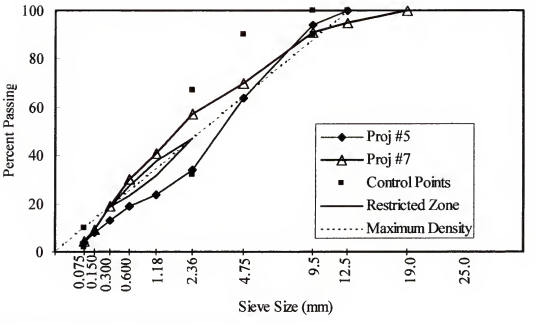

Figure 3-6 Gradations for field projects 5 and 7

2.2.3.6 Heavy vehicle simulator (HVS) mixture gradation

Finally, samples of plant mixtures for the Heavy Vehicle Simulator project, sampled and volumetrically analyzed by the Florida Department of Transportation (FDOT) State materials office were tested. Table 3-8 and Figure 3-7 show the gradation of the plant mixes for the mixtures tested (truck 4-Lift 2 for 67-22 and truck 3-Lift 2 for 76-22 mixtures). The mix comprises of Florida limestone aggregates.

The HVS mixtures were not produced in the laboratory. They were already mixed HMA mixture obtained directly from the project contractor's supply trucks. The aggregate and properties were therefore obtained from the Florida Department project supervising office. The gradations showed in Table 3-8 and Figure 3-7 are obtained from the ignition oven test on the field mixtures.

3.3 Mixture design

Before the production of test specimens, the mixture design process was verified for the mixture volumetric properties. The original Superpave design procedure was used for all the mixtures. The Servopac Superpave gyratory compactor was used in this process. Figure 3-8 shows a picture of the Servopac gyratory compactor. Table 3-9 displays the Superpave compaction requirements for specified traffic levels as a guide for the design of asphalt paving mixtures. The mixture volumetric properties are calculated based on the design number of gyrations (N_{des}). At this number of gyrations, a specified air voids level of 4% provides the optimum design asphalt content. All mixtures, with the exception of the projects and the HVS mixes were designed for a traffic level of 10-30 million ESALS, that is an N_{des} of 109 and N_{max} of 174. The project mixes except project 7, were designed at an Ndes of 96 and Nmax of 152.

Project 7 has an N_{des} of 84, while the HVS mixes have an N_{des} of 100. The Servopac compaction parameters used for the design are 1.25° gyratory angle, 600-kPa ram pressure and 30 revolutions per minute.

For each mixture, two pills were produced at the specified asphalt content, compaction of the mixtures was made to 109 gyrations with the Servopac gyratory compactor, after which the bulk densities were measured. To verify the volumetric properties of the mixtures, the maximum theoretical specific gravity was measured using the Rice maximum theoretical specific gravity method specified in AASHTO T 209/ASTM D 2041 standards. In this case, the mixtures were allowed to cool down in the loose state. Tables 3.10 to 3.16 show the volumetric properties of all the mixtures used in this research.

Table 3-8 HVS plat mix gradations

Sieve Size (mm)	Mixture 67-22	76-22
25(1")	100.0	100.0
19(3/4")	100.0	100.0
12.5(1/2")	97.4	97.1
9.5(3/8")	95.7	94.6
4.75(#4)	76.3	76.5
2.36 (#8)	54.2	55.2
1.18(#16)	44.1	45.3
0.6(#30)	37.8	39.2
0.3(#50)	23.7	24
0.15(#100)	8.9	8.8
0.075(#200)	4.2	3.9

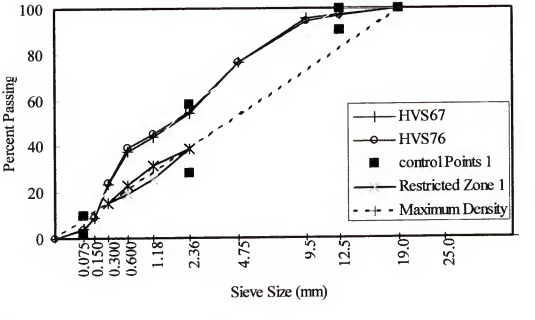

Figure 3-7 Gradation charts for HVS plant mixtures.

Figure 3-8 Servopac Superpave gyratory cpmpactor

Table 3-9: Superpave Gyratory Compaction Effort

Design ESALs (millions)	Average design high air temperature < 39°C		
	Ninitial	Ndesign	Nmaximum
< 0.3	7	68	104
<1	7	76	117
<3	7	86	134
<10	8	96	152
<30	8	109	174
<100	9	126	204
>100	9	143	233

(After Asphalt Institute Superpave Series No. 2)

Table 3-10: Volumetric Properties of Coarse Graded Mixtures (FAA Effects)

		Mixture				
Property	Symbol	WRC	CGC	RBC	CALC	CHC
Maximum Theoretical Density	Gmm	2.328	2.386	2.393	2.454	2.394
Specific Gravity of Asphalt	Gb	1.035	1.035	1.035	1.035	1.035
Bulk Specific Gravityof Compacted Mix	Gmb	2.235	2.295	2.300	2.353	2.289
Asphalt Content	Pb	6.5	6.5	6.25	5.8	5.7
Bulk Specific Gravityof Aggregate	Gsb	2.469	2.418	2.576	2.540	2.535
Effective Specific Gravity of Aggregate	Gse	2.549	2.625	2.622	2.680	2.601
Asphalt Absorption	Pba	1.1	1.2	1.2	1.2	1.0
Effective Asphalt Content In Mixture	Pbe	5.3	3.3	5.6	3.7	4.7
Percent VMA in Compacted Mix	VMA	15.4	11.2	16.1	12.6	14.8
Percent Air Voids in Compacted Mix	Va	4.0	3.8	3.9	4.1	4.4
Percent VFA in Compacted Mix	VFA	74.0	66.5	77.3	67.4	70.6
Dust/Asphalt Ratio	D/A	1.0	1.7	0.9	1.4	1.1
Surface Area (m^2/kg)	SA	4.2	4.4	4.3	4.3	4.3
Theoretical Film Thickness	FT	11.2	6.7	11.7	9.8	7.7
Effective VMA in Compacted Mix	VMAe	35.4	28.6	38.4	31.7	35.6
Effective Film Thickness (microns)	Fte	39.2	25.1	42.5	27.4	36.0

Table 3-11: Volumetric Properties of Fine Graded Mixtures (FAA Effects)

		Mixture				
Property	Symbol	WRF	CGF	RBF	CALF	CHF
Maximum Theoretical Density	Gmm	2.338	2.381	2.416	2.480	2.407
Specific Gravity of Asphalt	Gb	1.035	1.035	1.035	1.035	1.035
Bulk Specific Gravityof Compacted Mix	Gmb	2.244	2.288	2.372	2.386	2.315
Asphalt Content	Pb	6.3	6.7	5.9	5.3	5.5
Bulk Specific Gravityof Aggregate	Gsb	2.488	2.403	2.599	2.524	2.549
Effective Specific Gravity of Aggregate	Gse	2.554	2.630	2.637	2.691	2.608
Asphalt Absorption	Pba	1.1	1.2	1.2	1.2	1.0
Effective Asphalt Content In Mixture	Pbe	5.3	3.2	5.7	3.4	4.8
Percent VMA in Compacted Mix	VMA	15.6	11.2	16.0	10.5	14.1
Percent Air Voids in Compacted Mix	Va	4.0	3.9	3.7	3.8	3.7
Percent VFA in Compacted Mix	VFA	74.2	65.2	76.8	63.8	73.7
Dust/Asphalt Ratio	D/A	0.8	1.4	0.7	1.3	0.9
Surface Area (m^2/kg)	SA	5.4	4.8	4.7	4.7	4.7
Theoretical Film Thickness	FT	9.0	6.3	10.2	5.2	8.7
Effective VMA in Compacted Mix	VMAe	25.7	21.3	27.3	18.8	24.7
Effective Film Thickness (microns)	Fte	19.3	14.6	22.8	11.7	19.7

Table 3-12: Volumetric Properties of Coarse Graded Mixtures (Gradation Effects)

		Mixture				
Property	Symbol	WRC1	WRC2	WRC3	WRC4	WRC5
Maximum Theoretical Density	Gmm	2.328	2.347	2.349	2.347	2.338
Specific Gravity of Asphalt	Gb	1.035	1.035	1.035	1.035	1.035
Bulk Specific Gravityof Compacted Mix	Gmb	2.235	2.255	2.254	2.254	2.244
Asphalt Content	Pb	6.5	5.8	5.3	5.6	6.3
Bulk Specific Gravityof Aggregate	Gsb	2.469	2.465	2.474	2.478	2.467
Effective Specific Gravity of Aggregate	Gse	2.549	2.545	2.568	2.555	2.550
Asphalt Absorption	Pba	1.3	1.3	0.9	1.1	1.1
Effective Asphalt Content In Mixture	Pbe	5.3	4.6	4.5	4.5	5.3
Percent VMA in Compacted Mix	VMA	15.4	13.2	14.0	16.2	15.4
Percent Air Voids in Compacted Mix	Va	4.0	3.9	4.0	3.9	4.0
Percent VFA in Compacted Mix	VFA	74.1	71.6	70.2	71.8	74.0
Dust/Asphalt Ratio	D/A	0.7	0.8	1.2	1.0	0.9
Surface Area (m^2/kg)	SA	4.9	4.6	5.7	5.6	4.2
Theoretical Film Thickness	FT	11.2	10.1	8.0	8.1	10.5
Effective VMA in Compacted Mix	VMAe	35.4	35.3	30.4	30.6	34.2
Effective Film Thickness (microns)	Fte	39.2	39.3	24.1	25.0	36.3

Table 3-13: Volumetric properties of fine graded whiterock mixtures (Gradation effects)

		Mixture				
Property	Symbol	WRF1	WRF2	WRF4	WRF5	WRF6
Maximum Theoretical Density	Gmm	2.338	2.375	2.368	2.326	2.341
Specific Gravity of Asphalt	Gb	1.035	1.035	1.035	1.035	1.035
Bulk Specific Gravityof Compacted Mix	Gmb	2.244	2.281	2.272	2.233	2.244
Asphalt Content	Pb	6.3	5.4	5.7	6.7	6.1
Bulk Specific Gravityof Aggregate	Gsb	2.488	2.489	2.491	2.485	2.489
Effective Specific Gravity of Aggregate	Gse	2.554	2.565	2.568	2.555	2.550
Asphalt Absorption	Pba	1.1	1.2	1.2	1.2	1.0
Effective Asphalt Content In Mixture	Pbe	5.3	4.2	4.5	5.6	5.2
Percent VMA in Compacted Mix	VMA	15.6	13.2	14.0	16.2	15.4
Percent Air Voids in Compacted Mix	Va	4.0	3.9	4.0	4.0	4.2
Percent VFA in Compacted Mix	VFA	74.2	70.1	71.2	75.0	72.8
Dust/Asphalt Ratio	D/A	0.8	1.4	1.3	0.8	1.1
Surface Area (m^2/kg)	SA	5.4	5.7	6	6.5	4.1
Theoretical Film Thickness	FT	9.0	6.9	6.3	9.7	8.2
Effective VMA in Compacted Mix	VMAe	25.7	25.8	23.5	26.8	28.9
Effective Film Thickness (microns)	Fte	19.3	17.1	13.2	20.7	20.9

Table 3-14: Volumetric properties of granite mixtures

		Mixture					
Property	Symbol	GAC1	GAC2	GAC3	GAF1	GAF2	GAF3
Maximum Theoretical Density	Gmm	2.442	2.500	2.492	2.473	2.532	2.505
Specific Gravity of Asphalt	Gb	1.035	1.035	1.035	1.035	1.035	1.035
Bulk Specific Gravity of Compacted Mix	Gmb	2.442	2.399	2.391	2.473	2.433	2.404
Asphalt Content	Pb	6.63	5.26	5.25	5.68	4.56	5.14
Bulk Specific Gravityof Aggregate	Gsb	2.687	2.687	2.686	2.686	2.687	2.687
Effective Specific Gravity of Aggregate	Gse	2.710	2.719	2.709	2.706	2.725	2.720
Asphalt Absorption	Pba	0.37	0.43	0.31	0.28	0.53	0.46
Effective Asphalt Content In Mixture	Pbe	6.32	4.85	4.96	5.42	4.06	4.70
Percent VMA in Compacted Mix	VMA	18.5	15.4	15.7	16.6	13.6	15.1
Percent Air Voids in Compacted Mix	Va	4.0	4.0	4.1	4.0	3.9	4.0
Percent VFA in Compacted Mix	VFA	78.5	73.8	74.2	75.9	71.2	73.3
Dust/Asphalt Ratio	D/A	0.6	0.8	0.9	0.6	1.2	1.2
Surface Area (m^2/kg)	SA	3.3	3.5	4.2	4.1	5.3	4.9
Theoretical Film Thickness	FT	19.9	14.3	12.1	13.4	7.7	9.9
Effective VMA in Compacted Mix	VMAe	42.9	39.0	35.1	28.4	26.6	33.5
Effective Film Thickness (microns)	Fte	67.3	50.8	35.7	27.3	17.8	28.4

Table 3-15: Volumetric properties of field projects

		Mixture				
Property	Symbol	Proj #1	Proj #2	Proj #3	Proj #7	Proj #8
Maximum Theoretical Density	Gmm	2.509	2.523	2.216	2.334	2.382
Specific Gravity of Asphalt	Gb	1.035	1.035	1.035	1.035	1.035
Bulk Specific Gravityof Compacted Mix	Gmb	2.407	2.445	2.122	2.229	2.284
Asphalt Content	Pb	5.5	5.0	8.3	6.1	6.0
Bulk Specific Gravityof Aggregate	Gsb	2.691	2.694	2.325	2.47	2.503
Effective Specific Gravity of Aggregate	Gse	2.736	2.725	2.475	2.573	2.598
Asphalt Absorption	Pba	0.6	0.4	2.7	1.7	1.4
Effective Asphalt Content In Mixture	Pbe	4.9	4.5	5.7	5.2	4.5
Percent VMA in Compacted Mix	VMA	15.5	14.8	16.4	16.0	14.0
Percent Air Voids in Compacted Mix	Va	4.1	4.4	4.2	4.5	3.9
Percent VFA in Compacted Mix	VFA	73.7	70.6	74.1	71.9	72.4
Dust/Asphalt Ratio	D/A	1.2	0.6	0.6	0.6	1.0
Surface Area (m^2/kg)	SA	5.2	3	3.7	4.6	4.3
Theoretical Film Thickness	FT	9.2	8.7	11.3	7.7	8.9
Effective VMA in Compacted Mix	VMAe	31.1	38.1	35.4	22.1	34.3
Effective Film Thickness (microns)	Fte	24.4	52.3	48.3	18.6	35.3

Table 3-16. HVS plant mixtures

		Mixture	
Property	Symbol	67-22	76-22
Maximum Theoretical Density	Gmm	2.276	2.273
Specific Gravity of Asphalt	Gb	1.035	1.035
Bulk Specific Gravityof Compacted Mix	Gmb	2.185	2.186
Asphalt Content	Pb	8,2	7.90
Bulk Specific Gravityof Aggregate	Gsb	2.346	2.346
Effective Specific Gravity of Aggregate	Gse	2.525	2.532
Asphalt Absorption	Pba	3.10	3.10
Effective Asphalt Content In Mixture	Pbe	4.97	4.90
Percent VMA in Compacted Mix	VMA	14.4	14.2
Percent Air Voids in Compacted Mix	Va	4.0	3.7
Percent VFA in Compacted Mix	VFA	72.0	73.0
Dust/Asphalt Ratio	D/A	0.8	0.8
Surface Area (m^2/kg)	SA	6.1	6.1
Theoretical Film Thickness	FT	13.7	12.3
Effective VMA in Compacted Mix	VMAe	25.2	24.4
Effective Film Thickness (microns)	Fte	17.5	16.5

3.4 Testing of HMA Mixtures

The testing plan adopted for this research is displayed in Figure 3-9 below. This figure illustrates the testing that was performed to evaluate the ability of the Servopac to differentiate mixtures with respect to their rutting resistance base on the outcome of tested procedures such as the APA and the creep compliance, as well as mixture properties that affect the rutting performance of asphalt paving mixtures. The flow diagram below shows the testing for fine aggregate effects, however, the same testing protocol was followed for the testing for aggregate gradation effects.

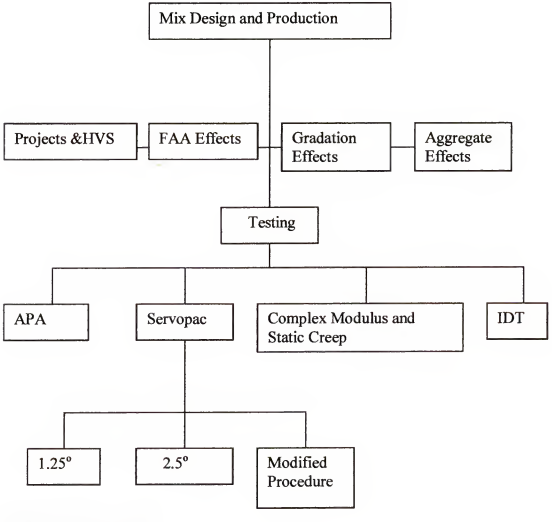

Figure 3.9 Research testing plan

3.4.1 Testing Methodology with the Servopac Gyratory Compactor

Testing with the Servopac was performed on six inch diameter samples having 4500 grams for the Whiterock limestone mixtures. The weight of the other FAA mixtures depended on the equivalent volume of the fine aggregates and their specific gravities. All mixtures were initially tested at gyratory angles of 1.25 degrees. In addition to this, the FAA mixtures were, tested at 2.5 degrees. For the AC-30 (PG 67-22) asphalt cement used, the mixing temperature was 300°F (150°C). The mixes were subjected to short-term oven aging (STOA) for approximately two hours at 275°F (135°C). The samples were stirred after one hour during aging to allow for uniform aging of all particles. They were then compacted in the Servopac to the maximum number of gyrations of 174. Two replicates of all mixtures were compacted. The gyratory shear resistance and height during compaction were recorded. The vertical pressure remained constant at 600 psi. The compaction rate was 30 revolutions per second.

3.4.2 Testing Methodology for Modified Servopac Compaction

- 4500g samples of the Whiterock limestone mixtures or equivalent weights of the FAA mixtures are batched in accordance with the gradations in section 3.2.4 and 3.2.5. The batched aggregates and asphalt binder are preheated separately to 300°F for about 3 hours after which they are mixed in a rotating mixer until all the aggregate particles are completely coated with the binder.

- The mixture is thereafter subjected to 2 hours of short-term oven aging (STOA) at 275°F in accordance to AASHTO PP2 specifications.

- The aged sample is compacted in the Servopac Gyratory compactor at an angle of 1.25° to a predetermined height/number of cycles (from the testing in section 3.4.2) which will produce air voids levels of 7.0 ± 1% within the mixture.

- Immediately after the end of the compaction to 7.0% air voids, the Servopac angle was set to 2.5° and the compaction cycle resumed for another 100 revolutions.
- The compaction heights and corresponding gyratory shear resistance were recorded for all cycles.

- Two replicate samples were tested per mixture.

3.4.3 Testing Methodology with the Asphalt Pavement Analyzer (APA)

Figure 3-10 shows the APA chamber

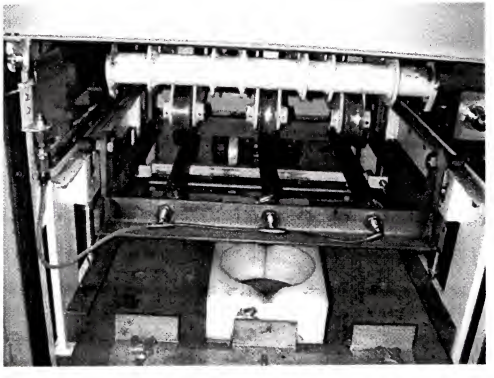

Figure 3-10 APA Chamber showing rutting wheels and pressure hoses.

Testing with the Asphalt Pavement Analyzer (APA) was performed at 60°C on cylindrical samples compacted with the Servopac Superpave Gyratory compactor as follows:

- 4500g samples of the Whiterock limestone mixtures or equivalent weights of the FAA mixtures are batched in accordance with the gradations in Section 3.2.4 and 3.2.5.

- The batched aggregates and asphalt binder are preheated separately to 300°F for about 3 hours after which they are mixed in a rotating mixer until all the aggregate particles are completely coated with the binder.

- The mixture is thereafter subjected to 2 hours of short-term oven aging (STOA) at 275°F in accordance to AASHTO PP2 specifications.

- The aged sample is compacted in the Servopac Gyratory compactor to a predetermined height which will produce air voids levels of 7.0 ± 1% within the mixture.

- The specimen is left to cool to room temperature for a minimum of 24 hours. The bulk specific gravity is then measured in accordance with AASHTO T 166 or ASTM D 2726. Using this result and the maximum theoretical density from the rice test, the air voids in the sample is determined in accordance with AASHTO T269 or ASTM F 3203 to verify if the actual air voids content is within the limits specified for the APA testing protocol.

- The specimen is trimmed to a height of 75-mm and allowed to air dry for about 48 hours.

- Two replicates of a sample are placed in the same APA mold and preheated in the APA test chamber to a temperature of 60°C (140°F) for a minimum of 6 hours but not exceeding 24 hours before the test is performed.

- The hose pressure gauge reading was set to at 100 ± 5 psi.

- The load cylinder reading for each wheel was adjusted to obtain a load of 100 ± 5lbs.

- 25 wheel strokes were applied to seat the specimen before initial measurements of rut depths were taken.

- After the initial 25 strokes, the elevations at two locations on the surface of each sample were measured using a dial gage.

- The molds containing the specimens, are securely positioned in the APA chamber, the doors are closed and the temperature of the sample allowed to stabilize in 10 minutes.

- The testing is continued for the next number of cycles and measurements taken after the APA is stopped.

- This procedure is repeated until 8000 cycles are reached.

- Rut depths are obtained by determining the average difference in specimen surface profile before and after testing. A template with seven slots that fits over the sample mold and a micrometer were used to measure the rut depth. The

equipment is stopped and rut depth measurements are taken at 0, 200, 400, 600, 800, 1000, 1500, 2000, 3000, 4000, 6000 and 8000 cycles.

- The difference between the initial measurement and that at a given cycle is Figure 3-9 shows the APA equipment.

- The rut depth is computed for each of 4 locations for a given mixture and averaged. The average rut depth at a specified cycle is reported for the particular mixture.

- After the test, the samples are removed from the molds and visually observed for shear cracks or any other development of note.

3.4.4 The Indirect Tension (IDT) Test

For comparison purposes, parameters from the Superpave IDT test are measured to observe any correlation with the APA rut depths measured and results from the Servopac Gyratory compactor. The creep compliance from this test was of particular interest in this research.

3.4.5 Methodology for IDT Testing

The methodology for the indirect tensile creep test are set up in AASHTO TP 9, the overall IDT testing protocol can be found in LTPP testing protocol P07, test methods for determining the creep compliance, resilient modulus and strength of asphalt materials using the indirect tensile strength. This protocol was followed and is described briefly below.

- All mixtures are short –term oven aged.

- Two 6-inch specimens compacted to air voids levels of 7±0.5% in the gyratory compactor were produced for each mixture type.

- A gyratory pill was cut to obtain two 2-inch thick specimens each. Three replicates for each mixture were tested in the Superpave IDT.

- Sample thickness was obtained by measuring at four different positions and averaging the results.

- Sample diameters were measures by measuring two perpendicular diameters and averaging the results.

- Four gage points were placed on each face of the cut specimen to perform the resilient modulus, creep compliance and tensile strength tests using the Superpave indirect tensile test (IDT). This was done using a special gage point placement device. The specimen was placed carefully on the gage placement device making sure that it was perfectly aligned and centered as shown in the figure. A special steel template was later used to check if all gages are properly aligned and mark the loading axis of the specimen to ensure that the specimen was perfectly aligned with the loading head. The loading head positions were marked on the vertical axis to for guidance during the testing.

- The specimen was then conditioned in a low relative humidity chamber for approximately forty-eight hours to reduce the effect of excess moisture in the test specimen.

- After removing the specimens from the humidifier, LVDT's were placed on gage points, after which they were placed in the environmental chamber of the Material Testing System (MTS).

- The resilient modulus, tensile strength and creep compliance tests were then conducted on the specimen. Only the creep compliance test was relevant to the purpose of this research and is therefore explained in the forgoing section.

- The tests were initially conducted at 10°C and followed by another series of tests at 25°C for the initial studies for FAA effects. However, the test results for the gradation effects were obtained from previous research (Nukunya, 2001) were at 10°C.

3.4.5 Creep Compliance.

In the creep test, a static load is applied to the HMA specimen, and the resulting time dependent deformation is measured. The creep compliance from this test at a higher temperature may be an indicator of the rutting potential of the mix. The compliance is calculated from this test by dividing the strain by the applied stress at a specified time in seconds. Equation 3-3 is used to calculate the creep compliance.

$$D(t) = \frac{\varepsilon_t}{\sigma} \qquad (3\text{-}3)$$

$D(t)$ = Creep compliance at the test temperature T and time of loading, t.

ε_t= Strain at time t (inch/inch), and

σ = applied stress, psi.

The creep test was run for a total 1000 seconds. The test load was chosen such that it produced a horizontal deformation of 150 – 200 micro-inches after 30 seconds of loading.

3.5 Material preparation and testing methodology for simple performance testing

This section describes the sample preparation and testing methodology for the dynamic modulus.

3.5.1 Sample Preparation for Testing

To produce cylindrical samples with a diameter of 100mm and height of 150mm, the following steps were used.

- Batchweight of 2700g of job mix formula for limestone based gradation or
- Batchweight of 2800g for granite based aggregates
- All mixtures prepared at the optimal asphalt content.
- Mixing and aging of mixtures are as previously described in chapter 3
- Compaction was done with the Servopac gyratory compactor using a100mm diameter mold.
- Air void levels in compacted samples were maintained at 7±0.5%
- The ends of the compacted samples were trimmed with a wet concrete saw to make them level.
- A total of 72 samples were prepared and tested comprising of 8 FAA mixtures 5 of the field mixtures, 2 HVS mixtures and 6 granite based mixtures all having 3 replicates.

3.5.2 Test and Sample Set Up

The complex modulus testing methodology used in this research was set up and has been fully described by Swan (2002) at the University of Florida infrastructural materials laboratory. The summary of the set up is as follows:

- MTS 810 load frame was used.

- Servo hydraulic controller attached.
- Applied stress measured and controlled using a 100kN (22kips) load cell.
- Samples were put in thin membrane to prevent water ingress.
- High viscosity vacuum grease and rubber membrane used between end platens to reduce end constraint effects.
- Two axial LVDT's mounted on clamps with an initial spacing of 50mm used.
- Clamp is mounted within the middle one third of the specimen.
- Data acquisition was performed using a Labview software.
- Axial deformations were recorded on two hermetically sealed LVDTs with a range of up to 5.0mm. These sensors have a maximum resolution of 0.076μm.
- After mounting the sample with the LVDTs on the MTS loading plate, a triaxial chamber was mounted on the sample to hold the heating fluid (water).
- Units were set up for the heating or cooling of the sample by circulating warm or chilled water respectively around the sample.
- The mounted sample was checked for no eccentricity by testing at room temperature to ensure that the two LVDTs give close strain values.
- Circulate chilled water at very low pressure and 10°C (about 5psi) for 1 hour to ensure that sample temperature is at equilibrium temperature of 10°C. Sample is ready for testing at this temperature.
- After the low temperature testing, drain the chilled water and fill sample with fresh water. Warm water at 40°C was circulated through the triaxial chamber at no pressure for 1 hour. Sample is ready for testing at this temperature.

Figure 3-11 shows the set up sample with the LVDT's and membrane in place while Figure 3-12 shows the MTS 810 frame with the test chamber in place.

A chilling unit was connected to the MTS system to control overheating of the system's pump. In this way continuous testing without interruption of pump shut down is

assured. Generally, the procedure takes approximately 4 hours from sample set up to test completion.

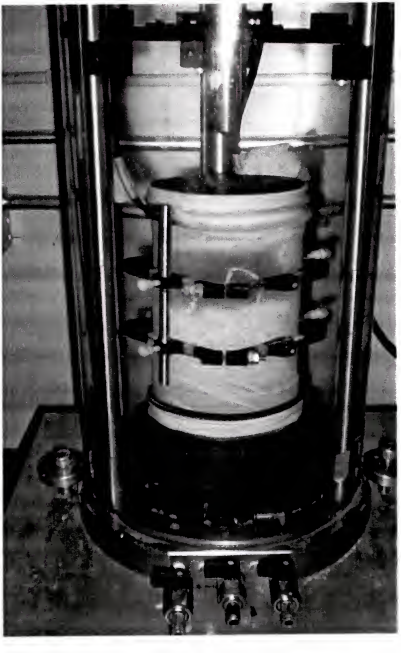

Figure 3-11. Dynamic test sample set up showing clamp, LVDT and membrane

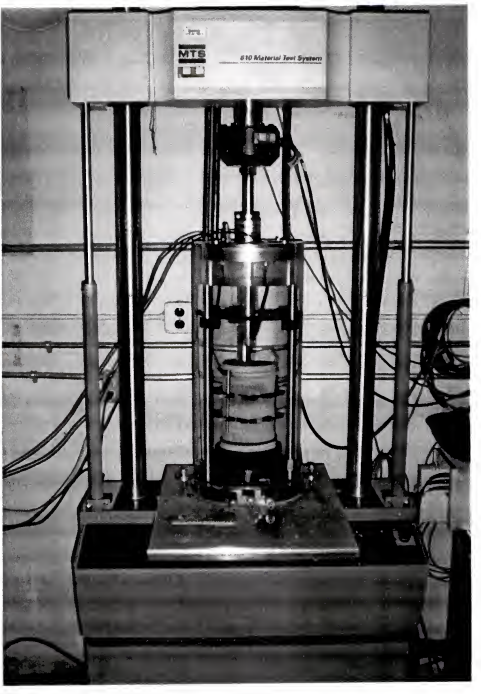

Figure 3-12. MTS 810 loading frame with the test chamber in place.

3.5.3 Testing Methodology

For testing at the low temperature of 10°C, the following procedure was used.

- A seating load of 220N (50lbs). was initially applied to the sample.
- A sinusoidal load of 4000N to 5000N (900 to 1125lbs.) applied to the sample at 10°C. These loads have been found to produce strain measurements between 50 and 250microstrains to ensure that the samples are not damaged.
- Loading was maintained for 50 cycles.
- Testing was repeated for loading frequencies of 16Hz., 10Hz, 4Hz., and 1Hz.
- After the dynamic testing, wait for 10 minutes to allow recoverable strains to be recovered.
- Apply a static or ramp load of between 1800 to 2200N (400-500lb) for a period of 1000 seconds for the static creep test. This load range produces a strain at 100cycles less than 1200 microstrains to prevent micro damage.

For testing at the low temperature of 40°C, the following procedure was used.

- A seating load of 45N (10lbs). was initially applied to the sample.
- A sinusoidal load of 1000N to 2000N (225 to 450lbs.) applied to the sample at 40°C. These loads have been found to produce strain measurements between 50 and 250microstrains to ensure that the samples are not damaged.
- Loading was maintained for 50 cycles.
- Testing was repeated for loading frequencies of 16Hz., 10Hz, 4Hz., and 1Hz.
- After the dynamic testing, wait for 20 minutes to allow recoverable strains to be recovered.

Apply a static or ramp load of between 220 to 550N (50-120lb) for a period of 1000 seconds for the static creep test (Texas DOT test procedure Tex-231-F).

3.5.4 Analysis of Test Data

A simple visual basic program developed at the University of Florida (Swan, 2002), was used to analyze the data from the complex modulus testing to obtain the dynamic modulus and phase angle.

Dynamic creep parameters were also computed.

Analysis of the static creep results was done by spreadsheet regression to fit a power law to obtain the creep parameters of D(t), Do, D_1, and m-values, as discussed in Chapter 7. .

CHAPTER 4
EVALUATION OF EXISTING ANALYSIS PROCEDURES OF GYRATORY COMPACTION PARAMETRS

The literature review presented in Chapter 2 provided a review of various proposed methods of analysis of gyratory compaction measurements from Superpave compatible gyratory compactors for the determination of mixture rutting performance. The most promising methods of analysis are the compaction slope (k), the terminal densification energy index (TDI), and the number of gyrations to the maximum stress ratio (N-SRmax). In this Chapter, the test results from the Servopac Gyratory Compactor are analyzed using these analysis methods. In addition, the product of the compaction slope and air voids at the design number of gyrations (Anderson, 2001) was evaluated. Table 4-1 shows a summary of these methods.

Table 4-1. Existing methods of analysis of SGC parameters

SGC Parameter	Description	Symbol	Reference
Compaction Slope	Slope of regression line of semi-logarithmic plot of percent Gmm versus number of cycles. (From 10 gyrations to 96%Gmm)	k	Anderson et al (1997); Corté and Serfass (2000)
Interaction of slope and air voids	The product of the compaction slope and the air voids(%) at the design number of gyrations	kxAV	Anderson (2002)
Densification Energy Index	The area under the compaction curve (Gmm vs. cycles) from 92%Gmm to 96%gmm.	$DEI_{92\text{-}96}$	Bahia (1998)
Number of Gyrations to maximum stress ration	Number of gyrations to maximum stress ratio obtained by fitting a quadratic equation to the compaction curve (stress ratio vs. cycles) and solving for N.	N-SRmax	Anderson (2002)

Analysis of the compaction parameters above was performed on the mixtures described in Chapter 3 to observe any relationship with rutting performance. Rutting performance in this study was based on test results performed on the samples using the Asphalt Pavement Analyzer (APA) rut depth measurement.

4.1 Analysis of Compaction Slope (k)

Figure 4-1 shows the plot of the compaction slope for all the mixtures tested.

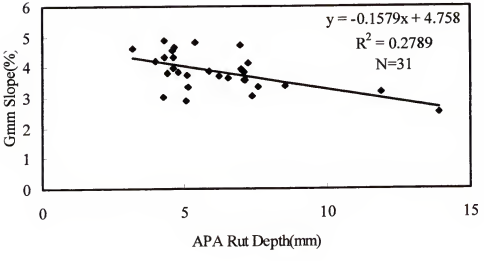

Figure 4-1 Compaction slope for all mixtures.

Generally, the plot shows a trend of the slope with the rut depth measurement from the APA as observed by other researchers (Corté et al (2000), Anderson (2002)). Mixtures with high slope values tend to have good rutting performance while a low slope is likely to be associated with mixtures with poor rutting performance. The correlation of the slope with the APA rut depths is, however, weak ($R^2 = 0.279$). In view of this weak correlation, the mixtures were further analyzed in groups of various categories, which are known to affect performance. These categories are: 1) whether mix is fine or coarse

graded and 2) design traffic level. Since almost all the mixtures were of 12.5-mm nominal aggregate size, analysis based on maximum nominal aggregate size was not performed.

4.1.1 Fine Graded Mixtures

Figure 4-2 shows the plot of the compaction slope versus the APA rut depths for all the fine graded mixtures.

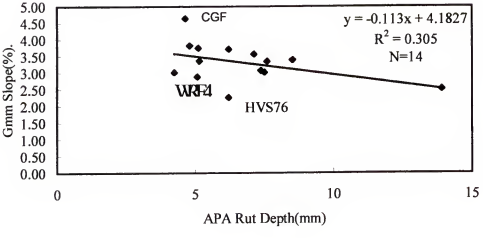

Figure 4-2 Compaction slope for the all the fine graded mixtures.

Figure 4-2 shows a slight improvement in the correlation (R^2 =0.305). Further observation of Figure 4-2 show CGF st of the outliers are mixtures with low VFA, low VMA or high dust to asphalt ratio (Mixtures which did not satisfy the Superpave volumetric criteria in one way or the other). On removing these substandard WRF4 mixtures (CGF and WRF2 and WRF4) a HVS76-22 mixture, which was the only mix with a different asphalt binder type, there was an improvement in the correlation (R2=0.4734) as shown in Figure 4-3.

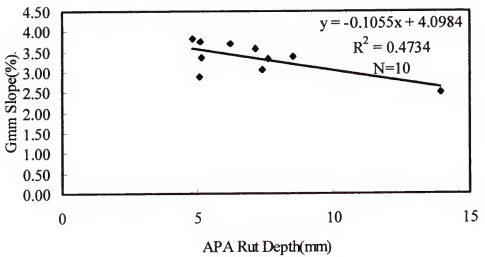

Figure 4-3 Slope of fine graded mixtures without substandard and HVS76-22 mixtures.

4.1.2 Coarse Graded Mixtures

Figure 4-4 shows a plot of the slope for all the coarse graded mixtures, while Figure 4-5 shows the coarse graded mixtures without the CGC mixture mixture, which is showed cracks in the APA. There was, however, only a slight improvement in correlation, R^2 increased from 0.2664 to 0.4068. Generally, the trend in the relationship is such that mixtures with high slope have low rutting in the APA, while mixtures with low slope values have high rutting in the APA. The low, R^2 values however, does not make this factor ideal for mixture rutting evaluation. This calls for the need for the evaluation of the shear resistance measurements with the equipment. The CGC mixture was an outlier probably because the cracks developed during the APA testing might have influenced the overall rut depth measured.

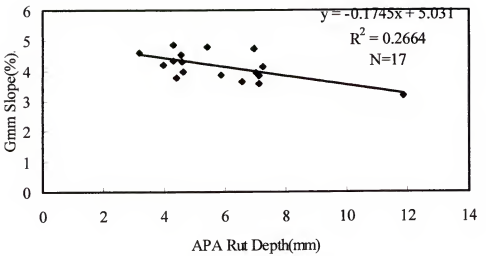

Figure 4-4 Slope of all coarse graded mixtures

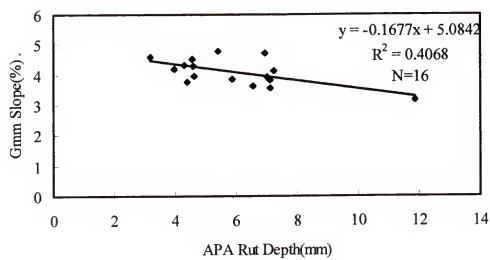

Figure 4-5 Slope of all coarse graded mixtures without the CGC mixture.

4.1.3 Analysis Based on Different Traffic Levels

At the onset of this research, the Superpave traffic level used (< 30 million ESALS), which was the prevalent level used in Florida, was such that the Ndesign value was 109 gyrations. The field mixtures tested at the latter stages of this work however, were designed with an Ndesign value of 96 gyrations (These are P1, P2, P3, P5, and P8). The exception is field project number 7, which has an Ndesign value of 84. It will therefore be ideal to separate the mixtures based on their level of traffic to ensure that the comparison is based on equal design parameters. Figures 4-6 to 4-8 show the plot based on traffic levels. These plots do not include the substandard mixtures WRF2, WRF4, WRF5, CGF, CGC and the HVS 76-22 mixtures. The substandard mixtures are mixtures on which cracks were observed after the APA test.

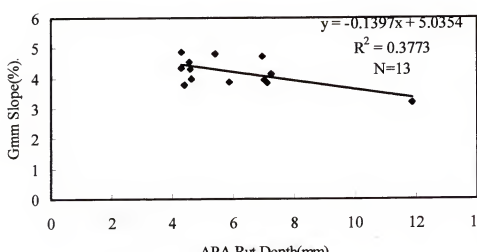

Figure 4-6 Compaction slope for coarse mixtures designed with Ndesign=109

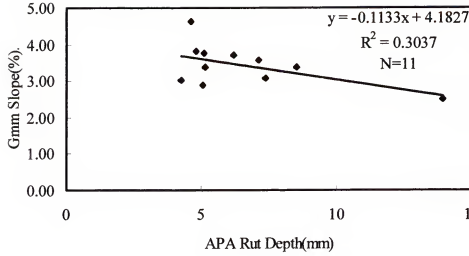

Figure 4-7 Compaction slope for fine mixtures designed with Ndesign=109

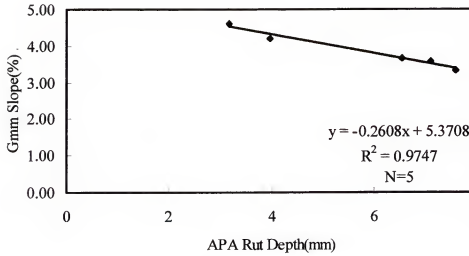

Figure 4-8 Compaction slope for field mixtures designed with Ndesign=96

The plots based on design traffic level show an improvement in the correlation with the APA rut depths measured for all categories of mixtures.

Generally, the slope showed some trend with the rutting performance of both fine and coarse graded mixtures. However, the correlation was weak. Also the analysis shows that substandard mixtures may show up as outliers in the slope plot.

Comparison of mixtures based on the slope of the compaction curve should be made on mixtures of similar nature with regards to position of the gradation curve and traffic level used for design

4.1.4 Interaction of Slope and Air Voids (kxAV)

Figures 4-9 to 4-11 show plots of the interaction of compaction slope versus APA rut depths.

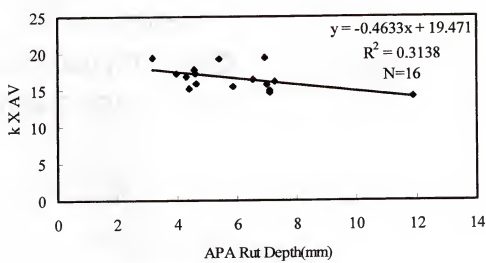

Figure 4-9 kxAv for all coarse graded mixtures designed with Ndesign=109.

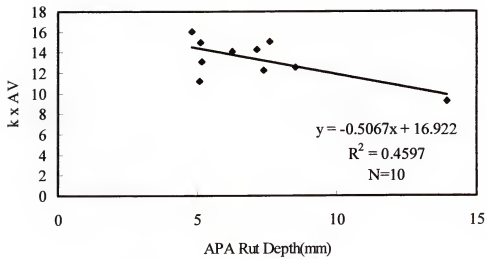

Figure 4-10 kxAv for fine mixtures designed with Ndesign=109 (Without substandard mixtures).

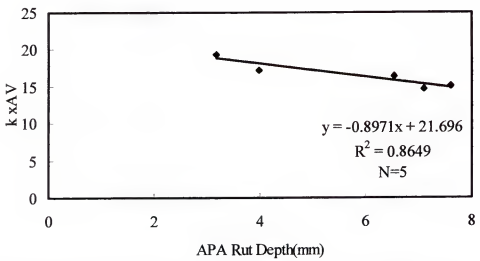

Figure 4-11 k xAv for field project mixtures designed with Ndesign=96.

This parameter is the product of the slope (k) as defined in Table 4-1 and the air voids (%) at Ndesign.

Comparison of Figures 4-6 to 4-8 for the analysis based on compaction slope on one hand and Figures 4-9 to 4-11 for the analysis based on compaction slope interaction with air voids, show little difference in correlation for the two analysis methods. There was no improvement for the analysis for coarse graded mixtures- both the laboratory and field mixtures. There was a slight reduction of the R^2 when the interaction of the slope with air voids was used in comparing the mixtures. In the case of the fine graded mixtures however, the R^2 increased slightly.

This analysis indicates that there is no advantage in using the interaction of slope and air voids in analyzing the mixtures in this work over the use of the slope alone for mixture performance when mixtures are designed at the same level of traffic and gradation position. There may however be a difference in the analysis of mixture sensitivity to asphalt content as changes in asphalt content at a constant level of traffic will be reflected in changes in air voids at the design number of gyrations.

4.2 Analysis of Densification Energy Index (DEI_{92-96})

All mixtures in this work were compacted to Superpave Nmax, which is the number of gyrations required to produce a density in the laboratory that should absolutely never be exceeded in the field. The air voids at this point are required to be at least 2%. Based on this procedure, almost all the mixtures tested in this work never reached an air void level of 2%. The use of the Terminal Densification Energy (TDI_{92-98}) parameter for the evaluation of these mixtures therefore was not possible. The densification energy index (DEI_{92-96}) was however calculated for all the mixtures and used to evaluate these

mixtures. $DEI_{92\text{-}96}$ is the area under the compaction curve (%Gmm versus cycles) from the 8th cycle to the cycle when the mixture attains an air void level of 4%.

4.2.1 Analysis of all Mixtures

Figure 4-12 through 4-14 show the plot of the $DEI_{92\text{-}96}$ for all the mixtures evaluated.

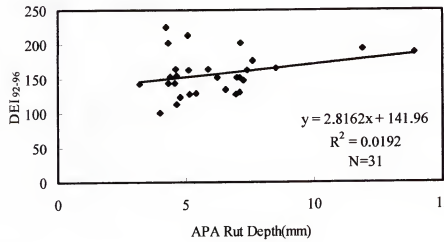

Figure 4-12 Densification energy index versus APA rut depth for all mixtures.

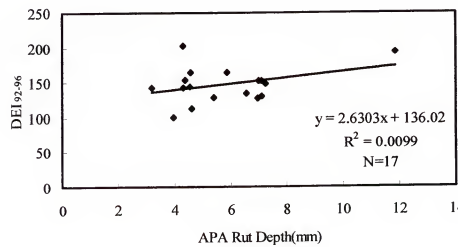

Figure 4-13 Densification energy index versus APA rut depth for coarse graded mixtures.

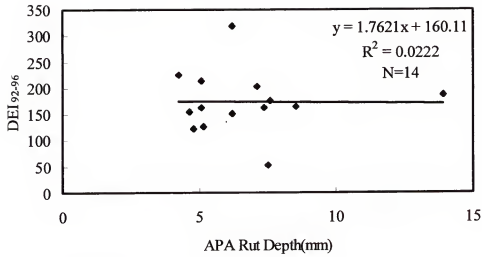

Figure 4-14 Densification energy index for all fine graded mixtures.

The above figures show no correlation of the densification energy index with rutting performance as measured with the APA, even when the mixtures are categorized into fine- and coarse- gradations. Similar observations were made when the plots were made based on traffic levels and even the removal of substandard mixtures did not appreciably improve the correlation with rutting performance as measured with the APA.

The densification energy index parameter was therefore considered to be not beneficial for the evaluation of the mixtures tested in this work.

4.3 Evaluation of Number of Gyrations to Maximum Stress Ratio (N-SRmax)

Figures 4-16 to 4-18 show plots of the number of gyrations to the maximum stress ratio versus the APA rut depth for all the mixtures, coarse graded mixtures and fine graded mixtures respectively. This parameter is the cycles to the maximum ratio of the normal stress to the gyratory shear.

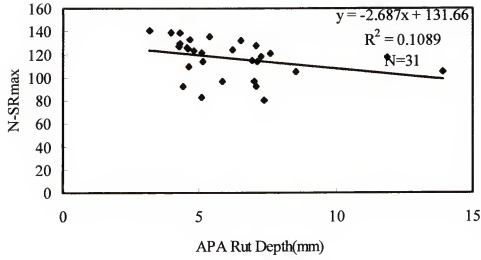

Figure 4.15. Cycles to maximum stress ratio for all mixtures.

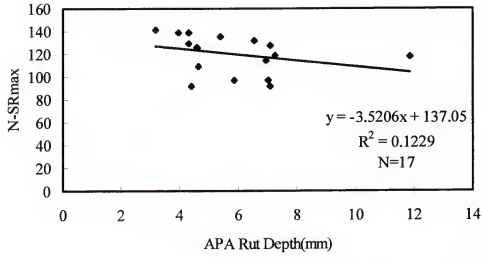

Figure 4-16. Cycles to maximum stress ratio for all coarse graded mixtures.

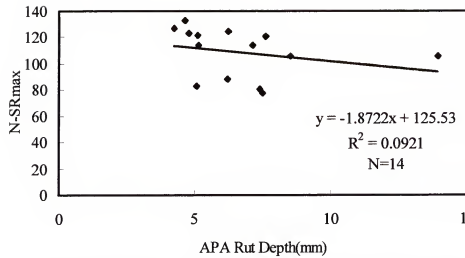

Figure 4-17. Cycles to maximum stress ratio for all fine graded mixtures.

Figures 4-15 to 4-17 show little correlation with rutting performance as measured with the APA. However, all the plots show a trend in the relationship. Mixtures with high N-SRmax values are likely to have good rutting performance while mixtures with low N-SRmax values tend to have relatively poorer performance. In view of this general trend, plots were made without substandard mixtures and into traffic categories as for the evaluation of the compaction slope in section 4.1. The removal of substandard mixtures however did not improve the correlation as shown in Figures 4-18 and 4-19 for coarse- and fine-graded mixtures respectively. In general, compaction in the SGC is such that drier mixtures have higher number of gyrations irrespective of whether they are good performers or not. A mixture with high effective asphalt content, will likewise have a low number of gyrations to the maximum gyratory shear. However, the plots indicates that relating this parameter alone to mixture rutting performance based on the categories evaluated so far is questionable.

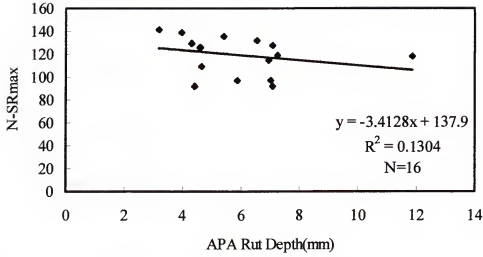

Figure 4-18. Cycles to maximum stress ratio for coarse graded mixtures, without CGC.

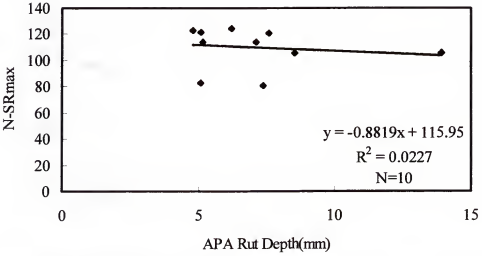

Figure 4-19. Cycles to maximum stress ratio fine graded mixtures, without substandard mixtures and HVS76-222

4.3.1 Analysis Based on Grouping of Mixtures by Aggregate Type

In view of the poor correlation of the N-SRmax parameter with rutting performance based on rut depth measurements with the APA, further grouping of the mixtures with respect to aggregate type was performed. Figure 4-20 shows the plot of the N-SRmax parameter with mixtures grouped by aggregate type (Granite or Limestone in this work). The plot shows a better correlation for the limestone-based mixtures (R^2=0.4435).

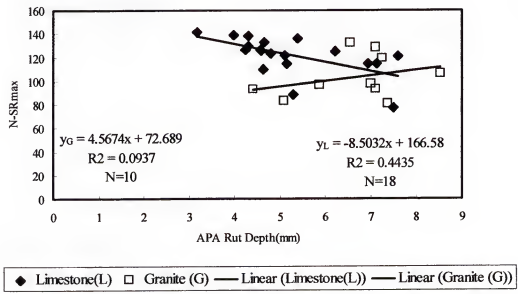

Figure 4-20. Cycles to maximum stress ratio for granite and limestone mixtures.

There is however no correlation between the N-SRmax parameter and rut depth measurements from the APA for the granite based mixtures R2=0.0937). The granite mixtures also showed the wrong trend. It is worth mentioning that the original work on the N-SRmax parameter (Anderson, 2002 and Anderson et al, 2002) was performed on

gravel and limestone-based mixtures. The analysis method has not yet been applied for other aggregate types.

Based on the analysis of the above parameters, the slope of the compaction curve appears to be a better parameter for the evaluation of the mixtures in this research. The slope has however been observed to be insensitive to asphalt content (Anderson et al, 2002).

In view of the shortcomings of the various methods reviewed, there is a need for a better understanding of the measurements from this equipment, as well as further development of an analysis method that can be used to address the shortcomings of the existing analysis methods.

CHAPTER 5
EVALUATION OF GYRATORY SHEAR RESISTANCE

5.1 Introduction

The first part of this study focused on a detailed study of the relationship between gyratory shear strength and the number of gyrations in the Superpave gyratory compactor. A close look at the typical compaction plots as shown in Figures 5-1 and 5.2 show that the curve can be divided into four distinctive regions or segments, namely: 1) the region up to the initial break point, 2) volumetric compaction region, 3) the shear driven densification region, and 4) the post-peak part of the curve. In the following, these different regions will be evaluated with respect to determining possible relationships between mixture rutting performance and engineering parameters obtained from these different regions.

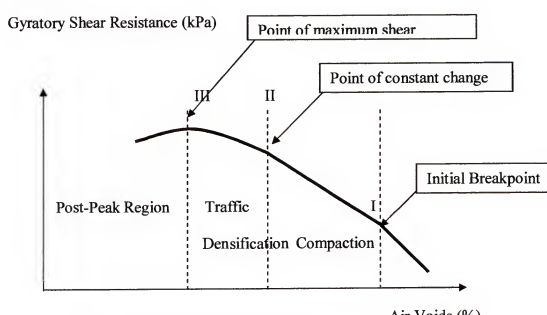

Figure 5-1 Gyratory shear versus air voids

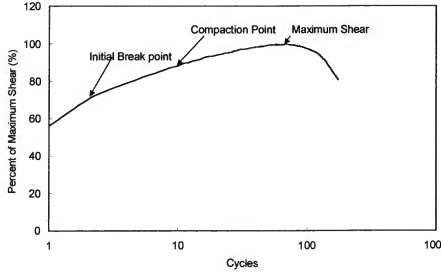

Figure 5-2: Compaction curve for WRF

5.1.1 Initial Break

The very first part of the curve up to the point of initial break (labeled I in figure 5-1) is normally reached within 2 or 3 cycles of compaction. It is the point at which the aggregates have moved close enough together for gyratory compaction to take place.

5.1.2 Volumetric Compaction

In the volumetric compaction region, shown between points I and II in Figure 5-1, the dominant compaction process can be described by controlled shearing causing the aggregates to move volumetrically into a denser, lower air voids structure by aggregate re-orientation. Hence, in this region of the compaction curve, a relationship should exist between the change in gyratory shear strength and the change in air voids.

Figures 5-3 and 5-4 show typical plots of the relationship between the rate of change of air voids, d(AV) and the rate of change of gyratory shear strength $d(G_s)$, for the part of the compaction curve from the point of initial break, for a fine-graded and coarse-

graded mixture respectively. From these figures, a linear relationship appears to exist between the rate of change of air voids and the rate of change of gyratory shear strength for both fine and coarse graded mixtures. However, as the peak gyratory shear strength is approached, this relationship ceases to be linear.

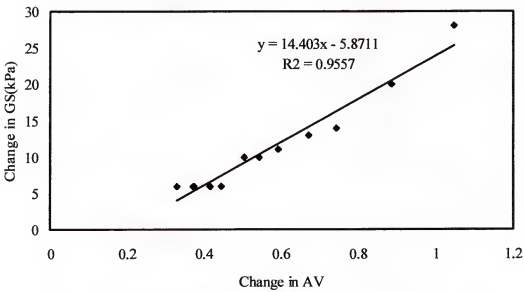

Figure 5-3. Rate of change of shear stress versus rate of change of air voids (CGC)

At the point where the linearity in the curve appears to end (labeled as point II in Figure 5-1), the rate of change of gyratory shear strength becomes constant and thereafter begins to fluctuate. The percent air voids still keeps decreasing beyond that point, indicating that the process of compaction has changed from being primarily volumetric compaction in which the coated particles are pushed together into a closer arrangement to shear driven densification. Once the aggregate particles have reached a tight enough packing, shear driven densification will be the primary mode of compaction, causing

aggregate particles to roll and slide over each other, gradually squeezing the mastic outward and the aggregates into a tighter structure, resulting in lower air voids.

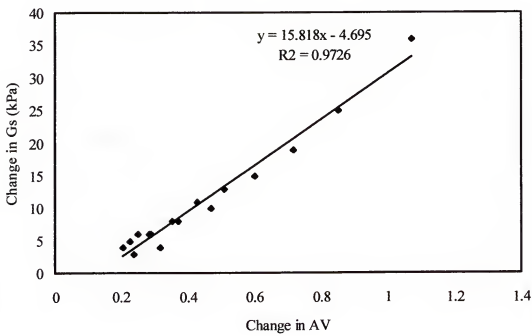

Figure 5-4. Rate of change of shear stress versus rate of change of air void (CGC).

5.2 Evaluation of the Volumetric Compaction Zone

Mixture compaction and related aggregate packing is affected by the frictional characteristics of the aggregates. Therefore, mixtures containing fine aggregates of different angularities and surface texture, but the same limestone (whiterock) coarse-graded aggregate structure were used to evaluate the compaction behavior in the volumetric compaction zone. Refer to Figure 3-1 for the base whiterock coarse and fine gradations and Tables 3-1 and 3-2 for the coarse and fine gradations with the different aggregates respectively. Ten mixtures, comprising of five fine graded mixtures and five coarse graded mixtures were evaluated. The rate of change of the gyratory shear strength with change in air voids was evaluated as a parameter for assessing the resistance of the

mixtures to compaction. Figures 5-5 and 5-6 show plots of the change in gyratory shear strength versus change in air voids for the coarse- and fine- graded mixtures respectively.

To evaluate the compaction slope as a tool to differentiate between the mixtures, Figures 5-7 to 5-9, for the fine mixtures, were plotted to study any relationship between the slope with the fine aggregate angularity of the fine portion (passing #4 sieve) of the aggregate used, which is a qualitative measure of the frictional resistance of the mixtures. The plots were made from the point of initial break to the first point when the change in gyratory shear begins to fluctuate.

Figure 5-9 shows no definite relationship in the trend of FAA with the slope as depicted by the low R^2 value of 0.0516. However Figure 5-8 shows that the Chattahoochee mixture did not fall in line with the trend observed for the other four mixtures. The Chattahoochee mixture contains river gravel, which is uncrushed. This might be a factor in the higher than expected slope. The findings of Brown et al.,(2001) confirms the behavior of the gravel mixtures, they found that gravel mixtures had high Marshall stability, low permanent strain in both unconfined and repeated creep, yet they developed high rut depths with APA measurements. Comparing the behavior of the gravel mixture and the other mixtures on the same basis may therefore be erroneous. The R^2 value improved substantially to 0.7568 when this mixture is removed from the plot as shown in Figure 5-9. The same trends were observed for coarse graded mixtures as shown in Figures 5-10 to 5-12. Figure 5-13 shows the plot for all the FAA mixtures without the Chattahooche mixtures

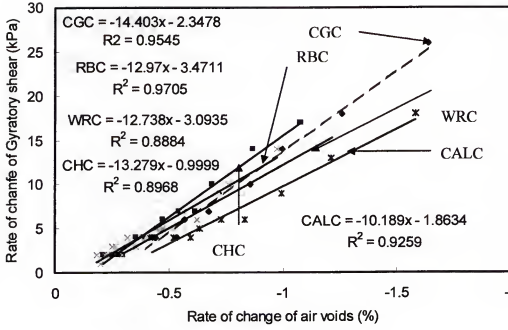

Figure 5-5. Regression for coarse mixtures.

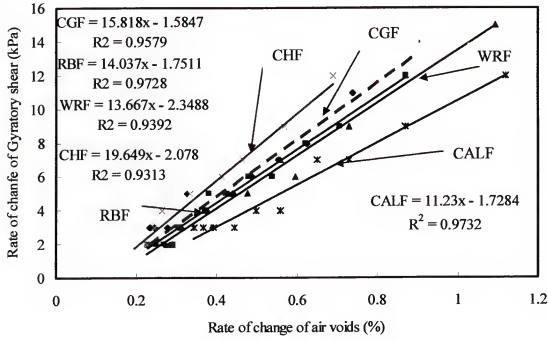

Figure 5-6. Regression for fine graded mixtures

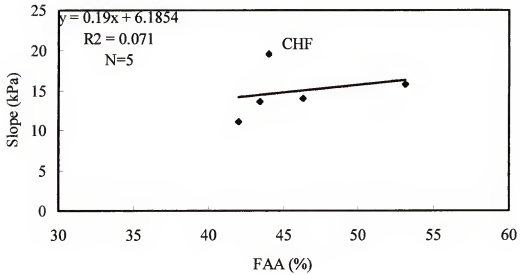

Figure 5-7 Slope in volumetric compaction zone versus FAA for the fine mixtures.

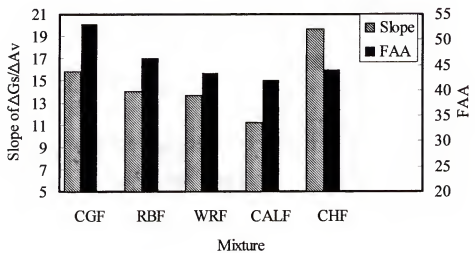

Figure 5-8 Slopes in volumetric compaction zone versus FAA-the fine mixtures.

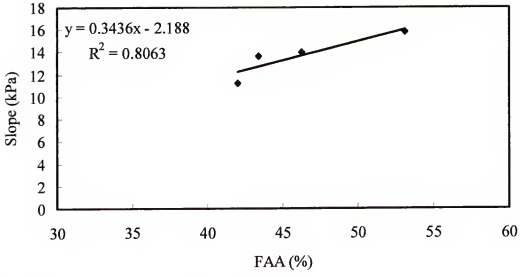

Figure 5-9 Slopes versus FAA for fine-graded mixtures without the CHF.

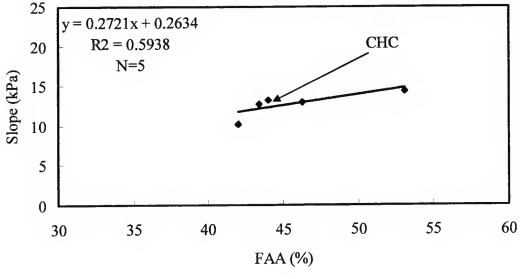

Figure 5-10. Slopes in volumetric compaction zone versus FAA -coarse mixtures.

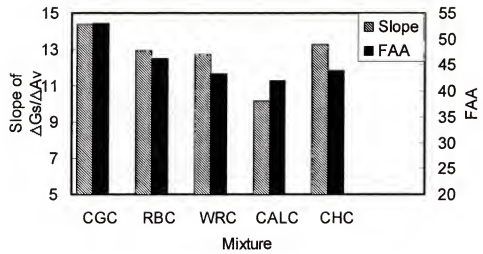

Figure 5-11 Slopes in volumetric compaction zone versus FAA -coarse mixtures.

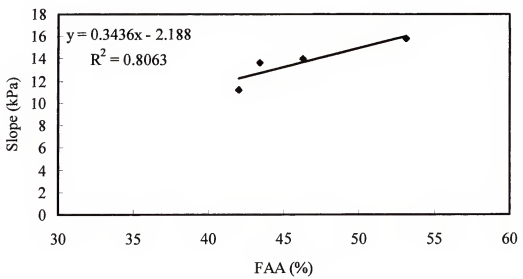

Figure 5-12 Slopes versus FAA for coarse mixtures without CHC.

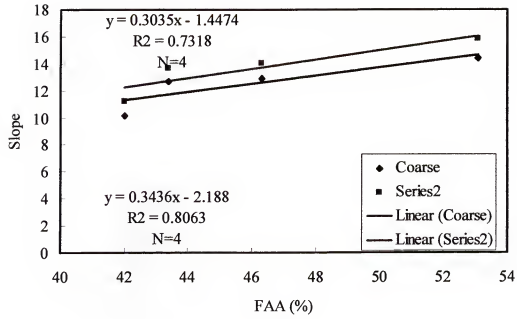

Figure 5-13. Slopes for all the FAA mixtures without the Chattahoochee mixtures

From this limited testing, it can be concluded that the slope of the change in gyratory shear versus the corresponding change in air voids may be related to aggregate properties that affect the compaction and packing of mixtures, such as the FAA. The influence of the FAA on mixture resistance to compaction, has been observed by researchers (Stakston (2002) and Brown and Cross (1992)). The general observation is that at high air voids, the FAA and other aggregate surface properties influence the compaction of HMA mixtures.

Tables 5-1 and 5-2 show the number of cycles, percent air voids and percent of maximum shear for fine- and coarse-graded mixtures at which point the rate of change in gyratory shear strength becomes constant.

Table 5-1. Percent Air Voids and Corresponding Percent Gs at Point of Constant Change in Gs for Fine-graded Mixtures

Aggregate Blend	Number of Cycles	Percent Air Voids at point of Constant Change in Gs	Percent Gs At Point of Constant Change in Gs
Whiterock Coarse + Cabbage Grove Fine (CGF)	30	8.66	93.3
Whiterock Coarse + Ruby Fine (RBF)	20	8.13	97.24
Whiterock Aggregate (WRF)	18	10.24	92.96
Whiterock Coarse + Calera Fine (CALF)	10	12.93	91.37
Whiterock Coarse + Chattahooche Fine (CHF)	9	9.35	91.51
Average	17.4	9.86	93.28

Table 5-2. Percent Air Voids and Corresponding Percent Gs at Point of Constant Change in Gs for Coarse-graded Mixtures

Aggregate Blend	Number of Cycles	Percent Air Voids at point of Constant Change in Gs	Percent Gs At Point of Constant Change in Gs
Whiterock Coarse + Cabbage Grove Fine (CGC)	24	11.6	89.4
Whiterock Coarse + Ruby Fine (RBC)	14	12.55	89.97
Whiterock Aggregate (WRC)	14	13.8	86.25
Whiterock Coarse + Calera Fine (CALC)	13	14.22	88.57
Whiterock Coarse + Chattahooche Fine (CHC)	11	11.75	91.05
Average	15.2	12.78	89.05

The fine-graded mixtures peak out at air voids between 8 and 13 percent. In comparison, the coarse graded mixtures peak out anywhere from about 11 to 14 percent. The slope of the plot of change in shear resistance to change in air voids in this range may be an indicator of the resistance of the mixture to compaction.

Tables 5-3 and 5-4 show the number of cycles, percent air voids and percent of maximum gyratory shear at the point where linearity in the plot ceases for the granite and limestone mixes respectively. The tables also show the slopes of the plot of change in gyratory shear versus change in air voids. Generally, the fine graded mixtures have higher slopes than the coarse graded mixtures. The number of cycles to end of linear relationship appear are similar for both coarse and fine mixtures. Fine graded mixtures have lower air voids at the end of compaction, with a higher gain in shear strength

relative to the maximum shear. The granite mixtures attain a higher percentage of the shear strength than the limestone mixtures at the end of compaction.

Table 5-3. Percent Air Voids and Corresponding Percent Gs at Point of Constant Change in Gs for Granite Mixtures

Aggregate Blend	Number of Cycles	Percent Air Voids at point of Constant Change in Gs	Percent Gs At Point of Constant Change in Gs	Slope of ΔGs Vs. ΔAV
GAC1	15	11.9	87.6	28.6
GAC2	15	11.8	93.4	34.2
GAC3	15	11.5	94.9	32.6
Average	15	11.7	91.7	32.8
GAF1	14	10.5	95.2	35.0
GAF2	17	9.2	93.8	37.0
GAF3	14	11.9	93.4	32.5
Average	15	10.5	94.13	34.83

Table 5-4. Percent Air Voids and Corresponding Percent Gs at Point of Constant Change in Gs for Coarse Limestone Mixtures

Aggregate Blend	Number of Cycles	Percent Air Voids at point of Constant Change in Gs	Percent Gs At Point of Constant Change in Gs	Slope of ΔGs Vs. ΔAV
WRC2	15	13.4	84.5	31.2
WRC3	13	14.1	84.2	32.4
WRC4	18	12.7	87.6	32.0
WRC5	16	11.1	90.2	37.6
Average	15.5	12.8	86.6	33.3
WRF2	15	10.4	87.8	37.3
WRF4	16	10.9	88.7	36.7
WRF5	15	11.4	88.9	40.1
WRF6	16	10.3	88.8	33.3
Average	15.5	10.75	88.55	36.85

5.3 Zone of Shear Driven Densification

Past the point of linearity in the compaction curve, shear driven densification will be the primary mode of compaction, causing aggregate particles to roll and slide over each other, gradually squeezing the mastic outward and the aggregates into a tighter structure, resulting in lower air voids. As the mastic is squeezed outward, the compaction curve starts to become increasingly nonlinear, due to the decrease in mastic lubrication effect between aggregates.

5.3.1 Evaluation of the Shear Driven Densification Zone

Table 5-5 shows the maximum shear resistance, corresponding cycles and maximum theoretical density for the fine- and coarse- graded mixtures respectively. The average air void contents for the fine graded mixtures is 4.65% whilst that for the coarse graded mixtures is 4.33%. These air void contents are typical of traffic densified pavements in the field. Further densification far beyond these points is likely to result in aggregate crushing and shear failure.

5.3.2 Simple Index Parameters for Permanent Deformation

Roberts et al (1996) observed that dense graded HMA pavements become highly permeable to water at approximately 8% air voids. Mixtures will be relatively impermeable as long as the air voids contents remain below 8%. Also, rapid oxidation which leads to cracking and raveling will be avoided. With this in mind, most construction specifications require that dense HMA mixtures be compacted to 7% air voids levels before opening to traffic. Generally, further densification of the HMA by traffic within a few years after paving is required to compact the mixture to an air void level of about 4%.

Table 5-5. Gyratory shear stress, number of cycles and Gmb. at maximum shear stress

AGGREGATE BLEND	1.25 Degrees			2.5 Degrees		
	N	Gmb	Gs(kPa)	N	Gmb	Gs(kPa)
COARSE AGGREGATE BLEND						
Whiterock Coarse +Cabbage Grove Fine (Coarse Blend)	134	2290	498	49	2301	557
Whiterock Coarse + Calera Fine (Coarse Blend)	142	2374	525	45	2382	541
Whiterock Aggregate (Coarse Blend)	117	2271	476	42	2233	515
Whiterock Coarse + Chattahooche Fine (Coarse Blend)	100	2284	447	27	2334	537
Whiterock Coarse + Ruby Fine (Coarse Blend)	131	2310	459	106	2310	485
FINE AGGREGATE BLENDS						
Whiterock Coarse + Calera Fine (Fine Blend)	70	2392	533	60	2403	565
Whiterock Aggregate (Fine Blend)	97	2226	483	48	2274	535
Whiterock Coarse + Cabbage Grove Fine (Fine Blend)	93	2284	498	63	2305	568
Whiterock Coarse + Ruby Fine (Fine Blend)	66	2289	472	40	2352.	521
Whiterock Coarse + Chattahooche Fine (Fine Blend)	57	2303	483	131	2370	550

The HMA material should be able to accommodate the traffic without shearing or any other type of failure. In this section, an attempt is made to develop a simple parameter that relates to the resistance of the HMA mixture to traffic densification within the air void levels in the range between 7 and 4 percent.

In Section 5.2, it was observed that beyond the compaction point the relationship between the gyratory shear and air voids is nonlinear. It was also observed in Chapter 4 that the slope (k) (Corte and Serfass, 2000) of the compaction curve in terms of density or percent of maximum theoretical density was the best parameter for evaluating the rutting resistance of the mixtures tested. However, not much work has been done in evaluating the slope of the gyratory shear strength versus number of revolutions from Superpave compatible gyratory compactors. In this study, it is assumed that this slope of the shear strength is a measure of the resistance of a mixture to densification in the shear driven densification zone. A mixture with a high density slope may have a high corresponding shear slope if the density of the mixture is actually related to its shear strength. Also, use of the gyratory shear resistance minimizes potential problems associated with using the slope of the density curve versus number of gyratory revolutions in mixtures that contain too much asphalt. In these mixtures, the change in density may occur very slowly, implying a high resistance to compaction. In contrast, the gyratory shear strength for these mixtures will drop once the mixture has been compacted to a low enough air voids level. Figure 5-14, the plot of the gyratory shear and the density for the RBF mixture at an asphalt content, 0.5% higher than the optimum asphalt content illustrates this.

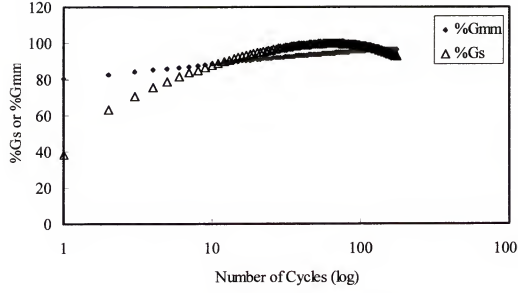

Figure 5-14. Variation of density and gyratory shear with cycles.

Initially, the gyratory shear strength versus the logarithm of the number of gyratory revolutions was studied at air void levels ranging either: a) 7 percent to 4 percent if the maximum gyratory shear strength was not reached at 4 percent air voids, or b) from 7 percent air voids to the air voids at maximum gyratory shear strength. Figures 5-15 and 5-16 show a series of regression results for the ranges of air voids studied for the FAA mixtures.

The results from the regression analyses on the semi-log plots of the gyratory shear resistance versus the number of cycles in the traffic densification zone of the compaction plots provided the best fit relationship in the form:

$$Gs = k_1 \ln(N) + k_2 \quad (5\text{-}1)$$

Where Gs = Gyratory shear resistance, N = Number of gyratory revolutions, and k_1 and k_2 are the slope and intercept of the regression lines respectively.

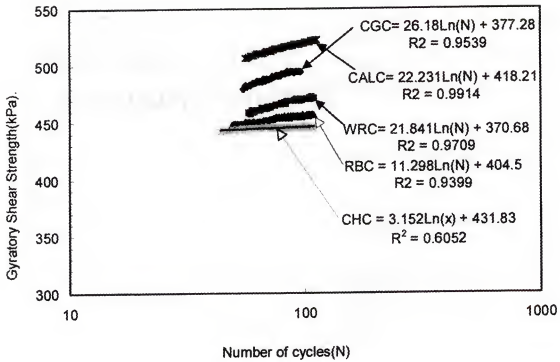

Figure 5-15. Slopes of gyratory shear strength versus cycles for coarse FAA mixtures.

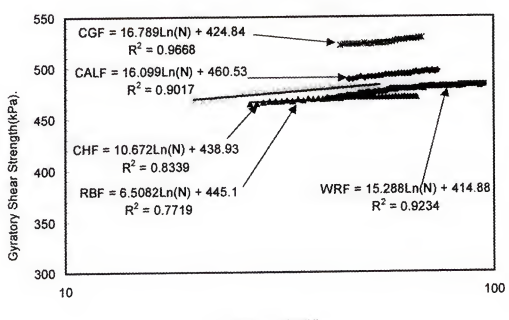

Figure 5-16. Slopes of gyratory shear strength versus cycles for fine FAA mixtures.

5.3.3 Comparison of Index to other Known Measures of Pavement Rutting

Rut depth measurements on the ten FAA mixtures with the APA were obtained (Kesory, 2000) for the purpose of comparison and to obtain an understanding of the meaning of the results with regards to the rutting resistance of the mixtures. Also as a baseline for comparison, Superpave IDT creep tests were conducted on these mixtures and the 1000 seconds creep compliances at both 10°C and 25°C were measured and reported. Table 5-6 shows the APA rut depths and creep compliances in addition to the slopes of the Gs versus log of number of cycles plots for the traffic densification zone for the coarse- and fine-graded mixtures.

Table 5-6. Comparison of Measurements of Shear Resistance Slope to Creep Compliance and APA Rut Depth Measurements.

AGGREGATE BLEND	APA Rut Depth (mm)	Slope of Shear Resistance	Creep Compliance (1/Gpa) @ 25°C	FAA (%)
		Coarse Graded Mixtures		
CGC	4.3	26.18	10.01	53.1
CALC	6.95	22.23	51.43	42.0
WRC	7.13	21.84	62.63	43.4
CHC	11.875	3.15	94.66	44.0
RBC	7.25	11.3	86.40	46.3
		Fine Graded Mixtures		
CGF	4.65	16.8	17.59	53.1
CALF	6.22	16.1	19.27	42.0
WRF	7.9	15.3	22.90	43.4
CHF	13.925	10.7	35.38	44.0
RBF	8.525	6.5	82.86	46.3

Generally, mixtures having high rut depth measurements on the APA, have high creep compliance and low rate of shear resistance and vice versa.

Table 5-7 displays the ranking of the fine- and coarse-graded mixtures with respect to their resistance to permanent deformation using the APA rut depth, creep compliance, and the rate of gyratory shear resistance. The correlation between the gyratory shear slopes and the APA rut depths were fairly good (R^2=0.8603) for all the coarse-graded mixtures, as shown in Figure 5-17. Similarly, the correlation between the gyratory shear slopes and the IDT creep compliances at 25°C(R^2=0.7835), was also fair for all the coarse-graded mixtures as shown in Figure 5-20 respectively. In the case of the fine-graded mixtures, the slope of the gyratory shear strength correlated well with the IDT creep compliance (R^2=0.9021). However, in Figure 5-18, there appears to be little correlation between the shear slope and the APA rut depths for the fine-graded mixtures studied. The apparent low R^2 value is due to the Ruby granite fine-graded mix, which has a low shear resistance. On removal of this mixture from the plot, the R^2 value improved to 0.988 as showed in Figure 5-19.

Table 5-7. Ranking of the mixtures with the three tests studied

AGGREGATE BLEND	APA Rut Depth	Slope of Shear Resistance	Creep Compliance (1/Gpa)
Coarse Graded Mixtures			
CGC	1	1	1
CALC	2	2	2
WRC	3	3	3
CHC	5	5	5
RBC	4	4	4
Fine Graded Mixtures			
CGF	1	1	1
CALF	2	2	2
WRF	3	3	3
CHF	5	4	4
RBF	4	5	5

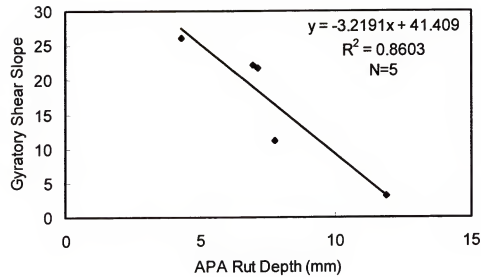

Figure 5-17. Gyratory shear slopes in the densification zone with APA test results (Coarse FAA Mixtures).

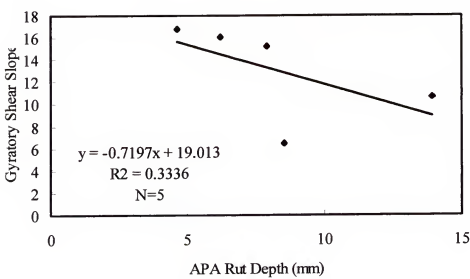

Figure 5-18. Gyratory shear slopes versus APA rut depths (Fine FAA Mixtures).

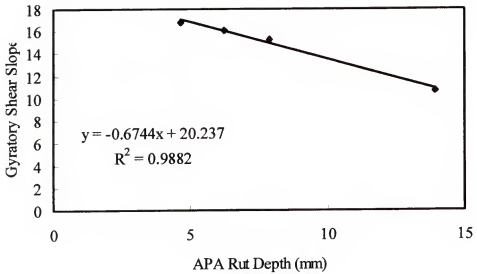

Figure 5-19 Gyratory shear slopes versus APA rut depths (Fine FAA mixtures) without the RBF.

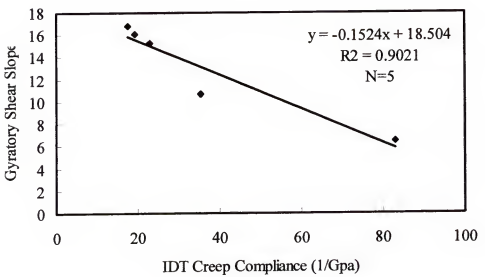

Figure 5-20 Gyratory shear slopes versus IDT creep compliance at 25°C (Coarse FAA mixtures).

The results of the APA rut measurements, the IDT creep compliance and the gyratory shear as given in Table 5-6 shows that within the range of air voids for which the plots were made, the Fine Aggregate Angularity (FAA) has little effect on the rutting resistance of the mixtures. However, the Cabbage Grove mixture, which has the highest FAA value of 53.1 has the greatest rut resistance, the Calera mixture, which has the lowest FAA value of 42.7, also has comparable rut resistance. Similarly, one would expect the Ruby granite mixture, which has a high FAA value of 46.3 not to have the poor rutting resistance measured. The rutting resistance correlated better with the effective volumetric properties of the mixtures as shown by the R^2 values in Table 5-8 after linear regression analysis was carried out between the three measured parameters for rutting performance and various volumetric properties of the mixtures.

Table 5-8. Correlation of mixture volumetric properties with measures of permanent deformation.

Parameter	Volumetric Property	Correlation coefficient (R^2)	
		Fine Graded	Coarse Graded
APA Rut Depth	Eff. Film Thickness	0.36	0.89
	VMA	0.64	0.77
	VFA	0.51	0.74
	Eff. AC Content	0.79	0.93
IDT Creep Compliance @25°C	Eff. Film Thickness	0.96	0.81
	VMA	0.57	0.87
	VFA	0.92	0.66
	Eff. AC Content	0.72	0.86
Servopac Gyratory Shear Resistance @1.25 Degree Angle	Eff. Film Thickness	0.89	0.52
	VMA	0.89	0.53
	VFA	0.72	0.52
	Eff. AC Content	0.98	0.59

Chowdhury et al, (2001), and Park et al.,(2001), found similar results that the FAA does not correlate well with the permanent deformation performance of mixtures.

5.3.4 Evaluation of other mixtures

Further testing on mixtures of different gradations extensively studied at the University of Florida (Nukunya, 2001, Asiamah 2001) was performed to confirm the outcome of the studies on the FAA mixtures. Ten limestone based mixtures, WRC1-WRC5 and WRF1,WRF2, WRF4, WRF5 and WRF6 , five field mixtures and six granite mixtures, GAC1, GAC2, GAC3, GAF1, GAF2 and GAF3 were tested with the Servopac and the APA and these results compared with results from IDT creep test results by Nukunya (2001). Figures 5-21 and 5-22 show the plot of the gyratory shear slope with the APA rut depth and IDT creep compliance respectively.

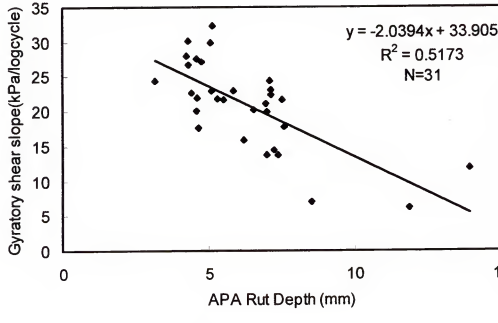

Figure 5-21. Gyratory shear slope Vs. APA rut depth for all mixtures

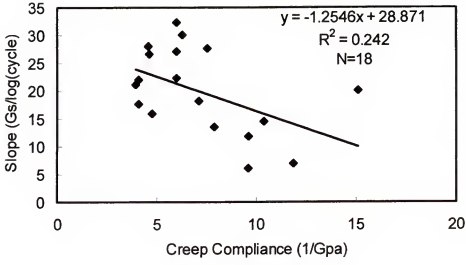

Figure 5-22. Gyratory shear slope Vs. IDT creep compliance

The plots show that generally, the slope of the gyratory shear versus logarithm of cycles correlates somewhat with the APA Rut depth measurements. The correlation is less definitive with the IDT creep compliance. Generally, the slope has an inverse relationship with the rut depth measured with the APA and the IDT creep compliance.

The IDT tests were conducted on 18 of the mixtures. These are the FAA study mixtures and the limestone mixtures. Since the IDT tests on the limestone mixtures (Nukunya 2001) were made at 10°C, the IDT test results used in Figure 5-23 are for testing at 10°C. This may be a reason why the correlation with the IDT results is not as good as with the APA test results, and the earlier correlation with the FAA test results at 25°C.

5.4 Post-Peak Zone

The post-peak zone is defined at the part of the gyratory shear strength curve that lies beyond the maximum gyratory shear strength. The maximum shear strength is reached at relatively low air voids. The gyratory shear begins to drop in most mixtures beyond this point. Since the gyratory angle in the Superpave gyratory compactor is fixed, the mixture is forced to shear continuously, leading to different degrees of aggregate breakdown from one aggregate type to another and possible mobilization of excessive pore fluid (mastic) pressure due to continued compaction. Also binder extrusion may occur at extremely low air voids. All these factors make the use of the post-peak zone for mixture stability evaluation questionable. However, for the same aggregate type and gradation, information in this zone may be useful for the evaluation of sensitivity to changes in asphalt binder content. At very low air voids, the drop in the gyratory shear strength may be attributed to pore pressures due to excessive asphalt in the pores of the aggregate skeleton. Comparison of mixture sensitivity to asphalt content may therefore be partly inferred from the relative drop in the gyratory shear.

5.4.1 Evaluation of the Post-Peak Zone

The gyratory shear strength can be thought of as the resistance of the mixture to compaction [Ruth & Schaub, 1966]. As a mix becomes denser, the gyratory shear will increase. From previous work on the Gyratory Testing Machine (e.g. Ruth and Schaub, 1966), it was observed that for mixtures with stability problems, the resistance to compaction and hence the gyratory shear, will reach a peak and drop off at some point during compaction. Conversely, stable mixtures will not show this decrease in gyratory shear in the Gyratory Testing Machine. Rather, the gyratory shear at low air void contents will tend to flatten out and become steady. In the following, the use of the

gyratory shear strength obtained from Superpave compatible gyratory compactors as an indicator of mixture stability will be examined.

The maximum gyratory shear strength (Gs_{max}), as well as a measure of the post peak drop, defined in this work by the ratio of the gyratory shear strength at the maximum number of gyrations divided by the maximum gyratory shear strength ($Gs@Nmax/Gs_{max}$) are evaluated. Anderson et al (2001) observed that one advantage of using a higher gyratory angle in compaction is that mixtures are compacted to the low air voids level associated with pavement instability in a faster time or with a lower number of gyrations than would have been obtained at a lower angle. In order to ensure that instability levels are attained, the ten FAA mixtures were compacted at both 1.25° and 2.5° angles. Figure 5-23 shows a plot of the gyratory shear resistance at 1.25 and 2.5 degrees angles for the RBF mixture.

Table 5-9 shows the maximum gyratory shear strength reached during compaction with 1.25 and 2.5 degree gyratory angles, as well as the gyratory shear ratio defined as shear strength at N_{max} (174 cycles) over the maximum shear strength achieved during compaction. The compaction curves for the two gyratory angles show a similar behavior up to the maximum shear stress. However, past the peak, the results differ drastically. The samples compacted at the 1.25 degree gyratory angle do not show a significant post-peak drop in the gyratory shear strength, whereas the samples compacted at 2.5 degrees show a drastic post-peak drop. This indicates that specimens compacted at 1.25 degrees may not have been sheared far enough to evaluate their stability using the gyratory shear strength, or that the mixtures sheared at the higher gyratory angle are undergoing particle crushing that is influencing the response unduly.

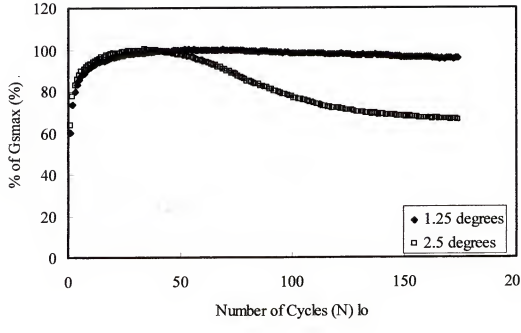

Figure 5-23 Gyratory shear strength versus cycles at 1.25° and 2.5° for the RBF at high asphalt content.

The Chattahooche fine and coarse mixtures did not show high post peak drop as would be expected of a natural gravel mixture.

The only reason N_{max} was selected was to ensure that any post-peak drop would be taken into account, if present. The coarse- and fine-graded Cabbage Grove and Calera mixtures tended to show the highest gyratory shear strength, followed by the Whiterock and Georgia Granite mixtures. With the exception of the Chattahoochee gravel mixtures, (CHC and CHF), the gyratory shear ratio also shows the similar trends at 2.5 degrees. However, the gyratory shear ratio obtained at a gyratory angle of 1.25 degrees does not clearly differentiate between the mixtures.

Finally, a comparison of the results in Tables 5-9 shows that the gyratory shear strength ratio, as well as the maximum gyratory shear strength do not rank the mixtures in

the same manner as the measured APA rut depths and the Superpave IDT creep compliance at 25oC

Table 5-9: Gyratory Shear Stress Ratio and Maximum Shear Stress

Aggregate Blend	1.25 Degrees		2.5 Degrees	
	$(Gs)@N_{max}/(Gs)_{max}$	Maximum Gs (kPa)	$(Gs)@N_{max}/(Gs)_{max}$	Maximum Gs (kPa)
Coarse Aggregat Blends				
CGC	0.99	525	0.86	541
CALC	0.985	498	0.90	557
WRC	1.00	476	0.75	515
RBC	0.99	459	0.69	485
CHC	0.998	447	0.98	538
Fine Aggregate Blends				
CGF	0.995	533	0.895	565
CALF	0.99	497	0.92	568
WRF	0.98	483	0.82	535
CHF	0.97	483	0.998	549
RBF	0.97	472	0.74	521

. This implies that the maximum gyratory shear strength and the post-peak part of the compaction curve may not be related to mixture stability in the Superpave gyratory compactor. Rather, the constant angle of shearing may cause aggregate breakdown and degradation in this region of the compaction curve for some aggregates, thus changing the mixture from its design gradation.

Extraction and recovery performed on these mixtures after compaction at 2.5 degree angle revealed extensive degradation of the Chattahoochee fine graded mixture (Kestory, 2000). Table 5-10 shows the gradation before and after compaction for this mixture. The other mixtures show little difference in gradation after compaction. The increase in fine portion, especially the percent passing the # 200 sieve size may increase the stiffness of the mix, hence the higher than expected shear ratio.

Table 5-10. Chattahoochee fine gradation before and after compaction.

Sieve Size mm(inch)	% Passing Original	% Passing After Compaction	Difference in % Passing
19 (3/4)	100	100	0
12.5 (½)	95	96.1	1.1
9.5 (3/8)	84.7	87.9	3.2
4.75 (#4)	67.9	71.7	3.8
2.36 (#8)	50.8	53.7	2.9
1.18 (#16)	34.04	38.3	4.3
600 (#30)	22.2	28.1	5.9
300 (#50)	14	20	6.0
150(#100)	6.9	12.6	5.7
75 (#200)	4.3	9.4	5.1

Using the gyratory shear ratio as a measure of stability will be erroneous in this case as the aggregate structure is changed and the exposure of fresh aggregate surface will lead to absorption, reduced more asphalt VFA and film thickness and hence higher shear strength. The use of the post peak shear ratio as a parameter for the evaluation of the rutting performance of mixtures of different aggregate types and gradations is

therefore questionable.

5.4.2 Use of the Gyratory Shear Strength to Evaluate Mixture Sensitivity

A proper understanding of mixture sensitivity with respect to asphalt content and gradation is important in all aspects of mix optimization, mix design, and mix production. To evaluate the usefulness of the shear measurements in assessing the sensitivity of mixtures to asphalt content, six of the FAA mixtures, comprising of the Cabbage Grove, Whiterock and Ruby Granite fine and coarse gradations were produced and tested at three different asphalt contents (optimum, optimum + 0.5% and optimum – 0.5%). These

mixtures were then compacted to N_{max} at both 1.25 and 2.5 degree angles. Figures 5-25 and 5-26 show typical plots of air voids versus percent of maximum gyratory shear strength for angles of 1.25 and 2.5 degrees, respectively. In both cases the slope of the gyratory shear before the peak gyratory shear does not show any appreciable difference, however, there is a marked difference in the post peak drop for the three asphalt contents. The sensitivity of the mix to asphalt content can be observed by the spacing between the compaction curves for the three asphalt contents shown. The magnitude of the shear drop, expressed as the ratio of the shear at N_{max}, to the peak shear (Gyratory shear ratio) may therefore be a useful parameter in evaluating the sensitivity of the mixtures to changes in asphalt content.

The larger compaction angle of 2.5 degrees appears to magnify the effects of mixture sensitivity as shown in Figures 5-24 and 5-25, in which the gyratory shear strength ratio is plotted versus asphalt content relative to the optimum asphalt content for coarse-graded mixes compacted at 1.25 and 2.5 degrees, respectively.

The curves for the coarse mixtures at 1.25 degrees (Figure 5-24) are all rather close together, whereas the curves in Figure 5-25 are spaced apart from each other, clearly showing the increase in definition by going to a higher gyratory angle.

The plots at 2.5 degrees angle clearly shows that the RBC mixture, which has a high VFA and VMA may already be saturated with asphalt. Changes in asphalt content therefore did not result in high changes in the gyratory shear.

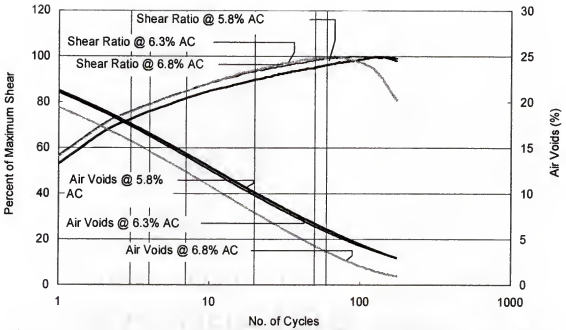

Figure 5-24. Effect of asphalt content on compaction curves (WRF) at 1.25 degrees

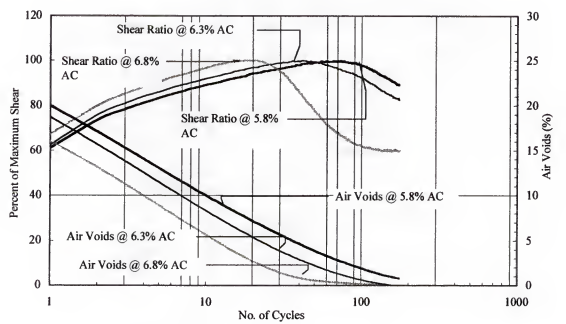

Figure 5-25. Effect of asphalt content on compaction curve (WRF) mix at 2.5 degrees

The dry CGC mix however show significant drop in shear strength with an increase in asphalt content. Similar observations were made for the fine mixtures, shown in Figures 5-26 and 5-27. In these plots, the relative asphalt content is the percent deviation of the asphalt content from the optimum asphalt content determined with the Superpave™ HMA design procedure.

In summary, the results shown in Figures 5-26 through 5-29 clearly show that a higher angle of compaction, along with the incorporation of the post-peak behavior of the mixtures may be useful in highlighting the sensitivity of a given mix to asphalt content during compaction. Unfortunately, since it was shown previously that aggregate breakdown in the post-peak region of the compaction curve may significantly affect the gyratory shear strengths in that region for certain mixtures, it has to be concluded that the use of the post-peak region of the compaction curve should be minimized, even though mixture sensitivity may be enhanced for certain mixtures in that region

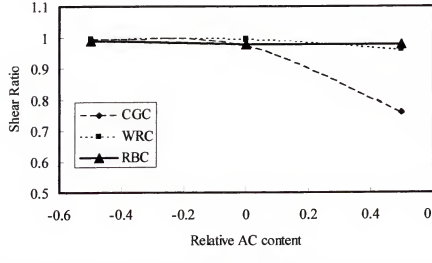

Figure5-26. Shear stress ratio versus relative asphalt content for coarse comp at 1.25 degrees

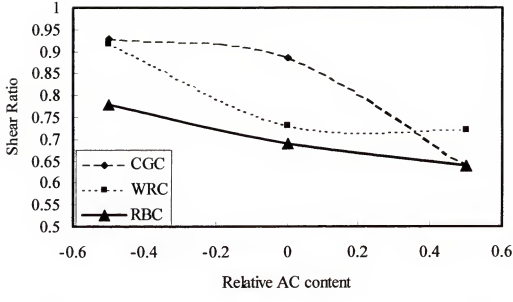

Figure 5-27. Shear stress ratio versus asphalt content for coarse mixtures at 2.5 degrees

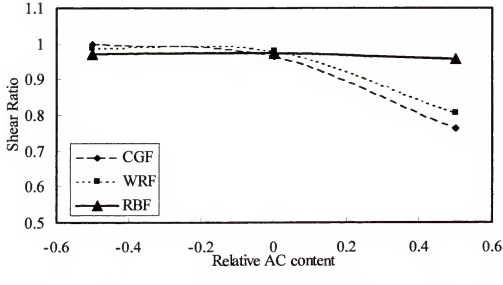

Figure 5-28. Shear stress ratio versus asphalt content for fine mixtures at 1.25 degrees

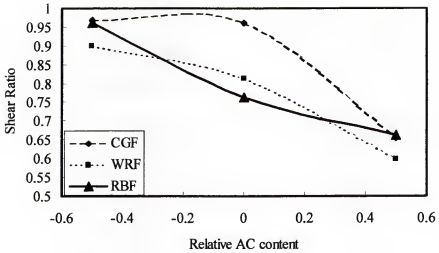

Figure 5-29. Shear stress ratio versus asphalt content for fine mixtures at 2.5 degrees

CHAPTER 6
MODIFIED COMPACTION PROCEDURE

6.1 Introduction

The results in Chapter 5 showed that the slope of the gyratory shear resistance versus the logarithm of cycles from Superpave gyratory compaction (gyratory angle of 1.25°) may be an indicator of a mixture's resistance to permanent deformation. However, the behavior of some mixtures, for example those with low VFA (dry mixes) that are likely to perform poorly (raveling susceptible), could not be explained. Such mixtures show high slopes, which is indicative of mixtures with good rutting performance.

To study the rutting behavior of asphalt mixtures, a comprehensive look at the critical conditions necessary to trigger pavement instability rutting is needed. The gyratory compaction procedure was modified to simulate this critical condition as closely as possible, using the gyratory compactor. Table 6-1 shows a comparison of the Superpave gyratory compaction protocol to field conditions.

Table 6-1 The differences between the field conditions and conditions during gyratory compaction

	Superpave Gyratory compactor	Field
Construction Compaction	• 135°C • 1.25° Angle • Constant angle of compaction	• 135°C • Variable resistance (angle) • Compacted to 6.0%-7.0% air voids
Traffic	• Compacted to 4% air voids at Ndesign and about 2% air voids at Nmax.	• ≤ 60°C • 7.0 – 4% air voids • Low strain levels • Variable shear resistance

6.1.1 Temperature Considerations

Pavements in service are generally subjected to variable temperature conditions which are normally less than 60°C with the exception of pavements placed in hot regions where pavement temperatures might be a bit higher. Compaction at these temperature conditions with the Superpave gyratory compactor in its current form may not be desirable for fear that the stiff asphalt mixture could damage the equipment components.

Generally, compaction temperatures are selected in such a way that irrespective of the type of asphalt used, the compaction is made within a specified band of asphalt viscosity. In this regard, asphalt binder effects may not be properly captured by the results of testing in this form of equipment. Aggregate effects and asphalt binder content effects are therefore the main focus of the outcome of testing with this equipment.

6.1.2 Loading Considerations

Asphalt mixtures are viscoelasto-plastic materials. Therefore the load response depends on both load magnitude and load duration. Responses due to loading time can be effected in the gyratory compactor by varying the rate of compaction, i.e. the number of cycles per minute. Butcher (1998), however showed that asphalt concrete response does not vary significantly at different loading rates with the gyratory compactor at the compaction temperature and at the same angle of compaction. The magnitude of loading (represented by angle of gyration) however affected the responses of mixtures because of the influence of frictional resistance between aggregate particles and degree of aggregate packing. Butcher (1998), found out that the higher the angle of gyration, the higher the shear resistance of a mixture at a given cycle. However, the shape of the compaction curve is similar for different angles.

6.1.3 Critical Loading Conditions to Trigger Instability

Generally, pavement instability rutting may be triggered by stationary or slow loading as observed at most intersections, and heavy loading after a new pavement is opened to traffic. Slow or stationary loading may result in a loading response that is equivalent to a heavier load traveling at higher speeds. It would be ideal to simulate the shear stresses due to these heavy loads as much as practicable during testing to evaluate the resistance of mixtures to such conditions. The testing protocol with the gyratory compactor was therefore modified in an attempt to simulate these effects.

6.2 Modified Compaction Procedure

To simulate the above pavement critical loading conditions with the Servopac gyratory compactor, the Superpave compaction protocol was modified as follows:

- The number of cycles to achieve an air voids level of 7% at a compaction angle of 1.25° was established from the design mixture compaction curve. This is about the average air voids level to which most pavements are compacted in the field before opening to traffic. Table 6-2 shows the number of cycles to 7% air voids for the mixtures.
- Mixtures are prepared following the Superpave protocol of mixture preparation described in Section 3.3 and compacted in the Servopac initially to 7.0% air voids at 1.25° angle.
- At the end of the number of cycles to 7.0% air voids, the gyratory angle setting was changed to 2.5° and the mixture was compacted for another 100 cycles (to about 2.0% air voids) to observe the shear response of the mixture.
- The compaction curve during compaction at 2.5° angle was analyzed and comparison made with measurements from the APA and the Superpave IDT test.
- The compaction temperature was 135°.

It is worth to note that the compaction of the mixture at this high temperature is not likely to bring out the binder influence on the mixtures' rutting performance. Aggregate properties are therefore the main response that can be measured.

Table 6-2. Number of cycles to 7.0% air voids

Fine Graded Mixtures		Coarse Graded Mixtures	
Mixture	Average cycles to 7% Va	Mixture	Average cycles to 7% Va
WRF1	52	WRC1	65
WRF2	38	WRC2	58
WRF4	50	WRC3	61
WRF5	47	WRC4/F3	62
WRF6	42	WRC5	40
CGF	46	CGC	57
RBF	41	RBC	53
CALF	51	CALC	60
CHF	33	CHC	48
Proj # 7	35	Proj # 1	39
GAF1	38	Proj # 2	43
GAF2	34	Proj # 3	62
GAF3/C4	45	Proj # 5	49
HVS67-22	18	Proj # 8	42
HVS76-22	38	GAC1	47
-	-	GAC2	47
-	-	GAC3	44
Average	40.4		52

6.3 Modified Compaction Results

During compaction at the 1.25 degrees angle, the behavior of the mixture is the same as previously observed in Chapters 4 and 5. Figures 6-1 and 6-2 show plots of the gyratory shear strength before and after the gyratory angle is changed to 2.5 degrees.

On the application of the 2.5 degree angle, the gyratory shear starts at a very high value, and drops with subsequent cycles to an initial minimum value after a few cycles. The shear resistance then increases in most of the mixtures to a secondary maximum before finally dropping again. The behavior of the mixtures during the initial stages when the angle is switched to the higher angle may be a mixture property that may lead to an understanding of the shear behavior of pavements when loaded with high instantaneous loads.

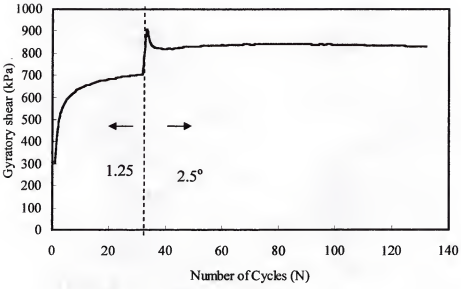

Figure 6-1. Gyratory shear for the modified compaction -CHF

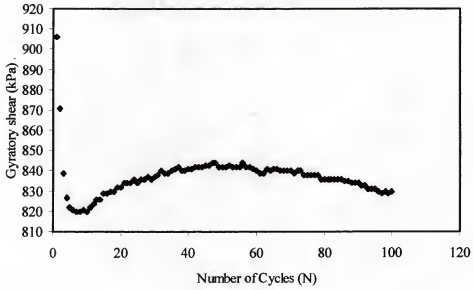

Figure 6-2. Gyratory shear for modified (2.5° only)-CHF

6.4 Destabilization of Aggregate structure

The instantaneous application of the higher angle of 2.5 degrees may have the following effects:

- A tendency of aggregate particles to move outwards or roll over each other instantaneously and thereby disturbing the already formed aggregate structure during compaction at 1.25°. This may lead to a temporary collapse of the aggregate structure.
- The tendency of aggregate particles to move out or roll over each other will result in high lateral stresses on the mold walls. Instantaneous high frictional forces are then developed between the mixture and the mold walls.
- The instantaneous high frictional force developed will result in the initial gyratory shear measured on the application of the 2.5° angle.
- With subsequent control shearing after the initial shock, the initial frictional force is gradually dissipated when the aggregate particles are gradually sheared back to their stable position.

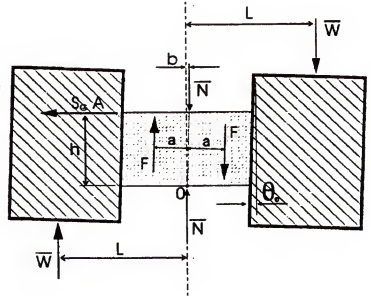

Figure 6-3: Force diagram during gyratory compaction.

Therefore,

$$S_G = 2(WL + Fa)/(Ah) \quad (6\text{-}1)$$

Where S_G = Gyratory shear, kPa

W = Average pressure exerted by the mixture

L = Load arm

F = Wall friction

a = Distance from center of the specimen to the mold wall

A = Cross sectional area of sample

H = height of sample.

In the conventional compaction procedure, the effect of wall friction was considered negligible. However with the modified procedure, on the instantaneous application of the higher angle, there is the likelihood of aggregate particles to spread out due to the shock loading. Restriction of outward movement by the mold walls and the vertical load plate will lead to high forces exerted by the mixture on the walls and loading platen. These forces will greatly increase the friction between the wall and the asphalt mixture. Further gyrations will reorient the aggregate particles and dissipate the high pressures on the mold walls. The friction induced by forces right after the change of gyratory compaction angle to 2.5 degrees cannot be neglected. In actual fact, the pressure transducers in the Servopac gyratory compactor that are used to obtain the gyratory shear strength are measuring the induced wall friction in addition to materials resistance to shear. In the analysis of the modified compaction curve, attempts will be made to evaluate the following effects: 1) the effects of degree of mixture disturbance after the application of the shock (2.5 degrees) on gyratory shear strength, and 2) the vertical strain present during the destabilized phase of the modified compaction procedure. The instantaneous gyratory shear strength, and the vertical strain during

aggregate particles reorientation, should both be lower for stable mixtures which are not substantially destabilized by the instantaneous shock load. A higher instantaneous gyratory shear strength and higher vertical strain on the other could be associated with unstable and more plastic materials.

- In view of the above explanation, both the instantaneous gyratory shear and axial strain during the period when the aggregate particles are reorienting themselves were evaluated for any correlation with the IDT creep compliance and the APA rut depths. Figure 6-4 shows a plot of the gyratory shear and axial strain as the mixture is compacted at a 2.5 degrees angle.

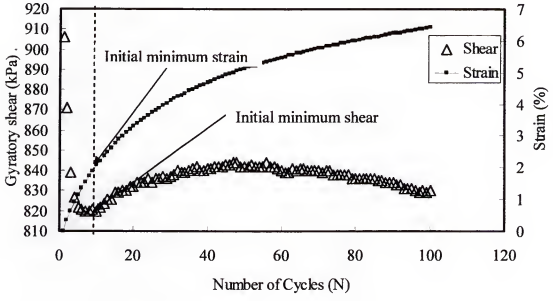

Figure 6-4 Gyratory shear strength and axial strain vs. number of cycles.

. Parameters used for the evaluation are also displayed on this figure and explained below:

- Shear strength at first cycle – The gyratory shear strength after one cycle of compaction at 2.5 degrees angle.

- Initial minimum shear – Minimum shear strength after the first few cycles of gyration at 2.5 degrees angle.
- Axial strain- Ratio of the compaction height at any number of gyrations divided by the height after the first gyration at 2.5 degrees angle of compaction.
- Vertical strain to initial minimum shear- The axial strain corresponding to the initial minimum shear.
- Intermediate maximum shear – The maximum shear strength after the initial minimum shear strength.

Minimum shear strength – The shear strength at the end of compaction

Figures 6.5 and 6.6 show plots of the ratio of the shear strength at the first cycle to the initial minimum shear strength in comparison with the measured APA rut depths and IDT creep compliance at 10°C respectively for the FAA mixtures. These plots show no definite relationships. The strain at the initial minimum shear strength was thereafter evaluated. In this case, the IDT creep compliance at 10°C was used for comparison because test results at this temperature were obtained for the limestone (Whiterock) mixtures from previous testing (Nukunya 2001). Figures 6-7 to 6-10 are plots of the vertical strain versus measurements from the APA and IDT creep compliance tests. The figures show some trend in the relationship between the vertical strain and the other measures of permanent deformation (IDT creep compliance and APA rut depth). Further investigation of this parameter was therefore pursued.

The Chattahooche mixtures however deviated from the trend. The behavior of the Chattahoochee mixtures may stem from the fact that the Chattahoochee gravels are natural and uncrushed, they are smooth and therefore may not roll over each other to the same extent as crushed particles.

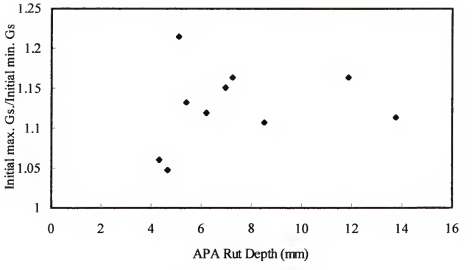

Figure 6.5 Gyratory shear ratio versus APA rut depth.

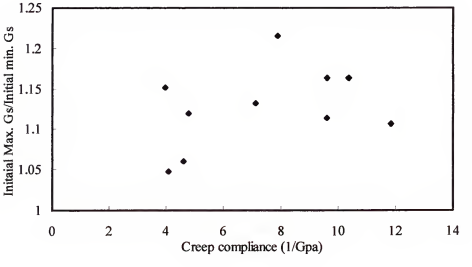

Figure 6.6 Gyratory shear ratio versus Creep Compliance.

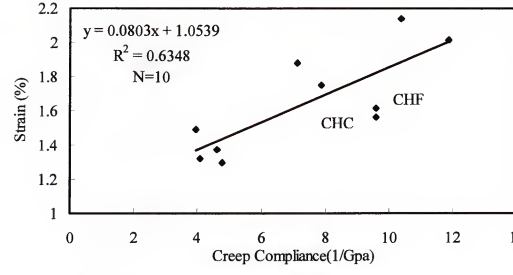

Figure 6.7 Strain at initial minimum shear versus IDT creep compliance for all FAA mixtures.

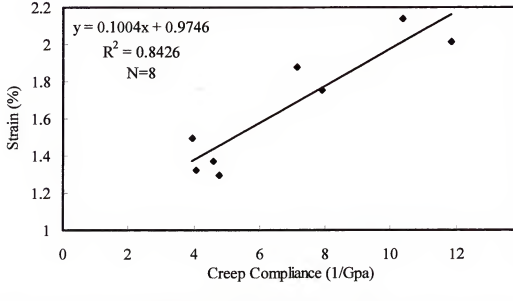

Figure 6.8 Strain at initial minimum shear versus IDT creep compliance for all FAA mixtures without the Chattahooche mixtures

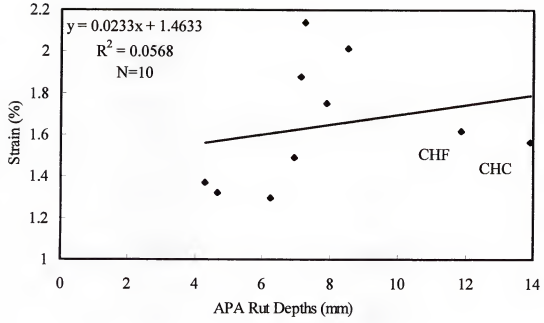

Figure 6.9 Strain at initial minimum shear versus APA rut depth for all FAA mixtures.

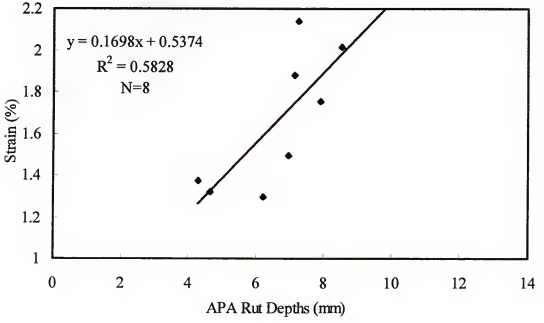

Figure 6-10 Strain versus APA rut depth (FAA mixtures without CHC and CHF..

As earlier observed in Chapter 5, the Chattahooche mixtures have low shear resistance and therefore the rutting behavior is mostly dictated by the low shear rather than destabilization in the modified procedure.

As observed from Figures 6-5 and 6-6, the shear stress ratios as computed from the modified Servopac procedure do not appear to give a true picture of the trend of the behavior of the mixtures. For a given mixture, the less the mixture is destabilized on the application of the instantaneous shock, the less will be the strain on further shearing. Thus, a more stable mixture will develop less vertical compressive strain than a mixture which has a high tendency to be destabilized.

Finally, all the other mixtures were tested using the modified procedure of compaction with the Servopac gyratory compactor (compacting to 7.0% at 1.25 angle followed immediately by compaction at 2.5 degrees for 100 gyrations). Figures 6-11 and 6-12 show the plot of the strain versus APA rut depths and IDT creep compliance at 10°C respectively. The IDT testing was performed on only the FAA and test results were obtained for the Limestone mixtures from previous testing at the University of Florida (Nukunya 2001). IDT testing of the other mixtures were discontinued and efforts were concentrated on testing in the APA due to the inability to test in the IDT at higher temperatures at which pavement rutting is more pronounced. Comparison of the parameters developed will be more credible in this case since specification limits exist for the APA testing protocol for which comparison could be made.

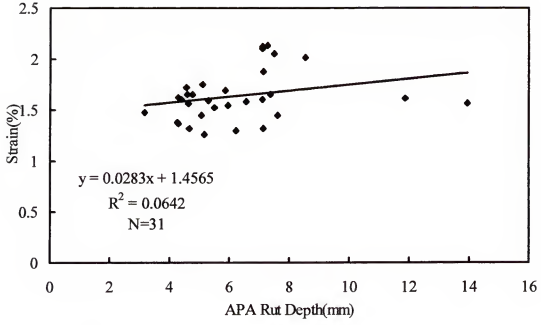

Figure 6-11 Strain versus APA rut depth for all mixtures

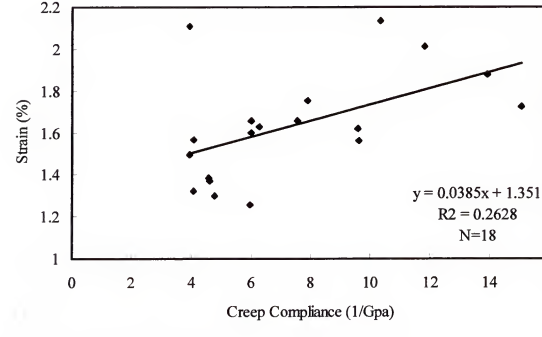

Figure 6-12 Strain versus IDT creep compliance for the FAA and Limestone mixtures.

There appears to be little correlation between the strain and the APA rut depth and IDT creep compliance. However, generally, a low strain level corresponds to a high rut resistance and vice versa. Asphalt mixtures are complex composite materials of aggregates and asphalt. Differences in aggregate type and aggregate structure (gradation) may result in significantly different load response behavior. Even with the same aggregate type and aggregate structure, other packing effects, such as particle orientation can have a significant impact on the resistance of mixtures to shear stress and deformation. In view of these complexities, grouping of asphalt mixtures with similar properties (fine gradation, coarse gradation, similar aggregate properties) for studies may be more appropriate for the initial identification of possible correlations. Figures 6-13 to 6-17 shows the plot for all these categories.

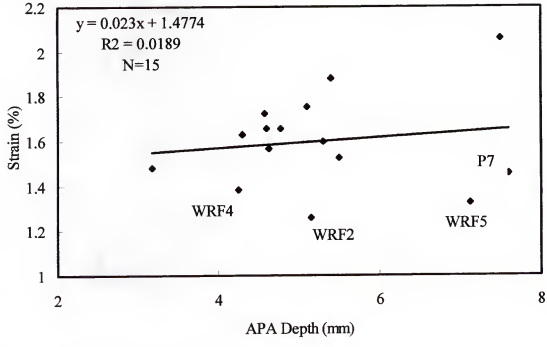

Figure 6-13 Strain versus APA rut depth for all limestone based mixtures

The plots show little correlation between the strain and the APA rut depths (R^2 = 0.0189). However, a closer look shows that mixtures F5 and F2 and project number 7 are outliers which might have skewed the results. Mixture F2 has a low VMA of 13.2 while mixture F5 is slightly gap graded. Project number 7 is the only 9.5-mm nominal maximum aggregate size gradation. Project 7 showed substantial rut depth, while F2 and F5 show failure by punching shear during the APA testing as illustrated in Figure 6-14. There is a better correlation (R^2 = 0.6902) when the plot is made without the outliers as shown in Figure 6-15.

The plots of the FAA mixtures and limestone mixtures show that the strain tolerance may be a useful parameter for assessing the rutting resistance of paving mixtures.

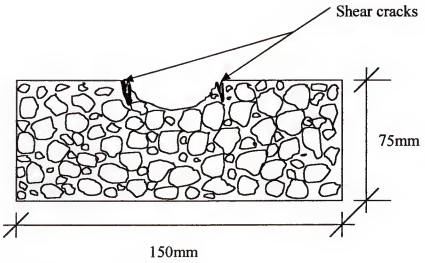

Figure 6-14 APA sample after testing showing shear cracks.

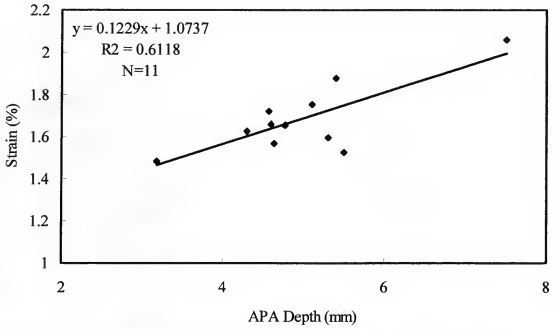

Figure 6-15 Strain versus APA rut depth for all limestone mixtures without WRF2, WRF4, WRF5 and project # 7.

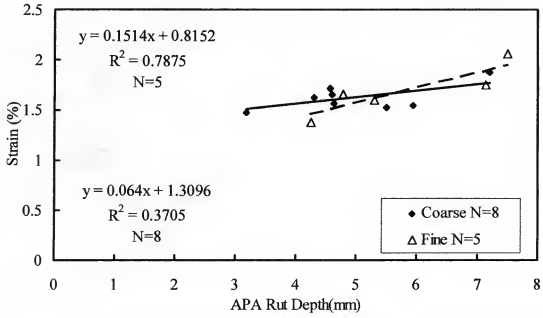

Figure 6-16 Strain versus APA rut depth for coarse and fine limestone mixtures without WRF2, WRF4, WRF5 and project # 7.

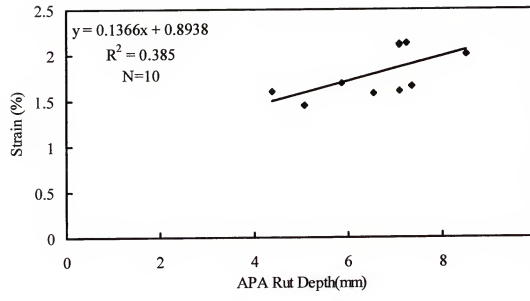

Figure 6-17 Strain versus APA rut depth for granite mixtures.

6.5 Combination of Shear and Destabilizing Effects

Results from Chapter 5 and the modified procedure presented above have shown that the following two parameters may be of interest for further evaluation: 1) the slope of the shear resistance versus the logarithm of cycles, and 2) the vertical strain when mixtures are dilating can be used to evaluate the rutting resistance of mixtures. These parameters, however, need to be evaluated in terms of both prevalent trends as well as outliers consisting of mixtures with undesirable properties. Criteria were set for screening these undesirable mixtures. Combined plots were made using these parameters for all 31 different types of mixtures tested and limits were set to screen these mixtures based on various mixture characteristics used in screening poor mixtures. The following section explains the criteria used in plotting the results for use as a mixture screening tools.

6.5.1 Summary of Presentation of Results

All the mixtures were compacted at 1.25 degrees angle using the Servopac and the shear strength plotted versus the number of cycles on a semi-log plot. The slope of the gyratory shear plot between 7% air voids and either: a) maximum gyratory shear strength, or b) 4% air voids (whichever is first) was calculated. Two replicate samples were compacted.

A second set of two replicate samples were compacted with a modified procedure by initially compacting the mixture in the Servopac at 1.25° to 7% air voids and immediately switching the angle to 2.5° and compacting to 100 cycles to obtain the shear compaction curve. The strain at the initial minimum gyratory shear strength was then recorded.

The two results were plotted on the same graph as follows:

- The slope of the gyratory shear strength during compaction at 1.25° angle was plotted on the y-axis.
- The strain to the initial minimum gyratory shear in the modified procedure of compaction was plotted on the x-axis.
- Limits were set for each parameter, which excludes the poor mixtures based on the observation of the results from the APA test.
- A mixture with an APA rut depth > 8.0 mm is considered rut susceptible as recommended by Kandhal and Cooley (2002).
- For the mixtures tested, a shear slope of less than 15 was set as the limit for rut prone mixtures.
- For the mixtures tested, a strain to the initial minimum gyratory shear of 1.4 (in the modified procedure) after switching the angle to 2.5°, was set as the minimum below which mixture performance is undesirable, based on observation of shear cracks in APA etc.

6.5.2 Comparison With Performance in APA

Figure 6-18 shows a plot of the gyratory shear strength slope from Chapter 5 versus the vertical strain to the initial minimum gyratory shear strength for all mixtures studied. Three different symbols are used to represent the observed rutting behavior in the APA: 1) solid squares refer to mixtures that did not exceed the threshold of 8.0 mm of rutting in the APA, 2) open squares refer to mixtures that exceeded the 8.0 mm APA rutting criterion used, and 3) open circles represent mixtures that showed surface cracking in the APA, but generally exhibited APA rutting of under 8.0 mm. The mixtures in category 3 all did not meet various Superpave mix design criteria.

All of these mixtures had a low VMA and a high D/A ratio, with three mixtures also having a low VFA (CALF, CGF, CGC)

These three categories of mixtures fall in three distinct regions, depending upon the observed APA behavior. Mixtures with a gyratory shear slope of 13.5 or higher generally did not exhibit rutting failure in the APA. Mixtures that exhibited cracking in the APA all had very low vertical strain at the initial minimum gyratory shear strength (less than 1.4 percent) after switching the gyratory angle from 1.25 degrees to 2.5 degrees. Therefore, a look at the APA rut depths alone may create the erroneous impression that these mixtures are good, whereas in fact they exhibited various other volumetric problems.

In summary, the criteria set screens mixtures with questionable APA rutting performance from mixtures with good APA rutting performance.

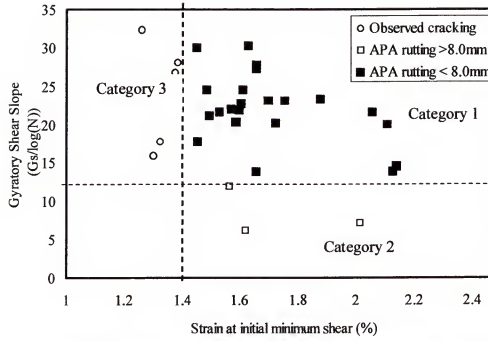

Figure 6-18. Summary plot based on APA rut measurements for all the mixtures.

6.5.3 Voids in Mineral Aggregates (VMA)

The voids in mineral aggregates (VMA), is a mixture volumetric measure used in screening HMA mixtures for stability and durability. The Superpave HMA design and analysis method sets minimum criteria for good performance. For the 12.5-mm nominal maximum aggregate size mixtures used in this work, the minimum Superpave criteria for VMA of 14% is used as a cut off value. VMA below this value is considered low. At the fixed design air void content of 4%, variations in VMA for different mixtures are due to variations in the effective asphalt content. Therefore a low VMA indicates low effective asphalt content. This may in turn lead to low asphalt film thickness on the aggregate particles. On the other hand, a high VMA indicates a mixture having high effective asphalt content. A mixture having excessive effective asphalt content will also have a high film thickness. Though asphalt film on the aggregates is beneficial for providing

aggregate bonding, excessive film thickness reduces inter-aggregate friction, leading to reduced shear resistance. Such mixtures may easily be saturated with asphalt on further compaction beyond the design air void level of 4%, and thereby have stability problems. Figure 6-19 illustrates mixtures with high and low VMA at the design asphalt content. Figure 6-20A shows a mixture with high effective asphalt content but having 4.0% air voids at the deign number of gyrations while figure 6-17B shows a mixture with low effective asphalt content and still have an air void content of 4.0% at the design asphalt content. The difference in the two mixtures is the asphalt binder (effective asphalt content) available to provide the required VMA. Figure 6-18 shows plots based on VMA.

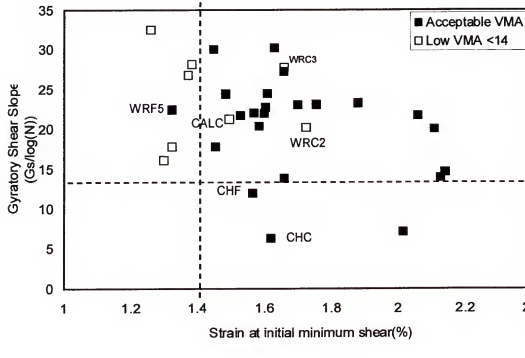

Figure 6-19. Summary plot based on VMA for all the mixtures

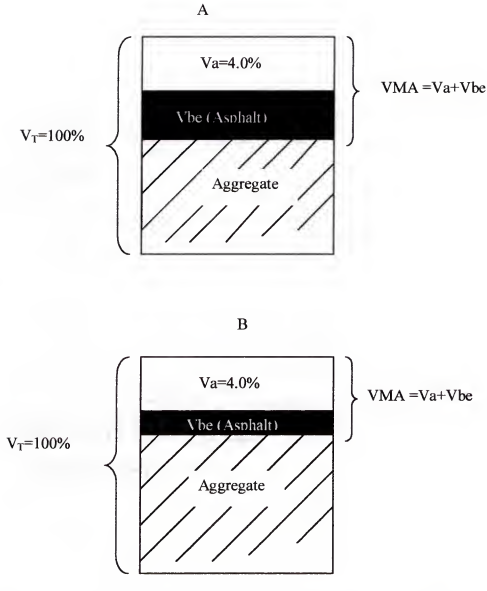

Figure 6-20. VMA and effective asphalt content at design asphalt content. A) High VMA, and B) Low VMA. V_T = Total volume, Va= volume of air voids, Vbe= effective volume of asphalt.

. The plot shows that most of the mixtures with low VMA values at the optimum asphalt content have vertical strain values less than 1.4 percent. The exceptions are the Chattahoochee mixtures, some coarse mixtures (CALC, WRC2, WRC3), and the gap graded WRF5 mixture.

6.5.4 Voids Filled With Asphalt

The voids filled with asphalt (VFA), is another volumetric parameter used in screening HMA mixtures. It is the percentage of voids in the mineral aggregate (VMA) filled with asphalt. Like the VMA, this affects the durability and stability of the mixture. The Superpave HMA method of design and analysis sets a criteria of 65% - 75% for 12.5 mm mixes. Figure 6-1-21 shows plots of the shear slope and strain based on VFA.

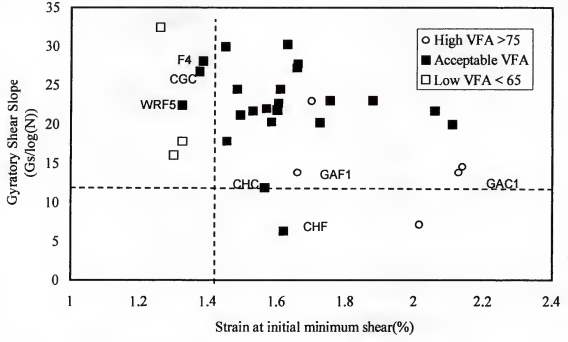

Figure 6-21. Summary plot based on VFA for all the mixtures

Mixtures which have low VFA are associated with low strain, with the exception of the WRF4, CGC and the WRF5 mixtures. The WRF4 and CGC mixtures have high dust proportion while the F5 mixture is a gap-graded mixture. With the exception of the CHF and CHC mixes, all mixtures which have acceptable VFA values have good rutting

performance in the APA. The GAF1 and GAC1 mixes have high VFA values but performed well in the APA.

6.5.5 Dust to Asphalt Proportion

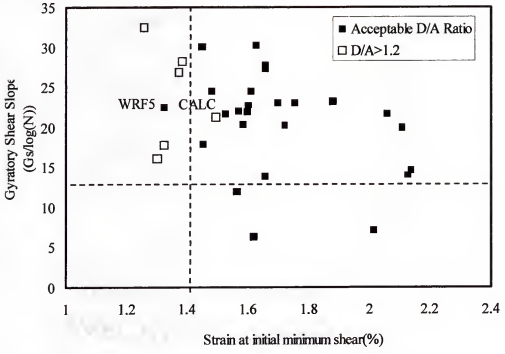

Figure 6-22. Plots based on dust proportion.

The dust proportion is defined as the material passing the 75 μm sieve opening size (i.e. passing the # 200 sieve) affects mixture performance. This material mixes with the asphalt binder to change the viscosity of the binder. The higher the dust content, the stiffer will the binder becomes. Too much dust will make the binder brittle and affect the performance of the mix. The Superpave mix design specifications specify a dust to asphalt ratio limits of 0.6<D/A<1.2. Figure 6-22 clearly shows that mixtures with D/A > 1.2 have low strain values. Figure 6-20 shows that high Dust to Asphalt Ratio may be detrimental to mixture performance.

With the exception of the gap-graded WRF5 mix and the CALC mix, mixtures which have high dust proportion (>1.2%) had low strain values and showed surface cracks in the APA.

6.5.6 Comparison with Overall Superpave™ Criteria

The Superpave level one mixture design depends on the proper selection of aggregate gradation, characterization of aggregates by the aggregate consensus properties, binder selection by the introduction of performance grading, and finally specifying mixture volumetric properties that are related to performance. He volumetric properties specified are the voids in mineral aggregates (VMA), voids filled with asphalt, (VFA), and the dust to asphalt ratio (D/A ratio). The Superpave design procedure specifies limits for these volumetric properties based on the design traffic of a pavement facility nd the niminal maximum aggregate size used in an HMA mixture. Figure 6-23 is based on whether or not a mixture passed or fails the Superpave volumetric screening criteria, a failed mixture is one which does not satisfy any of the following criteria. For the traffic level of <30 million ESALs used in this work, the Superpave volumetric criteria of acceptance are as follows:

$VMA \geq 14$

$65 \leq VFA \leq 75$, and

$0.6 \leq$ Dust proportion ≤ 1.2

The volumetric properties are computed at the Ndesign gyrations, at which the air voids within the mixture is 4.0%.

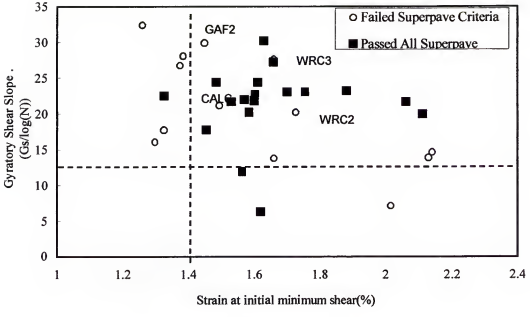

Figure 6-23 Summary based on Superpave criteria.

Of the mixtures that failed the Superpave volumetric criteria but performed well in the APA, GAF2 had a low VMA of 13.6%, GAF1 had a high VFA of 75.9%. The gap-graded WRF5 mixture passed all the Superpave criteria but developed surface cracks in the APA. All the three coarse mixtures which failed the Superpave volumetric criteria (CALC, WRC2 and WRC3) had low VMA values. Figure 6-21, identifies the GAF1 and GAF2 mixes as nominal mixes which lies close to the minimum criteria lines. Also, mixtures CHC and CHF, which showed excessive rutting in the APA and had gyratory shear slopes below 15, passed all the Superpave volumetric criteria, however the Chattahoochee aggregate is an uncrushed gravel and had rounded shape. Such aggregates are prone to rutting when used in a mixture. The need for a review of VMA criterion for mixtures has been an issue for a long time. Nukunya (2001) proposed the

use of the effective VMA as an alternative to the use of the traditional VMA for screening coarse graded mixtures.

The traditional VMA criterion was found to result in the potential for over asphalting of coarse graded mixtures, resulting in rut prone pavements. This implies that coarse graded mixtures, which may seem to be under asphalted based on the current VMA criteria, may have adequate asphalt for good rutting performance. The coarse graded CALC, WRC2 and WRC3 mixtures that failed the Superpave VMA criterion but were classified with acceptable rutting performance by this analysis may in actual fact have adequate VMA. The coarse-graded mixtures were therefore analyzed based on the effective VMA calculations as proposed by Nukunya (2001).

6.5.7 Analysis of Coarse Graded Mixtures Based on Effective Volumetric Properties

Figure 6-24 shows the analysis of the coarse-graded mixtures based on effective VMA. The effective VMA criteria (Nukunya, 2001) applied to the analysis, Figure 6-22 however, was able to improve the identification of substandard mixtures in accordance with their rutting performance. The only mixtures, which performed well in the APA but have high effective VMA values are Project # 2 and GAC2. The coarse-graded mixtures might have been over asphalted when the traditional VMA criteria was used for their design, leading to a higher rutting than will be expected. Over-asphalting may lead to slightly lower shear slope and higher strain in the modified compaction procedure. This observation further throws light on the need to reconsider the volumetric specifications, especially the VMA in the Superpave mix design.

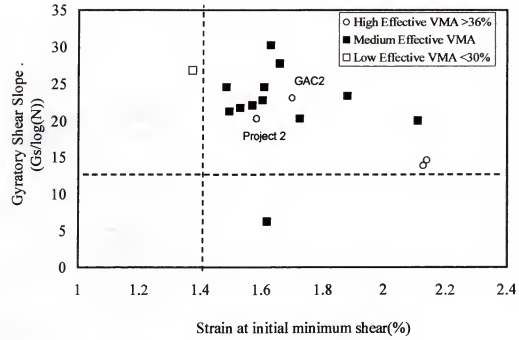

Figure 6-24. Summary based on Effective VMA criteria for the coarse graded the mixtures.

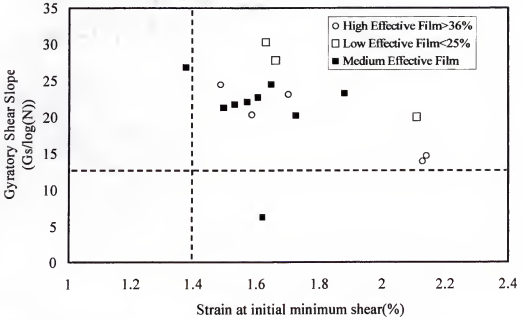

Figure 6-25. Summary based on Effective Film thickness criteria for all the coarse mixtures.

Figure 6-25 shows a plot based on effective film thickness. A comparison of Figures 6-16 and 6-25 shows that the effective film thickness did not identify mixtures with low rutting performance.

The theoretical film thickness was plotted for the fine mixtures to see if it has any influence on the rutting resistance of the mixtures tested. Figure 6-26 shows this plot.

With the exception of the WRF5 gap graded mixture, low theoretical film thickness is associated with mixtures which had low VMA, low VFA and showed cracks in the APA. The plot shows that the theoretical film thickness may be able to identify some good mixtures. However, low film thickness may be associated with the cracking performance of HMA mixtures, as binder oxidation is compromised.

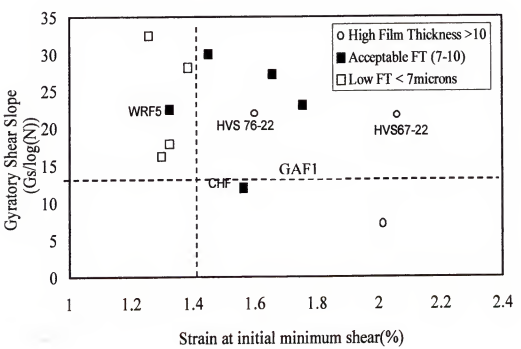

Figure 6-26. Summary based on theoretical film thickness for the fine graded mixtures.

6.5.8 Recommended Specification Limits for Rutting Classification

Based on the findings from Sections 6-2 to 6-8, the APA rut depth limit of 8.0 mm could not identify most of the mixtures which are substandard with respect to the Superpave™ volumetric criteria. Most mixtures that have high VMA, high VFA and high film thickness, and therefore may be prone to rutting were not identified. This observation calls for a review of the APA standards used for the mixtures tested. The maximum rut depth requirements was therefore reviewed downwards to 7.0mm, and the gyratory shear slope and strain from the modified procedure of testing replotted to. Figure 6-27 shows the plot to account for the behavior of majority of the mixtures. In Figure 6-27, the minimum gyratory shear slope was raised to 15 to account for all the mixtures with high VMA, VFA and rutted in the APA. A cut off line for the strain at initial minimum shear in the modified procedure was set at 2.0%. Mixtures that have high strain beyond this level are likely to be those which are plastic and are easily destabilized. All the five mixtures which plot beyond this strain level had APA rut depths greater than 7.0 mm. The only exceptions are project number 7 and the GAC3 mixtures, however, the recommended limits shows promise of being a screening tool for both substandard and rut prone mixtures. Project number 7 was designed for a lower traffic level (Ndesign = 84). However, the same number of cycles (8,000) is applied for all mixtures in the APA testing without consideration to traffic level. The specification for the same APA limit of rutting for project 7 may therefore be too severe. A review of the APA specifications to account for traffic level is therefore advocated.

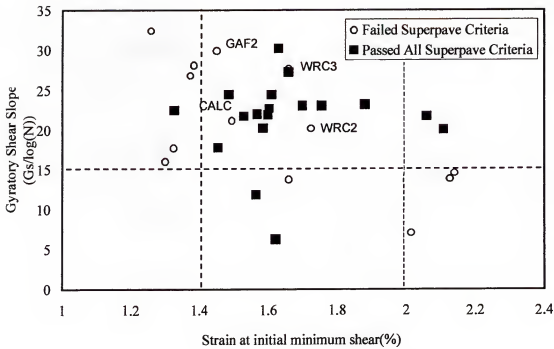

Figure 6-27. Recommended plot for characterization of mixtures with the gyratory compactor.

6.5.9 Comparison With NCHRP-9-16 (Asphalt Institute Method)

Anderson (2002) proposed the use of the parameter NSRmax (The number of gyrations to the maximum stress ratio) for screening mixtures with potential rutting problems. The stress ratio is defined as the ratio of applied normal stress to the induced gyratory shear stress. This parameter was able to differentiate between the mixtures evaluated by Anderson (8 limestone based and 8 gravel based mixtures) with respect to their rutting resistance (Anderson, 2002). The N-SRmax value is estimated by fitting a quadratic curve to the NSR versus number of cycles (N) curve. The N value at the maxima is then obtained from the curve fit (See Chapter 2 for details). Using this method and the proposed criteria for mixtures, all the mixtures tested in this work were evaluated

for NSRmax and classified in accordance with the proposed range of performance, as proposed by Anderson (2002). Figure 6-28 shows the plot of all mixtures based on this method.

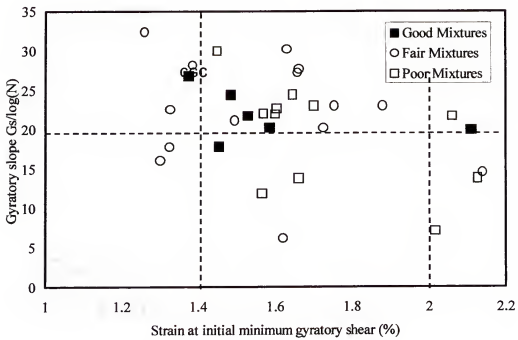

Figure 6-28 Analysis based on Asphalt Institute Method

This method classified most of the granite mixtures as poor mixtures while most of the limestone mixes are classified as fair. Also, mixtures with other volumetric problems did not get identified. For example, the CGC mixture from the FAA study, an extremely dry mix, low VFA, and high D/A ratio, showed up as a "good performer". This method is therefore considered not appropriate for the purpose of this research since it may fail to identify potentially dry mixtures.

6.6 Review of Marshall Test Parameters for Superpave Mixtures

The most widely used method of bituminous mix design before the advent of the Superpave HMA mix design and analysis method was the Marshall method developed by the U.S. Corps of Engineers. Most international specifications still use the Marshall method of mixture design. Marshall Stability and flow, together with density, air voids, voids in the mineral aggregate (VMA), and percentage of voids filled with asphalt (VFA) are determined at varying binder contents to determine an 'optimum' condition for asphalt mixture design. Limited correlation of the Marshall stability with the permanent deformation characteristics of HMA pavement has been found (Ford Jr., 1988 and Ford Jr. 1985). The Arkansas DOT (Ford Jr., 1988 and Ford Jr. 1985) found that a Marshall Modulus (Stability/Flow x 0.01 psi) has better correlation with field rutting performance. The same studies showed little correlation of Marshall flow with field performance.

In addition to binder content, stability and flow are also dependent on type of binder, grading of aggregate, the particle shape, geological nature of parent rock (most importantly, porosity), degree of compaction, etc. Test temperature is also a factor but, for the Marshall test, it is standardized at 60 °C. In the following, the Marshall stability, flow, and modulus criteria will be evaluated for use in screening mixtures with potential rutting problems from mixtures with adequate rutting performance.

6.6.1 Marshall Test Procedure (ASTM D1559)

The dimension and specifications of the Marshall apparatus are laid down in the American Society of Testing and Materials test specifications ASTM D1559-89

The diameter of the specimen is 101.6 mm with a nominal thickness of 6.5mm ASTM D1559, gives a correlation ratio hereby the stability of specimens that are not exactly 63.5 mm thick can be adjusted The basic steps for evaluating the mixture stability and flow are summarized as follows:

- Test specimens, prepared according to the Standard, are immersed in a water bath for 30 to 40 minutes or in an oven for 2 hours at 60 ± 1.0 °C.
- The testing heads and guide rods are thoroughly cleaned, guide rods lubricated and head maintained at a temperature between 21.1 and 37.8 °C.
- A specimen is removed from the water bath or oven, and placed between the lower jaw and the upper jaw of the specimen holder. The complete assembly is then placed in the compression testing machine and the flow meter adjusted to zero.
- The load is applied to the specimen at a constant strain rate of 50.8 mm/min until the maximum load is reached. The maximum force (called stability) and flow (deformation in units of 0.01 inches) at that force are read and recorded. The maximum time allowed between removal of the specimen from the water bath and maximum load is 30 seconds.

6.6.2 Analysis of Marshall Stability

The Marshall test was performed on all of the mixtures previously tested with the exception of the two HVS mixes. The Marshall stability of the mixtures was then plotted to evaluate if the test could screen mixtures with potential low rutting problems. Based on the Superpave traffic level used in this work (< 30 million ESALs), Marshall properties for Heavy traffic pavements are used in the analysis. In this regard, mixtures with stability values greater than 1800 lbs are considered acceptable while those with

stability values below 1800 lbs are considered " Low Stability Mixtures" Figure 6-29 shows the Marshall Stability plots.

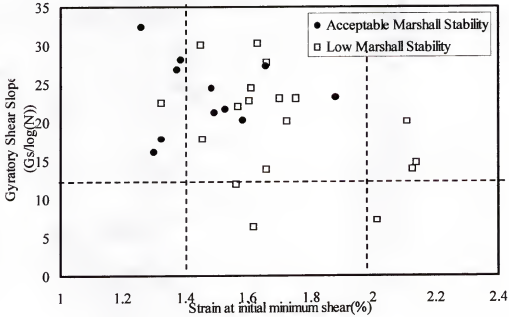

Figure 6-29 Analysis of mixtures based on Marshall stability.

This plot shows that the acceptable value of Marshall stability for heavy traffic may not be able to differentiate the mixtures with respect to their rutting performance. Most mixtures classified as having low stability showed adequate rutting peroformance in the APA and have a high gyratory shear slope. Also, dry mixtures (Low VFA, and high D/A ratio) showed high stability values implying that they were adequate performers.

6.6.3 Analysis of Marshall Flow

Figure 6-30 shows the plot of the Marshall flow for all the mixtures. For heavy traffic, the following categories of Marshall flow are plotted:

Marshall Flow < 8 considered "Low".

8 < Marshall Flow < 14 is acceptable.

Marshall Flow > 14 considered "High." None of the mixtures tested however has a low flow value.

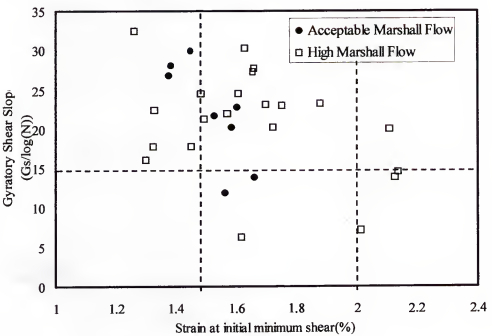

Figure 6-30 Analysis of Mixtures Based on Marshall Flow.

The Marshall flow is not able to differentiate between the mixtures with regard to rutting performance.

6.6.4 Analysis of Marshall Modulus

Based on the observation of the results, the Marshall modulus for all the mixtures were categorized as follows:

Marshall Modulus < 10,000 psi - considered low.

Marshall Modulus > 10,000 psi is acceptable.

The plot of the Marshall modulus is shown in Figure 6-29.

The Modulus identified most of the good performance mixtures, however, dry mixtures could not be identified.

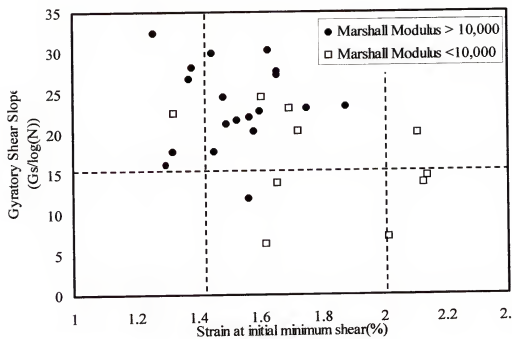

Figure 6-31. Analysis of mixtures based on Marshall modulus

6.7 Summary and Conclusions of the SGC Evaluation

The tests with the Servopac Superpave gyratory compactor have shown that both the shear resistance of a mixture and the resistance to destabilization by high shock loads effects of HMA mixtures are necessary for the mixture's resistance to permanent deformation. Using one of these factors alone may not be able to explain the behavior of all the different types of mixtures used in pavement construction. The slope of the plot of the gyratory shear resistance versus the logarithm of cycles at 1.25 angle of gyration was found to correlate well with the rutting resistance of the mixtures tested. However, the shear slope alone could not be used the rutting behavior of all the 31 mixtures tested.

A modified compaction procedure of initially compacting the mixtures at 1.25 degrees angle to 7% air voids followed immediately with compaction at 2.5 degrees angle to simulate excessively heavy loading immediately after construction was evaluated.

The shear resistance in this mode of compaction initially starts at a high value, drops to an initial minimum value after some few cycles, and thereafter begins to rise again to a maximum before finally dropping. The strain at the initial minimum shear, an apparent indication of the stability of the mixtures, was found to have some correlation with mixture rutting resistance.

Based on the results of the two testing modes, limits were set for the screening of Superpave mixtures in conjunction with the volumetric properties of the mixtures. A shear slope of 15 was set as a lower limit of acceptance while a strain of 1.40 was set as a lower limit of acceptance. Mixtures with shear slope values less than 15 are likely to be prone to stability problems, as such mixtures are likely to have excessively high VFA values. Mixtures with low strain values (<1.4%) are likely to be dry mixtures with excessively low VFA values or may have high dust to asphalt ratio, and are likely to have durability problems.

Limited testing at an angle of 2.5 degrees made of six mixtures showed that mixture behavior beyond the peak gyratory shear is influenced by a variety of factors, among which are aggregate shear strength, asphalt content and aggregate degradation. Comparing different mixtures based on observations of this region of the compaction curve will therefore be erroneous. However, for the same mixture, the effect of changes in asphalt content could be captured. The parameter of the ratio of the gyratory shear at the maximum number of cycles (Nmax) to the maximum gyratory shear resistance

(Gsmax) clearly distinguishes the sensitivity of the mixtures to changes in asphalt content. This may be a valuable tool in quality control/quality assurance during construction. The analysis presented should hold for different traffic categories because mixtures are expected to perform well for the traffic level they are designed for. Hence, in the range of 7% to 4% air voids, irrespective of the traffic level, the shear will characterize the mixture behavior.

6.8 Recommendations

The following recommendations are made for the use of the SGC procedure provided in this report as a tool for assessing the rutting resistance of HMA mixtures. This research is conducted solely on 12.5mm mixtures, and therefore the results need to be tested with mixtures of other nominal maximum size aggregate blends. Based on the results, the limits may either be maintained or reviewed to reflect the behavior of such mixtures.

The effect of mixture instability after the switch in angle need to be further studied. A device to measure the lateral pressure in the SGC may help in the understanding of the contribution of destabilizing resistance to mixture performance.

The specified APA rut depth of 8.0mm ((Kandhal and Cooley (2002)), may not be appropriate for the traffic level under which the mixtures in this research are designed. (< 30 million ESALS). If the APA is to be used for the characterization of mixtures, there is the need to set different limits for different traffic levels. The unexplained rutting behavior of project number 7, which was designed with a lower traffic level than all the other mixtures, is one example where the APA results may give some misleading conclusions. For the traffic level for project 7 (< 3 million ESALS), the Servopac

analysis shows the mixture to have good rutting resistance, however, the APA rut depth measurement was high. This is so because the mixture was subjected to the same number of APA wheel passes (8,000) as the other mixtures which were designed for higher traffic.

CHAPTER 7
RESULTS OF SIMPLE PERFORMANCE TESTING

7.1 Introduction

Test results of the proposed Superpave™ simple performance testing at 10°C and 40°C are presented. The various analysis methods described in Chapter 2 are used to analyze these test results and the outcome compared with the rutting resistance represented by the measured rut depths from the Asphalt Pavement Analyzer (APA). Twenty mixtures, comprising of 9 of the FAA mixtures (WRF, CGF, RBF, CALF, CHF, CGC, RBC, CALC, and CHC), 5 project mixes (P1, P2, P3, P5, and P7) and the six granite based mixtures (GAC1, GAC2, GAC3, GAF1, GAF2, and GAF3)..

7.2 Evaluation of Dynamic Test results for HMA Rutting Resistance

In this section, the dynamic modulus measurements and related parameters are compared to the rutting performance of the various mixtures as measured by the APA rut depths. Parameters which are found to correlate well with the rutting resistance of the mixtures are then compared with the parameters developed from the gyratory compactor in an attempt to differentiate the substandard mixtures based on the dynamic test results. For the evaluation of the rutting resistance of HMA mixtures, evaluation of the stiffness at high temperatures, when pavement rutting is likely to occur is performed. In this work, rutting resistance is evaluated at the high temperature of 40°C at the frequencies of 1 Hz, 4Hz and 10Hz. Berthelot et al. (1996), proposed the following ranges of testing frequencies for simulating various highway speeds:

- 0.02 – 0.2Hz to simulate parking

- 0.2 – 2.0Hz to simulate street and intersection speed
- 2.0 – 20Hz to simulate highway speed.

Shenoy and Romero (2002) and Witczak et al. (2002), used a testing frequency of 5.0Hz as representative of traffic speed that will trigger pavement rutting in the evaluation of the Superpave™ simple performance tests. Test results were therefore plotted for the lower frequencies of 1.0Hz and 4 Hz.

7.2.1 Evaluation of the Dynamic Modulus E*

Figure 7-1 shows the dynamic modulus, E*, plotted against the APA rut depth measurements for the mixtures tested.

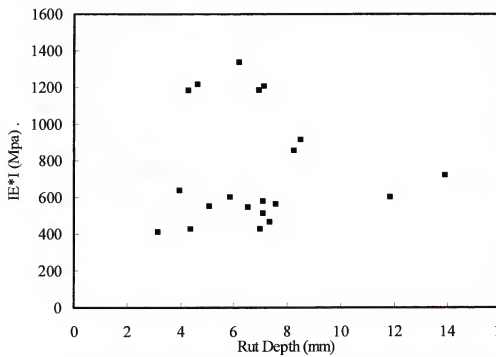

Figure 7-1. Plot of dynamic modulus, E* at 40°C for 1.versus APA rut depths

Figure 7-1 shows no correlation of dynamic modulus with the rutting resistance as measured by the APA for all the mixtures tested at 1Hz. frequency. The trend at 4Hz. was not different.

To check if the scatter in the plot might be due to gradation effects, Figures 7-2 was plotted for the fine graded and coarse graded mixtures for a frequency of 4Hz.

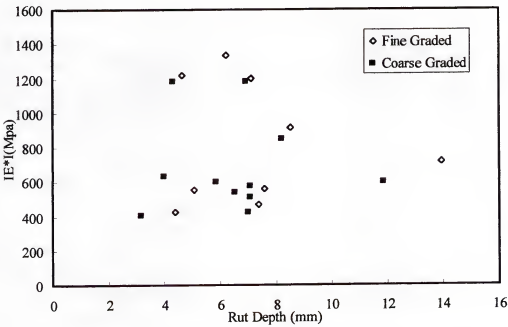

Figure 7-2. E* at 40°C and 1Hz, versus APA rut depth for the fine and coarse graded mixtures

The plot however, indicates no relationship between the dynamic modulus and the rut resistance for both fine and coarse graded mixtures at the high temperature of 40°C and low frequency of 1Hz. at which pavement rutting is most likely to occur. A similar trend was observed at 4Hz. testing frequency.

7.2.2 Evaluation of $|E^*|/\sin\phi$

The viscous stiffness based on the Maxwell model (Ullidtz (1987)), $|E^*|/\sin\phi$, at 40°C and 1 frequency was plotted against the APA rut depth to observe any relationship of this parameter with the rutting resistance of the mixtures tested.

Figures 7-3 and 7-4 show the plots for all the mixtures, the fine graded mixtures and the coarse graded mixtures respectively.

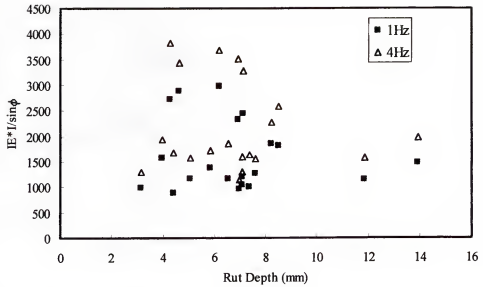

Figure 7-3. Plot of E*/Sinϕ at 40oC and 1 and 4Hz. versus the APA rut depths for all mixtures

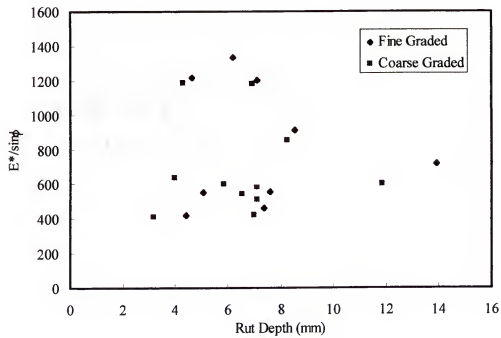

Figure 7-4. Plot of E*/Sinϕ at 40°C and 1Hz. versus the APA rut depths for the fine and coarse graded mixtures

7.2.3 Evaluation of |E*|sinϕ

The loss modulus, |E*|sinϕ, at 40°C and 1 frequency was plotted against the APA rut depth to observe any relationship of this parameter with the rutting resistance of the mixtures tested. Figure 7-5 shows the plot for all the mixtures, the trend with the APA rut depth is similar to the |E*| and |E*|/sinϕ plots. There was no correlation between this parameter and the rutting resistance of the mixtures as measured with the APA.

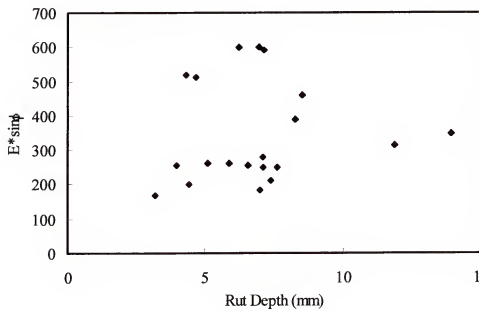

Figure 7-5. Plot of E*/Sinϕ at 40°C and 1Hz. versus the APA rut depths for the coarse graded mixtures

7.2.4 Evaluation of Dissipated Energy

Figures 7-6 shows the plot of dissipated energy for all the mixtures at 40°C and for 1Hz. frequency.

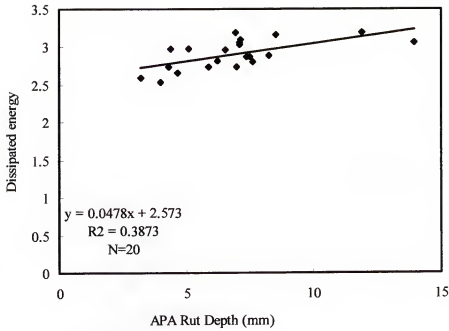

Figure 7-6. Dissipated energy versus APA rut depth at 40°C for all mixtures

There appear to be some trend in the data. However, in view of the low R^2 value, Figure 7-7 was plotted to examine the relationship of the dissipated energy with the rutting behavior of the fine and coarse graded mixtures. The plot shows better correlation of the dissipated energy with the rutting resistance of the mixtures tested. The R^2 for the fine graded mixtures was 0.4815 while the R^2 for the coarse graded mixtures was 0.7209. The dissipated energy may therefore be a measure of the internal resistance of the mixtures tested. Coarse graded mixtures have better aggregate to aggregate contacts and their shear performance is more driven by aggregate interlock than fine graded mixtures. Aggregate effects may therefore be more pronounced in coarse graded mixtures than in fine graded mixtures. The better correlation of the dissipated energy with rutting resistance as measured with the APA shows that the shear or interlock properties of mixtures are influencing the mixture behavior in these equipment.

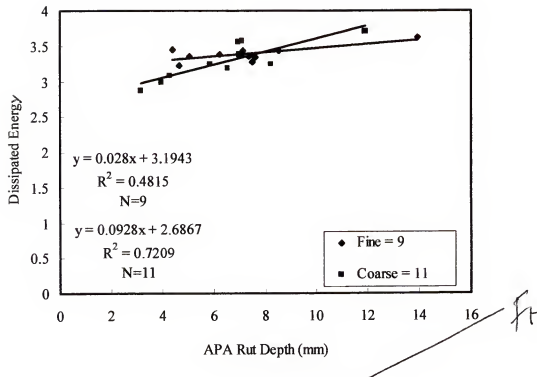

Figure 7-7: Plot of dissipated energy at 40°C and 1Hz versus APA rut depth for the fine and coarse graded mixtures.

7.2.4 Evaluation of Dynamic Creep Parameters

The dynamic creep parameters obtained by the method presented by Zhang et al (1997) are plotted against the APA rut depths for any correlation of the parameters with the rutting resistance of the mixtures tested.

Figure 7-8 –7-10 show plots of the dynamic creep parameters of D_1, m-value and estimated compliance at 100 seconds respectively versus the APA rut depth measurements for all the mixtures. These plots are for the 40°C temperature tests. The computations were effected using a Mathcad program, which calculates the m-value, D_1 value.

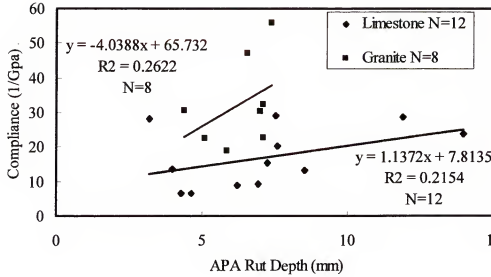

Figure 7-8. Dynamic creep parameter D_1 versus APA rut depth at 40°C

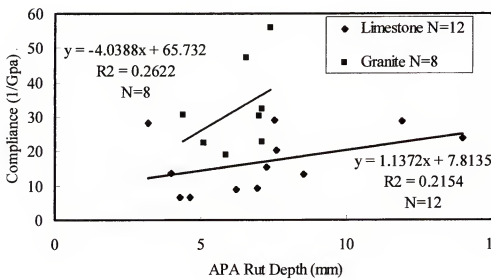

Figure 7-9. Dynamic creep parameter m-value versus APA rut depth at 40°C

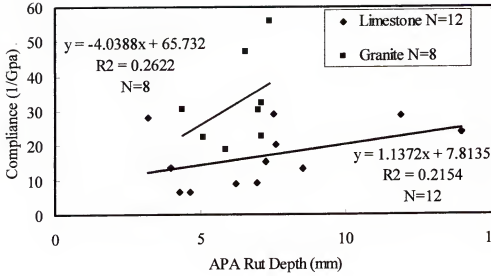

Figure 7-10. Estimated dynamic creep compliance at 100 seconds versus APA rut depth at 40°C

Generally, there appears to be a trend in the relationship for the dynamic creep parameters with the APA rut depth measurements for the limestone based mixtures. The m-value from the dynamic test has the highest correlation, R^2 value of 0.7999. Though the granite based mixtures displayed similar trend with the APA (lower the parameter, the lower the APA rut depth) as expected, the correlation is rather weak. The granite based mixtures appear to have higher creep parameters than the limestone based mixtures.

7.3 Evaluation of Static Creep Parameters

Figures 7-11 shows the variation of the static creep compliance parameters at 10°C with the APA rut depth for 17 of the mixtures tested (Without GAC1, GAC3 and CHC). In general, the lower the creep compliance, the lower the rut depth. However, the R^2 value of 0.3473 is low. The m-value and D_1 parameters are therefore plotted to observe how they vary with the rutting performance of the mixtures as measured with APA.

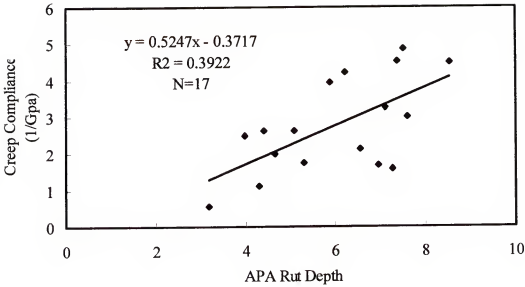

Figure 7-11. Static creep compliance versus APA rut depth at 10°C.

Figure 7-12 shows the plot of the m-value for the mixtures. The plot indicates that the m-value of coarse graded mixtures correlates with the rutting performance as measured with the APA. The m-value of the fine graded mixtures however did not correlate with the rutting performance as measured with the APA. As observed in the case of the dissipated energy, the m-value, may be more related to the shear/interlock properties of the mixtures. The good correlation for coarse graded mixtures may be an indication of the different interlocks provided by the different gradations. The fine graded mixtures may have formed their structure already and the shear at this time may not be a major influence in the behavior of the mixtures in the dynamic testing mode. Figure 7-13 shows the plot of the static creep parameter D_1.

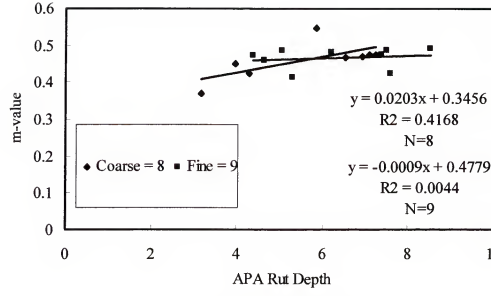

Figure 7-12. M-value versus APA rut depth at 10°C for fine and coarse graded mixtures

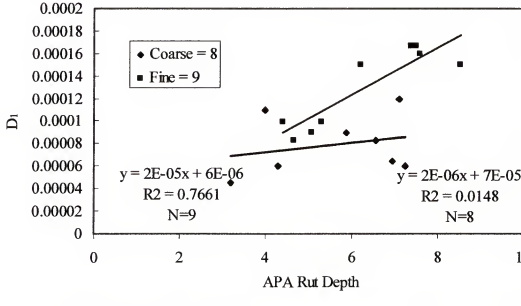

Figure 7-13. D_1 values from static creep test versus APA rut depth at 10°C for fine and coarse graded mixtures

The plot shows that the D_1 parameter has good correlation with the rutting performance of the fine graded mixtures, The R^2 for the correlation for the fine mixtures

is 0.766. The correlation of the m-value with the rutting performance of the coarse graded mixtures is however not so good. Both the fine and coarse graded mixtures followed the same trend. The lower the D1 value, the lower the rutting resistance as measured with the APA.

The static creep test at 40°C did not yield good results. The probable reason may be due to the short test duration of 1000 seconds (15 minutes). Generally the lstatic creep test at high temperatures is performed for long periods. The Texas Department of Transportation procedure recommends testing for a time period of 3 hours with a relaxation period of 10 minutes after the test. This procedure will allow for the evaluation of the secondary as well as the tertiary creep of the material.

7.4 Comparison with Servopac Results

The m-value and dissipated energy from the dynamic testing, which were found to have some correlation with the rutting performance of the mixtures, were compared with the results from the Servopac gyratory compactor to obtain an understanding of mixture behavior in the SGC.

7.4.1 Strain at Initial Minimum Gyratory Shear

Figures 7-14 and 7-15 show plots of the strain at the initial minimum gyratory shear with the damping energy and m-value respectively. The plots show no clear trend between the damping energy and the strain at the initial minimum gyratory shear from the modified Servopac compaction procedure. However, there appears to be some trend between the strain and the m-value, though the R2 of 0.0799 is rather low. The four mixtures with high strain values (>2.0%), project number 1, GAC1, RBC and RBF, appears to be separated from the rest of the mixtures.

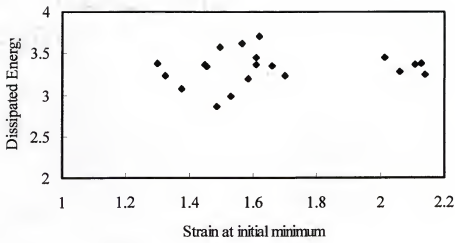

Figure 7-14 Dissipated energy versus strain at initial minimum gyratory stress.

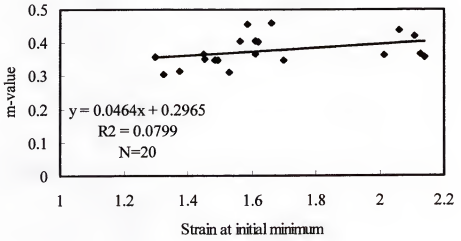

Figure 7-15 M-value versus strain at initial minimum gyratory stress

On removal of these mixtures from the plot, there was an improvement of the R^2 value to 0. 3517 as shown in Figure 7-16. Mixtures with low strain had low m-value. This behavior is as expected as mixtures with low strain values generate high internal confinement, leading to low m-values.

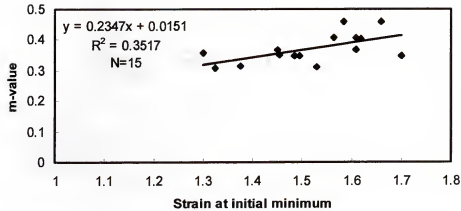

Figure 7-16 M-value versus strain at initial minimum gyratory shear without mixtures of high strain values.

Figure 7-17 shows the plot of the m-value versus the strain for the fine and coarse graded mixtures. The correlation of the m-value with the strain appears to be better for the fine graded mixtures.

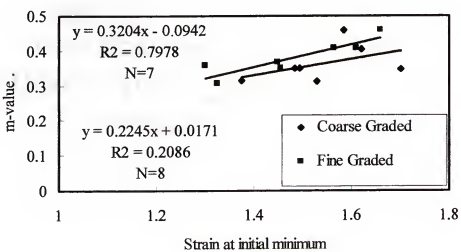

Figure 7-17 M-value versus strain at initial minimum gyratory shear for fine and coarse graded mixtures.

7.4.2 Gyratory Shear Slope

Figures 7-18 and 7-19 show the plot of the gyratory shear slope versus the dissipated energy and the m-value respectively.

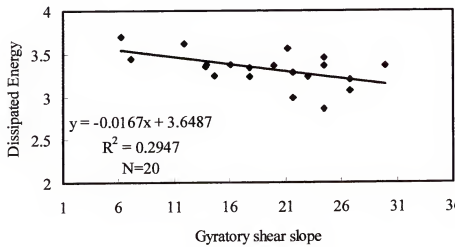

Figure 7-18 Dissipated energy versus gyratory shear slope

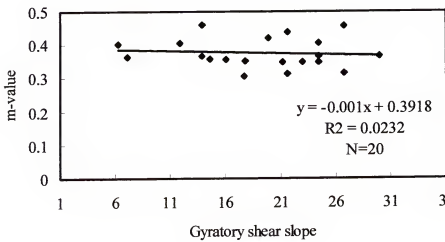

Figure 7-19 M-value versus gyratory shear slope

There appears to be a trend in the variation of the dissipated energy with the gyratory shear slope. Higher the dissipated energy, the lower the gyratory shear slope.

The dissipated energy, is a measure of the internal resistance of materials (Findley et al 1976). A correlation with the shear resistance of the material is therefore expected. There is however, no definite trend in the variation of the m-value with the gyratory shear slope. Figure 7-20 shows the plot of the fine and coarse graded mixtures.

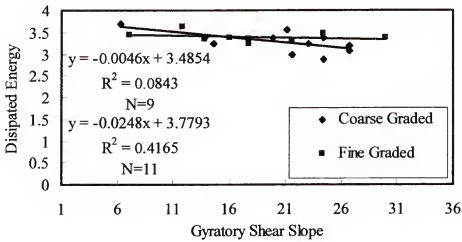

Figure 7-20 Dissipated energy versus gyratory shear slope for fine and coarse graded mixtures

The correlation of the dissipated energy with the gyratory shear slope is better for coarse graded mixtures. The dissipated energy may be more influenced by the coarse aggregates in the mixture. Generally, the coarse aggregates provide the required interlock in a mixture to resist shearing of the aggregates. The changes in aggregate interlock in fine gradations may not be adequate to be captured by the damping energy.

7.5 Summary of Simple Performance Testing

The complex modulus testing showed the following results.

- The dissipated energy at 1Hz testing frequency at a temperature of 40°C was found to be the best parameter that correlated with the rutting resistance of the mixtures tested in this work.

- The E*and E*/sinϕ parameters from the dynamic modulus test did not correlate well with the rutting resistance of the mixtures tested.
- The computed m-value from the dynamic test showed correlated well with the rutting resistance of the limestone mixtures tested. There was a good trend for the granite mixtures, however the correlation was weak.
- The static creep compliance at 10°C showed a good trend with the rutting resistance of the mixtures tested, however, the correlation was not very good (R^2=0.3437).
- The m-value from the static creep test showed a good trend with the rutting performance as measured with the APA. There was however no trend for the fine graded mixtures.
- The D_1 parameter from the static creep test showed a good trend and good correlation (R2=0.766) with the rutting performance as measured with the APA. The trend for the coarse graded mixtures was however not very good.
- The static creep testing at 40°C did not yield good results due to the short duration of testing. The testing time need to be reviewed to follow the Texas Department of Transportation procedure of testing for 3 hours.
- Correlation of the simple performance testing with the parameters developed from the SGC showed good trend, however, different parameters need to be used in characterizing coarse and fine graded mixtures, as the results show that the two gradations have different rutting behavior.

CHAPTER 8
CLOSURE

8.1 Summary of Findings

The gyratory shear strength from the Superpave gyratory compactor (SGC), was evaluated for use as a parameter in hot mix asphalt (HMA) evaluation and screening with respect to their rutting performance. A total of 32 mixtures, comprising of ten (10) mixes for fine aggregate angularity (FAA) effects, eight mixtures of limestone based for study of gradation effects, eight field mixtures and six granite based mixtures for aggregate type effects. Parameters developed in this work, the slope of the plot of gyratory shear versus the logarithm of cycles, and the strain at the initial minimum shear strength for a modified compaction procedure, correlated better with rut depth measurements from the APA test.

Evaluation of existing methods of analysis of measurements from the Superpave Gyratory Compactor on the mixtures tested gave the following results:

- The use of the compaction slope (%Gmm versus the logarithm of cycles), correlated well with both the APA rut depth measurements and IDT creep compliance. This method, however, does not provide a means of screening good mixtures from bad ones with respect to their rutting performance, Moreover, the range of the slope values (4 to 5) was too close to provide any meaningful insight into the performance of the different mixtures.
- The Densification Energy Index ($DEI_{92\text{-}96}$), proposed by Bahia et al (1998), did not be able to identify the mixtures tested with respect to their rutting behavior in

comparison with either the measurements from the IDT creep compliance or APA rut depths. The Terminal Densification Energy ($_{TDI92-98}$) was however not evaluated in this work. Mixtures which are dry (low VFA), and mixtures with soft aggregates which may breakdown during compaction, may seem to be good performing mixtures when evaluated with this method.

- The N-SRmax parameter proposed by Anderson (2002), did not work well for the granite mixtures tested, even though comparable results were obtained for the limestone based mixtures. The granite mixtures had very low N-SRmax values, which classify them as poor mixtures. APA measurements and field performance however, does not show these mixtures as poor performing.

This study provided a comprehensive study of the compaction curve in terms of the relationship between the gyratory shear strength and air voids as well as with compactive effort (number of cycles). Four distinctive zones of the compaction curve were identified. The initial contact zone where aggregate to aggregate contact is made, the volumetric compaction zone where the shear strength has a linear relationship with change in air voids, the densification zone which is representative of conditions in the field similar to when traffic densification occurs and finally the post peak zone after the maximum gyratory shear strength is attained. The findings in these zones are summarized below.

- On compaction, the gyratory shear strength increases rapidly during the initial 2 or 3 cycles, after which the increase becomes more gradual. The point of change in this increase was termed the point of initial contact when aggregate particles are in contact with each other.
- From the point of initial contact onwards, the plot of the change in gyratory shear strength versus change in air voids was linear up to a point when the linearity stops. The slope of these plots correlated well with the fine aggregate angularity of the

FAA mixtures. This is in agreement with the findings of Brown and Cross (1992), that at high air void levels, the FAA influences the performance of mixtures. In this region, the controlling process is aggregate reorientation, which leads to volume reduction. This region of the curve is termed the volumetric compaction zone.

- Air void levels at the point where the linearity in the plot of gyratory shear strength versus change in air voids stops are within the air voids levels when construction compaction is effected in the field.

- After the point where linearity ceases in the plot of change in gyratory shear strength versus change in air voids, the change in gyratory shear fluctuates, whilst the air voids keep on decreasing, an indication that the process of strength gain is principally shear driven. Plots of the gyratory shear strength versus the logarithm of cycles in this region were linear. The slope of the plots for the different mixtures correlated with the APA rut depth measurements and IDT creep compliance as well as field rut measurements. This region of the compaction curve is termed the densification zone.

- The portion of the curve after attaining maximum gyratory shear strength was termed the post peak zone. Most of the mixtures tested show a drop in gyratory shear strength on further compaction after the maximum gyratory shear strength is attained. Comparison of mixtures in this region by way of the drop in shear with the APA rut depth measurements did not show any trend. Extraction and recovery of the FAA mixtures after compaction showed substantial degradation of the aggregates in mixtures with soft aggregates such as Chattahooche. The degradation changes the gradation of the mixture, increases the total surface area of aggregates and subsequently the mixture volumetric properties. Comparing mixtures of different gradations and aggregate types in this zone could therefore be erroneous, however, for the same aggregate type and gradation, mixture sensitivity to changes in asphalt content was possible. Compaction at a higher angle of 2.5 degrees was able to define the post peak region better than the conventional compaction at 1.25 degrees even though the two give similar trends.

The use of the gyratory shear slope alone could not explain the behavior of substandard mixtures with respect to observations in the APA. Mixtures with low VFA and VMA, which do not satisfy the Superpave mix design criteria had low values of rut depths in the APA, while mixtures with rounded aggregates and high VMA and VFA showed high rut depths as expected. Khandal et al (2001), have set a maximum value of rut depth of 8.0mm from APA measurements as maximum acceptance rut depth for good

performance mixtures. There is however no lower limit for acceptance or screening dry mixtures.

A modified compaction procedure with the SGC to simulate a loading condition in the field likely to result in pavement rutting, by first compacting the mixture to 7% air voids at an angle of 1.25 degrees followed immediately with compaction at 2.5 degrees angle for 100 cycles was evaluated. The findings of this modified compaction procedure are summarized below.

- The gyratory shear stress initially starts at a high value on switching the angle to 2.5 degrees. This high shear reduces to a minimum after a few cycles and thereafter gradually increases to a secondary maximum before finally dropping.
- Evaluation of various parameters after switching to the 2.5 degree angle showed that the volumetric strain at the initial minimum gyratory shear strength correlated well with rut performance as measured with the APA. This parameter, might be an indication of the mixture's resistance to shock loads. Generally, mixtures with low strain have good rutting performance while those with high strain have poor rutting performance.

Based on the analyses above, mixtures with high gyratory shear slope with conventional compaction and low strain to the initial minimum gyratory shear strength with the modified procedure are expected to have good rutting performance and mixtures with low shear slope and high strain to have relatively poorer rutting performance.

The results of the two methods plotted on the same graph revealed the following:

- A lower limit of shear slope from the conventional SGC procedure at 1.25 gyratory angle set at 15 was able to screen most of the mixtures that rutted in the APA (rut depth > 8.0mm) and had either rounded aggregates or high VFA.
- A lower limit of volumetric strain at the initial minimum gyratory shear during compaction with the modified SGC compaction procedure of 1.4% was able to screen most of the substandard mixtures with low VFA and VMA.
- A higher limit of volumetric strain at the initial minimum gyratory shear during compaction with the modified SGC compaction procedure of 2.0% was able to screen most of the plastic mixtures which show high rutting potential in the APA.

- Some coarse graded mixtures with low volumetric properties performed well . This observation confirms the findings of Nukunya (2001) that coarse graded mixtures are over-asphalted, if the same volumetric standards used in the Superpave design are employed.

- The selected Superpave simple performance tests of dynamic modulus and static creep were evaluated to confirm the behavior of some of the mixtures tested and to further evaluate some parameters from this test methods. The following is a summary of the test.

- The parameters of E* and E*/sinϕ did not correlate with the rutting resistance as measured with the APA.

- The damping energy, which is a measure of energy dissipation during cyclic loading, correlated well with the rutting resistance of the mixtures tested. The damping energy is a function of the phase angle only and is frequency dependent.

- The creep parameters of m-value and creep compliance derived from dynamic testing correlated well with the rutting resistance as measured with the APA. There is however the need to improve on the result by increasing the number of cycles of testing to ensure good estimation of parameters.

8.2 Conclusions

Analysis of the gyratory shear strength from the Superpave gyratory compactor (SGS) has been made and parameters developed which correlates with the rutting performance of HMA mixtures tested. Further modification of the testing procedure by initially compacting at 1.25 degrees angle to 7% followed immediately with compacting at 2.5 degrees angle provided additional insight into the stability of HMA mixtures.

The strain to the initial minimum gyratory shear in combination with the slope of the conventional compaction method can correctly screen mixtures with respect to their rutting performance. Mixtures which are prone to rutting have either low shear slope or high strain to the initial minimum gyratory shear in the modified procedure or both. Mixtures which have very low strain to the initial minimum gyratory shear (1.4%, are detected to be mostly dry mixtures with low VMA and high dust to asphalt ratio.

However some coarse mixtures which appear to be dry performed well in accordance with the analysis.

Results from the dynamic modulus testing at 40°C and 4Hz. can be used for the assessment of the rutting resistance of HMA mixtures. However, there is the need for more testing to establish a relationship between the rutting resistance of field mixtures and the damping energy as well as creep parameters from the dynamic test.

8.3 Recommendations

The following recommendations are provided for consideration:

- Evaluation of mixtures for rutting resistance should be made by consideration of not only the shear strength of the mixtures alone, but in addition, the resistance of the mixtures to destabilization of the aggregate structure.
- Efforts to measure the lateral pressure during the modified compaction in the SGC is encouraged, as this will provide a true measure of the frictional forces developed in the modified compaction procedure.
- More tests on field mixtures to establish a clear relationship between the dissipated energy of HMA their field rutting resistance is recommended.
- The use of creep parameters from the dynamic modulus test for the evaluation of HMA mixture rutting resistance should be further pursued, as this shows the promise of providing an answer to the Superpave performance prediction model for rutting.

APPENDIX A
BATCHWEIGHTS

Table A-1: Batch weight for Whiterock coarse / with Cabbage Grove Fines, Coarse graded mixture

Sieve Size	S1a	S1b	Screen	Filler
12.5	116	429	1981	3989
9.5	318	600	1981	3989
4.75	429	1981	1981	3989
2.36	429	1981	3051	3989
1.18	429	1981	3485	3989
600	429	1981	3732	3989
300	429	1981	3900	3989
150	429	1981	4065	3989
75	429	1981	4141	3989
<75	429	1981	4141	4382

Table A-2: Batch weight for Whiterock coarse / with Alabama Calera Fines, Coarse graded mixture

Sieve Size	S1a	S1b	Screen	Filler
12.5	116	429	1981	4318
9.5	318	600	1981	4318
4.75	429	1981	1981	4318
2.36	429	1981	3138	4318
1.18	429	1981	3607	4318
600	429	1981	3875	4318
300	429	1981	4057	4318
150	429	1981	4235	4318
75	429	1981	4318	4318
<75	429	1981	4318	4559

Table A-3: Batch weight for Whiterock coarse / with Georgia Granite (Ruby) Fines, Coarse graded mixture

Sieve Size	S1a	S1b	Screen	Filler
12.5	116	429	1981	4427.14
9.5	318	600	1981	4427.14
4.75	429	1981	1981	4427.14
2.36	429	1981	3192.56	4427.14
1.18	429	1981	3683.5	4427.14
600	429	1981	3963.5	4427.14
300	429	1981	4154.06	4427.14
150	429	1981	4340.2	4427.14
75	429	1981	4427.14	4427.14
<75	429	1981	4427.14	4668.14

Table A-4: Batch weight for Whiterock coarse / with Chattahooche Gravel Fines, Coarse graded mixture

Sieve Size	S1a	S1b	Screen	Filler
12.5	116	429	1981	4354
9.5	318	600	1981	4354
4.75	429	1981	1981	4354
2.36	429	1981	3156	4354
1.18	429	1981	3633	4354
600	429	1981	3904	4354
300	429	1981	4089	4354
150	429	1981	4270	4354
75	429	1981	4354	4354
<75	429	1981	4354	4595

Table A-5: Batch weight for Whiterock coarse / with Cabbage Grove Fines, Fine graded mixture

Sieve Size	S1a	S1b	Screen	Filler
12.5	231	853	1475	4140
9.5	633	922	1475	4140
4.75	853	1475	1475	4140
2.36	853	1475	2192	4140
1.18	853	1475	2893	4140
600	853	1475	3387	4140
300	853	1475	3733	4140
150	853	1475	4031	4140
75	853	1475	4140	4140
<75	853	1475	4140	4336

Table A-6: Batch weight for Whiterock coarse / with Alabama Calera Fines, Fine graded mixture

Sieve Size	S1a	S1b	Screen	Filler
12.5	231	853	1475	4357
9.5	633	922	1475	4357
4.75	853	1475	1475	4357
2.36	853	1475	2251	4357
1.18	853	1475	3009	4357
600	853	1475	3543	4357
300	853	1475	3917	4357
150	853	1475	4239	4357
75	853	1475	4357	4357
<75	853	1475	4357	4553

Table A-7: Batch weight for Whiterock coarse / with Georgia Granite (Ruby) Fines, Fine graded mixture

Sieve Size	S1a	S1b	Screen	Filler
12.5	231	853	1475	4495.51
9.5	633	922	1475	4495.51
4.75	853	1475	1475	4495.51
2.36	853	1475	2287.38	4495.51
1.18	853	1475	3080.88	4495.51
600	853	1475	3640.21	4495.51
300	853	1475	4031.63	4495.51
150	853	1475	4368.53	4495.51
75	853	1475	4492.41	4495.51
<75	853	1475	4492.51	4688.41

Table A-8: Batch weight for Whiterock coarse / with Chattahooche Gravel Fines, Fine graded mixture

Sieve Size	S1a	S1b	Screen	Filler
12.5	231	853	1475	4402
9.5	633	922	1475	4402
4.75	853	1475	1475	4402
2.36	853	1475	2263	4402
1.18	853	1475	3033	4402
600	853	1475	3576	4402
300	853	1475	3955	4402
150	853	1475	4282	4402
75	853	1475	4402	4402
<75	853	1475	4402	4598

Table A-9: Batch weight for Whiterock coarse mixture WRC1

Sieve Size	S1a	S1b	Screen	Filler
12.5	116	459	3306	4454
9.5	318	630	3306	4454
4.75	429	2011	3306	4454
2.36	445	2987	3472	4454
1.18	449	3127	3804	4454
600	450	3149	4054	4454
300	451	3158	4230	4454
150	452	3192	4376	4454
75	454	3226	4424	4454
<75	459	3306	4454	4500

Table A-10: Batch weight for Whiterock coarse mixture WRC2

Sieve Size	S1a	S1b	Screen	Filler
12.5	403	1591	3273	4409
9.5	1103	1692	3273	4409
4.75	1486	2508	3273	4409
2.36	1543	3084	3438	4409
1.18	1556	3167	3766	4409
600	1559	3180	4014	4409
300	1562	3185	4188	4409
150	1567	3206	4332	4409
75	1573	3226	4380	4409
<75	1591	3273	4409	4500

Table A-11: Batch weight for Whiterock coarse mixture WRC3

Sieve Size	S1a	S1b	Screen	Filler
12.5	122	1215	2970	4365
9.5	358	1320	2970	4365
4.75	1018	2171	2970	4365
2.36	1179	2773	3172	4365
1.18	1188	2859	3575	4365
600	1191	2873	3880	4365
300	1193	2879	4093	4365
150	1197	2900	4270	4365
75	1215	2921	4329	4365
<75	1215	2970	4365	4500

Table A-12: Batch weight for Whiterock coarse mixture WRC4

Sieve Size	S1a	S1b	Screen	Filler
12.5	122	1215	2970	4365
9.5	358	1320	2970	4365
4.75	1018	2171	2970	4365
2.36	1179	2773	3172	4365
1.18	1188	2859	3575	4365
600	1191	2873	3880	4365
300	1193	2879	4093	4365
150	1197	2900	4270	4365
75	1215	2921	4329	4365
<75	1215	2970	4365	4500

Table A-13: Batch weight for Whiterock coarse mixture WRC5

Sieve Size	S1a	S1b	Screen	Filler
12.5	119	462	2417	4500
9.5	462	462	2417	4500
4.75	462	2417	2417	4500
2.36	462	2417	3057	4500
1.18	462	2417	3642	4500
600	462	2417	3898	4500
300	462	2417	4076	4500
150	462	2417	4223	4500
75	462	2417	4351	4500
<75	462	2417	4351	4500

Table A-14: Batch weight for Whiterock Fine mixture WRF1

Sieve Size	S1a	S1b	Screen	Filler
12.5	231	914	2056	4454
9.5	633	983	2056	4454
4.75	853	1536	2056	4454
2.36	886	1928	2404	4454
1.18	893	1984	3097	4454
600	895	1993	3619	4454
300	897	1997	3986	4454
150	900	2010	4291	4454
75	903	2024	4392	4454
<75	914	2056	4454	4500

Table A-15: Batch weight for Whiterock Fine mixture WRF2

Sieve Size	S1a	S1b	Screen	Filler
12.5	416	1980	1980	4275
9.5	990	1980	1980	4275
4.75	1742	1980	1980	4275
2.36	1940	1980	2554	4275
1.18	1940	1980	2976	4275
600	1940	1980	3476	4275
300	1944	1980	3827	4275
150	1950	1980	4119	4275
75	1958	1980	4266	4275
<75	1980	1980	4275	4500

Table A-16: Batch weight for Whiterock Fine mixture WRF4

Sieve Size	S1a	S1b	Screen	Filler
12.5	210	696	1433	4374
9.5	696	696	1433	4374
4.75	696	1433	1433	4374
2.36	696	1433	2208	4374
1.18	696	1433	2801	4374
600	696	1433	3314	4374
300	696	1433	3734	4374
150	696	1433	4108	4374
75	696	1433	4374	4374
<75	696	1433	4374	4500

Table A-17: Batch weight for Whiterock Fine mixture WRF5

Sieve Size	S1a	S1b	Screen	Filler
12.5	209	693	1801	4427
9.5	693	693	1801	4427
4.75	693	1801	1801	4427
2.36	693	1801	2200	4427
1.18	693	1801	3069	4427
600	693	1801	3585	4427
300	693	1801	3939	4427
150	693	1801	4204	4427
75	693	1801	4427	4427
<75	693	1801	4427	4500

Table A-18: Batch weight for Whiterock Fine mixture WRF6

Sieve Size	S1a	S1b	Screen	Filler
12.5	211.5	693	1431	4369.5
9.5	693	693	1431	4369.5
4.75	693	1431	1431	4369.5
2.36	693	1431	2606.5	4369.5
1.18	693	1431	3042	4369.5
600	693	1431	3559.5	4369.5
300	693	1431	3928.5	4369.5
150	693	1431	4234.5	4369.5
75	693	1431	4369.5	4369.5
<75	693	1431	4369.5	4500

Table A-19: Batch weight for Georgia Granite Coarse mixture GAC1

Sieve Size	#7 stone	# 89 stone	W-10 scr	Filler
12.5	128.0	539.5	2182.5	4727.6
9.5	539.5	539.5	2182.5	4727.6
4.75	539.5	2182.5	2182.5	4727.6
2.36	539.5	2182.5	3447.6	4727.6
1.18	539.5	2182.5	3957.2	4727.6
600	539.5	2182.5	4247.1	4727.6
300	539.5	2182.5	4444.3	4727.6
150	539.5	2182.5	4637.3	4727.6
75	539.5	2182.5	4727.6	4727.6
<75	539.5	2182.5	4727.6	4895.0

Table A-20: Batch weight for Georgia Granite Coarse mixture GAC2

Sieve Size	#7 stone	# 89 stone	W-10 scr	Filler
12.5	444.1	1328.9	2649.4	4705.6
9.5	1328.9	1328.9	2649.4	4705.6
4.75	1328.9	2649.4	2649.4	4705.6
2.36	1328.9	2649.4	3520.2	4705.6
1.18	1328.9	2649.4	3972.3	4705.6
600	1328.9	2649.4	4252.8	4705.6
300	1328.9	2649.4	4445.8	4705.6
150	1328.9	2649.4	4626.0	4705.6
75	1328.9	2649.4	4705.6	4705.6
<75	1328.9	2649.4	4705.6	4898.9

Table A-21: Batch weight for Georgia Granite Coarse mixture GAC3

Sieve Size	#7 stone	# 89 stone	W-10 scr	Filler
12.5	134.0	511.6	2175.6	4653.0
9.5	511.6	511.6	2175.6	4653.0
4.75	511.6	2175.6	2175.6	4653.0
2.36	511.6	2175.6	3227.0	4653.0
1.18	511.6	2175.6	3758.9	4653.0
600	511.6	2175.6	4098.8	4653.0
300	511.6	2175.6	4333.2	4653.0
150	511.6	2175.6	4547.8	4653.0
75	511.6	2175.6	4653.0	4653.0
<75	511.6	2175.6	4653.0	4881.3

Table A-22: Batch weight for Georgia Granite Coarse mixture GAF1

Sieve Size	#7 stone	# 89 stone	W-10 scr	Filler
12.5	255.0	774.6	1626.9	4689.7
9.5	774.6	774.6	1626.9	4689.7
4.75	774.6	1626.9	1626.9	4689.7
2.36	774.6	1626.9	2461.3	4689.7
1.18	774.6	1626.9	3264.2	4689.7
600	774.6	1626.9	3829.6	4689.7
300	774.6	1626.9	4223.7	4689.7
150	774.6	1626.9	4564.1	4689.7
75	774.6	1626.9	4689.7	4689.7
<75	774.6	1626.9	4689.7	4849.1

Table A-23: Batch weight for Georgia Granite Coarse mixture GAF2

Sieve Size	#7 stone	# 89 stone	W-10 scr	Filler
12.5	458.7	1092.2	1921.0	4577.5
9.5	1092.2	1092.2	1921.0	4577.5
4.75	1092.2	1921.0	1921.0	4577.5
2.36	1092.2	1921.0	2745.9	4577.5
1.18	1092.2	1921.0	3192.8	4577.5
600	1092.2	1921.0	3722.3	4577.5
300	1092.2	1921.0	4098.3	4577.5
150	1092.2	1921.0	4413.3	4577.5
75	1092.2	1921.0	4577.5	4577.5
<75	1092.2	1921.0	4577.5	4836.5

Table A-24: Batch weight for Georgia Granite Coarse mixture GAF3

Sieve Size	#7 stone	# 89 stone	W-10 scr	Filler
12.5	260.6	724.8	1698.7	4581.4
9.5	724.8	724.8	1698.7	4581.4
4.75	724.8	1698.7	1698.7	4581.4
2.36	724.8	1698.7	3169.6	4581.4
1.18	724.8	1698.7	3597.5	4581.4
600	724.8	1698.7	3981.6	4581.4
300	724.8	1698.7	4256.4	4581.4
150	724.8	1698.7	4489.2	4581.4
75	724.8	1698.7	4581.4	4581.4
<75	724.8	1698.7	4581.4	4863.9

Table A-25: Cumulative Batch Weight for Project #1

	#89 Stone	W-10 Gra	M-10 Gra
Sieve, mm			
19.0	0	2250	3092
12.5	0	2250	3092
9.5	0	2250	3092
4.75	1530	2284	3106
2.36	2205	2477	3345
1.18	2228	2696	3655
0.600	2228	2847	3866
0.300	2228	2965	4035
0.150	2228	3041	4162
0.075	2241	3069	4270
0	2250	3092	4500

Table A-26: Cumulative Batch Weight for Project #2

	#7 Stone	#89 Stone	W-10 Sc 1	W-10 Sc 2
Sieve, mm				
19.0	0	909	3065	4019
12.5	91	909	3065	4019
9.5	473	931	3065	4019
4.75	882	2439	3084	4019
2.36	891	3000	3322	4019
1.18	891	3021	3570	4019
0.600	891	3021	3732	4192
0.300	900	3021	3847	4317
0.150	900	3021	3933	4409
0.075	900	3043	3980	4457
0	909	3065	4019	4500

Table A-27: Cumulative Batch Weight for Project #3

	S-1-A Stone	S-1-B Stone	200 Scrn
Sieve, mm			
19.0	0	864	2372
12.5	346	864	2372
9.5	518	864	2372
4.75	812	1392	2478
2.36	812	2266	3095
1.18	812	2296	3542
0.600	821	2296	3883
0.300	829	2311	4074
0.150	838	2326	4330
0.075	838	2326	4415
0	864	2372	4500

Table A-28: Cumulative Batch Weight for Project #5

	FC-3 Stone	Med. Asph Scr	W-10 Scrns
Sieve, mm			
19.0	0	2826	3762
12.5	0	2826	3762
9.5	254	2826	3762
4.75	1667	2826	3762
2.36	2656	2901	3969
1.18	2713	3079	4168
0.600	2713	3275	4293
0.300	2741	3416	4375
0.150	2741	3622	4434
0.075	2769	3715	4470
0	2826	3762	4500

Table A-29: Cumulative Batch Weight for Project #7

Sieve, mm	S-1-A Stone	S-1-B Stone	Asphalt Scrns
19.0	0	1103	1665
12.5	287	1103	1665
9.5	584	1148	1665
4.75	1036	1457	1665
2.36	1036	1631	2034
1.18	1047	1637	2827
0.600	1047	1643	3423
0.300	1058	1648	3876
0.150	1058	1648	4273
0.075	1069	1648	4401
0	1103	1665	4500

APPENDIX B
SERVOPAC COMPACTION CURVES FOR FAA MIXTURES

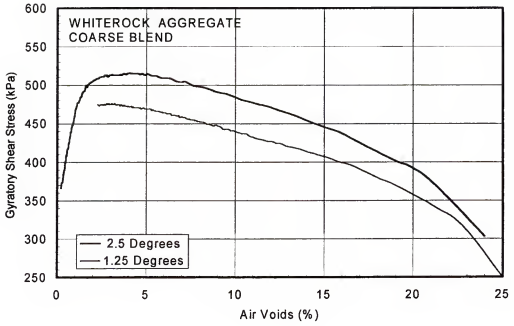

Figure B-1 Compaction Curve for WRC

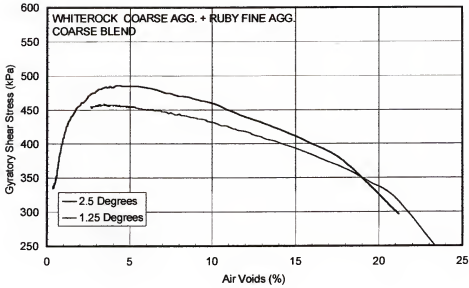

Figure B-2 Compaction Curve for RBC

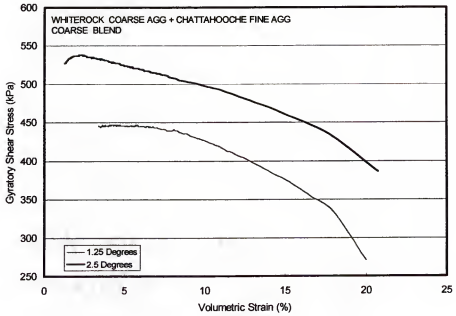

Figure B-3 Compaction Curve for CHC

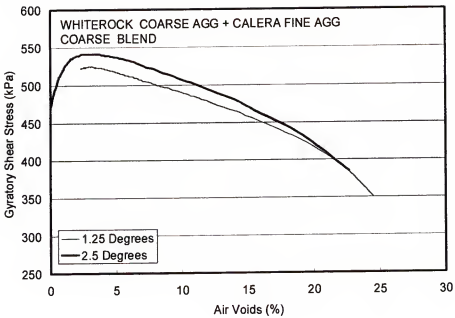

FigureB-4: Compaction Curve for CALC

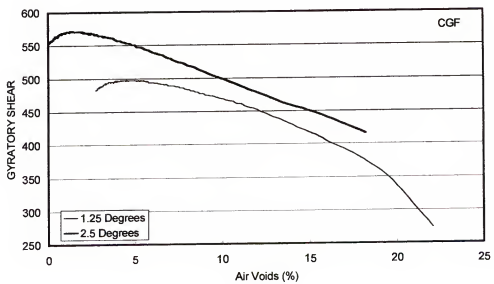

Figure B-5: Compaction Curve for CGF

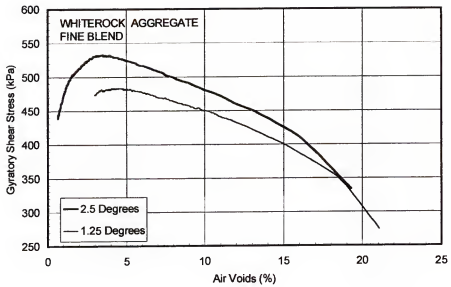

Figure B-6: Compaction Curve for WRF

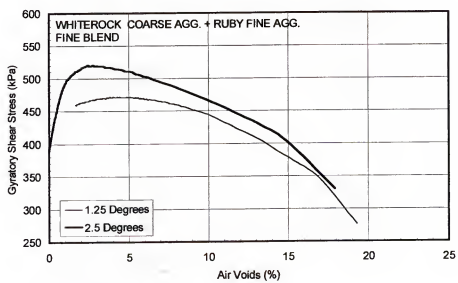

Figure B-7: Compaction Curve for RBF

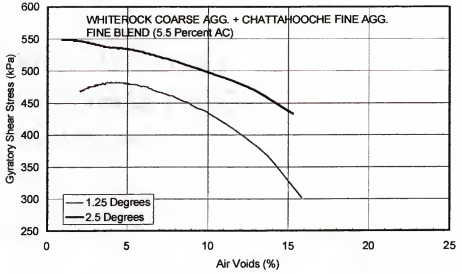

Figure B-8 Compaction Curve for CHF

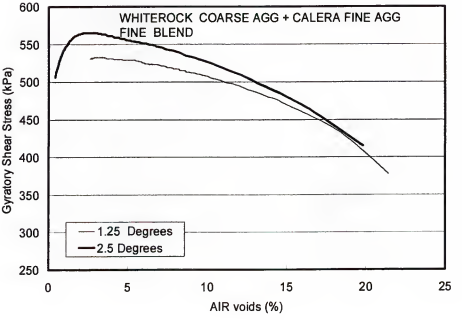

Figure B-9 Compaction Curve for CALF

APPENDIX C
GYRATORY SHEAR PLOTS FOR MODIFIED COMPACTION PROCEDURE

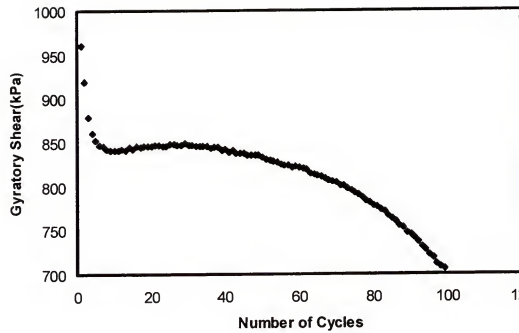

Figure C-1: Modified Compaction Plot for WRC1

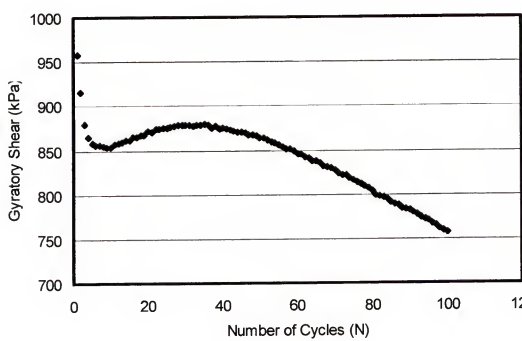

Figure C-2: Modified Compaction Plot for WRC2

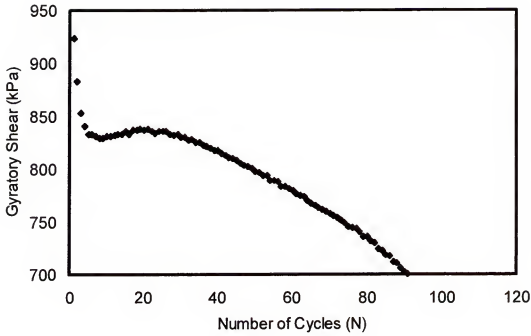

Figure C-3: Modified Compaction Plot for WRC3

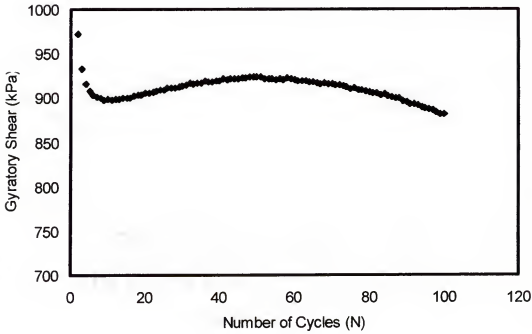

Figure C-4: Modified Compaction Plot for WRC4/F3

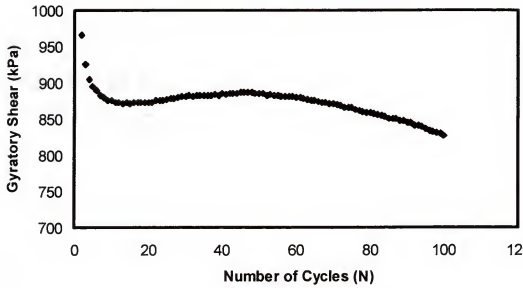

Figure C-5: Modified Compaction Plot for WRC5

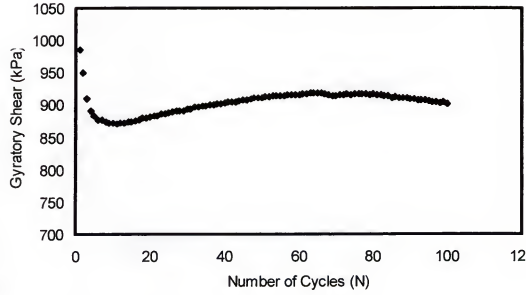

Figure C-6: Modified Compaction Plot for WRF1

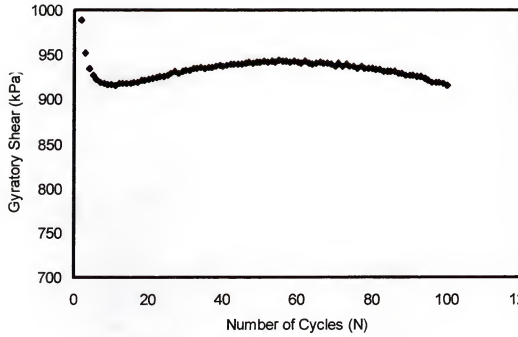

Figure C-7: Modified Compaction Plot for WRF2

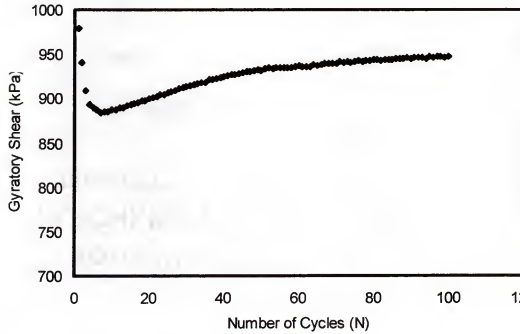

Figure C-8: Modified Compaction Plot for WRF4

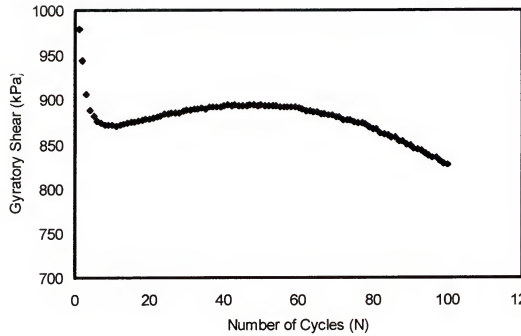

Figure C-9: Modified Compaction Plot for WRF5

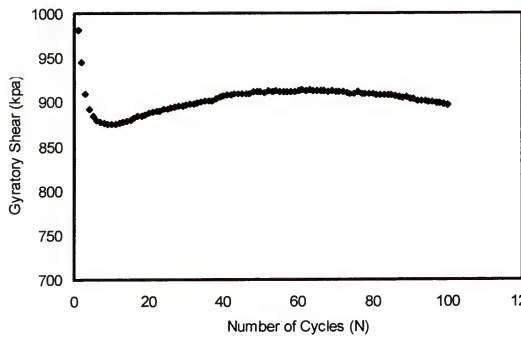

Figure C-10: Modified Compaction Plot for WRF6

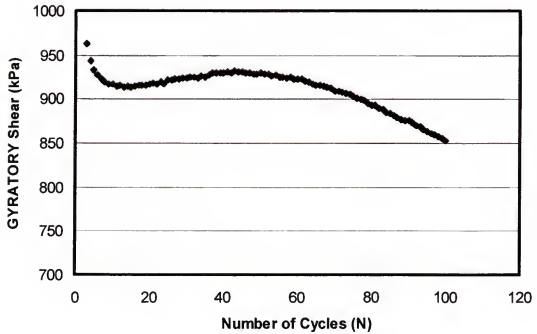

Figure C-11: Modified Compaction Plot for CGC

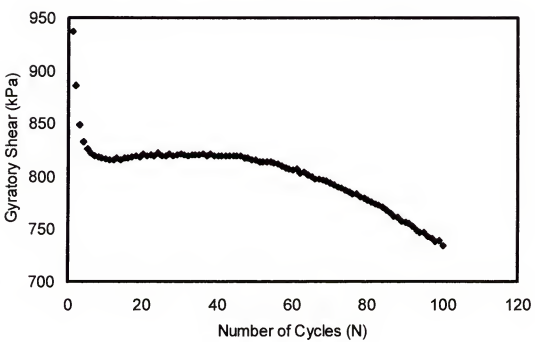

Figure C-12: Modified Compaction Plot for RBC

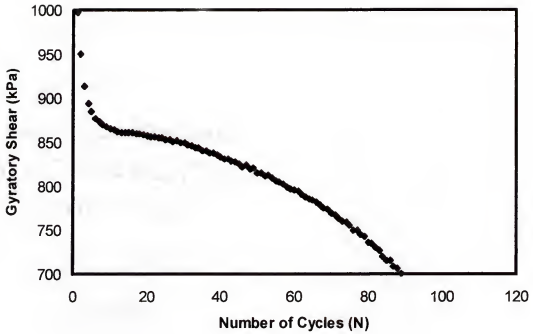

Figure C-13: Modified Compaction Plot for CALC

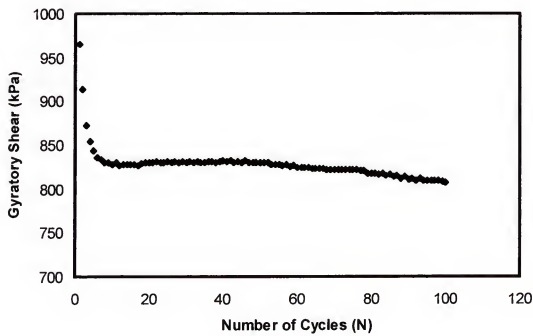

Figure C-14: Modified Compaction Plot for CHC

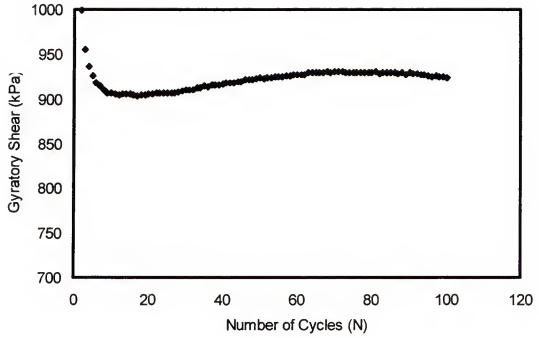

Figure C-15: Modified Compaction Plot for CGF

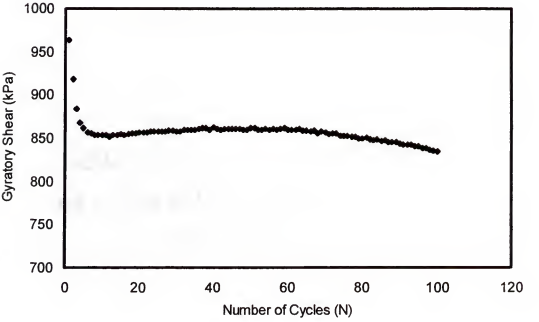

Figure C-16: Modified Compaction Plot for RBF

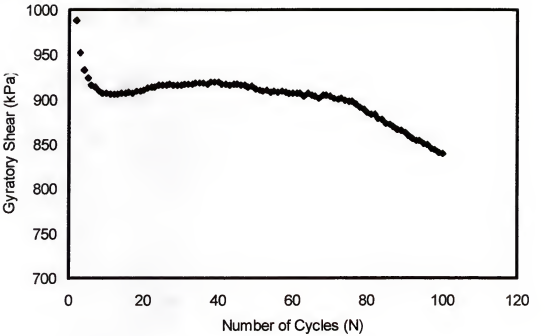

Figure C-17: Modified Compaction Plot for CALF

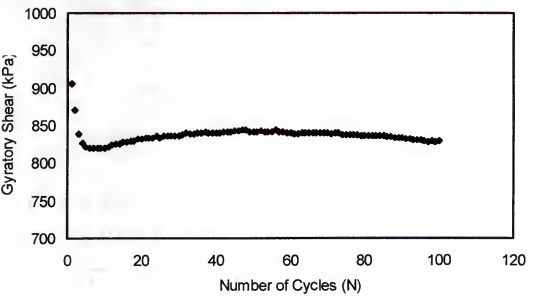

Figure C-18: Modified Compaction Plot for CHF

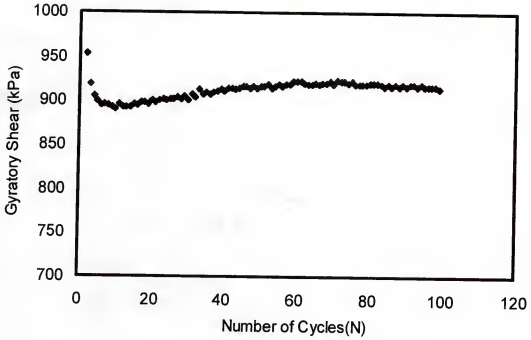

Figure C-19: Modified Compaction Plot for Project #1

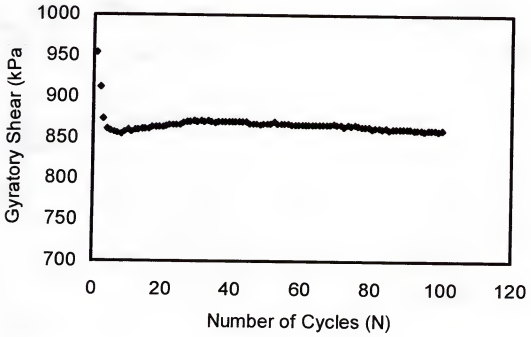

Figure C-20: Modified Compaction Plot for Project #2

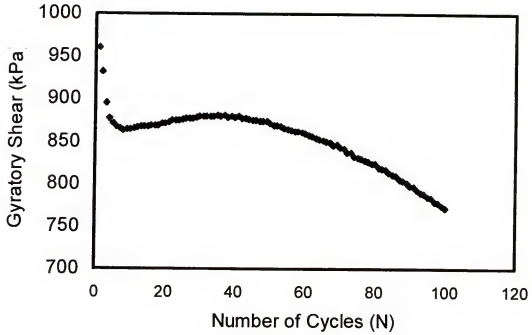

Figure C-21: Modified Compaction Plot for Project #3

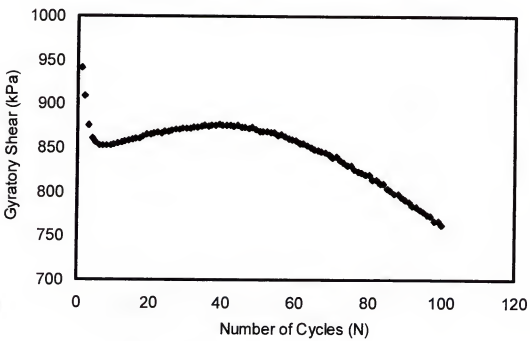

Figure C-22: Modified Compaction Plot for Project #7

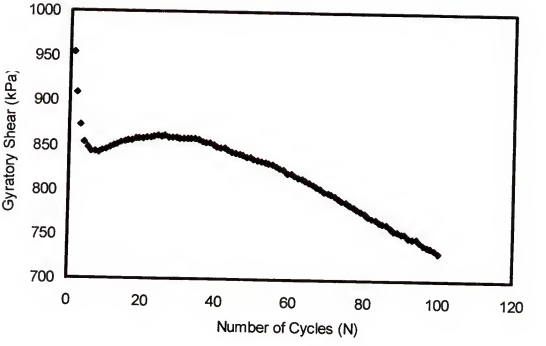

Figure C-23: Modified Compaction Plot for Project #8

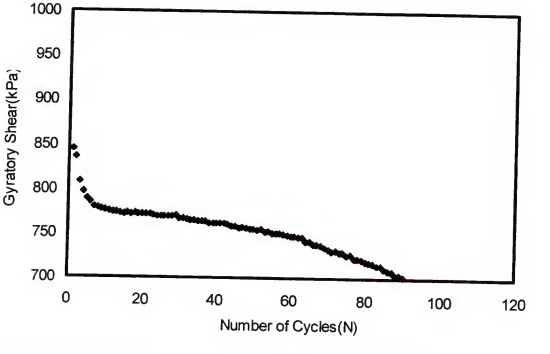

Figure C-24: Modified Compaction Plot for Granite Coarse Mix GAC1

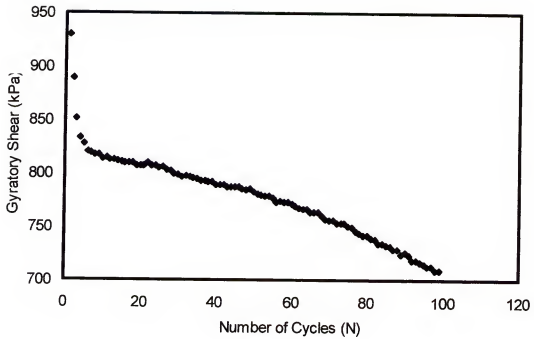

Figure C-25: Modified Compaction Plot for Granite Coarse Mix GAC2

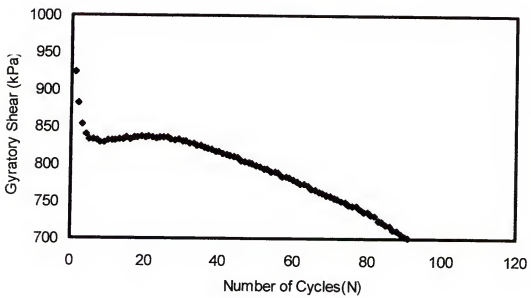

Figure C-26: Modified Compaction Plot for Granite Coarse Mix GAC3

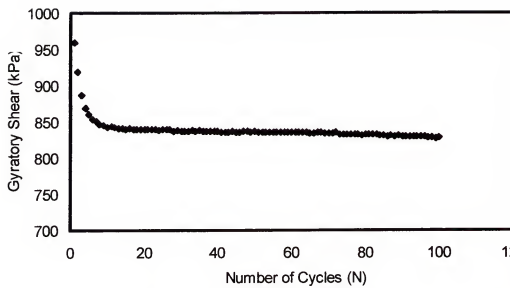

Figure C-27: Modified Compaction Plot for Granite Fine Mix GAF1

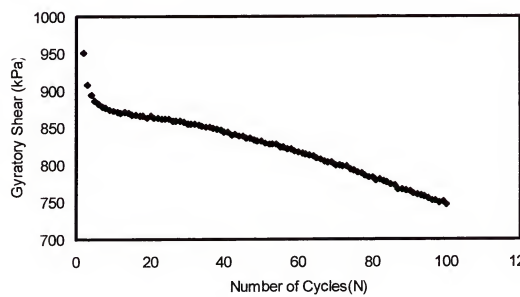

Figure C-28: Modified Compaction Plot for Granite Fine Mix GAF2

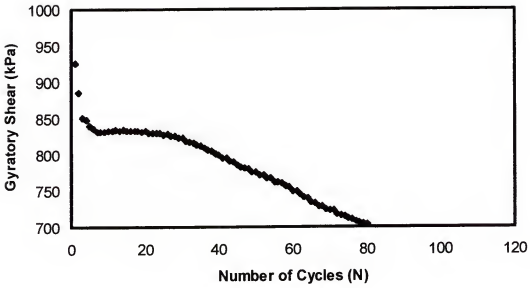

Figure C-29: Modified Compaction Plot for Granite Fine Mix GAF3

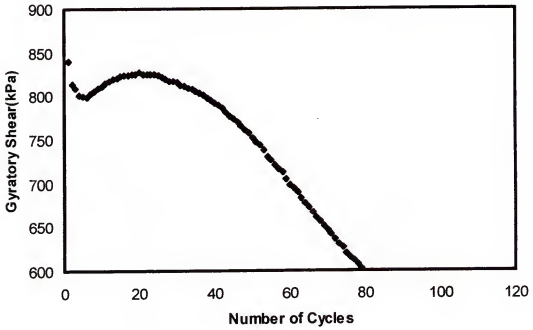

Figure C-30: Modified Compaction Plot for HVS 67-22 Mixture

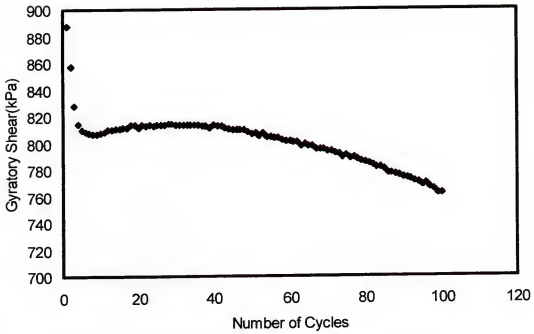

Figure C-29: Modified Compaction Plot for the HVS 76-22 mixture.

APPENDIX D
SEROPAC TEST RESULTS

Table D-1 FAA Mixtures

Mixture	Gs Slope in densification Zone	Strain at initial minimum Gs	APA rut depth(mm)
WRC	21.84	1.88	5.4
CGC	26.18	1.375	4.3
RBC	14.61	2.14	7.25
CALC	22.23	1.495	6.95
CHC	3.15	1.62	11.875
WRF	15.3	1.755	5.1
CGF	17.76	1.325	4.65
RBF	6.51	2.015	8.525
CALF	16.05	1.30	6.22
CHF	10.67	1.565	13.925

Table D-2 Whiterock Mixtures

Mixture	Gs Slope in densification Zone	Strain at initial minimum Gs	APA rut depth(mm)
WRC1	23.24	1.88	5.40
WRC2	20.17	1.725	4.57
WRC3	27.7	1.66	4.60
WRC4	30.22	1.63	4.30
WRC5	22.0	1.57	4.63
WRF1	23.04	1.755	5.10
WRF2	32.43	1.26	5.15
WRF4	28.11	1.385	4.25
WRF5	22.46	1.325	7.13
WRF6	27.22	1.66	4.775

Table D-3 Granite Mixtures

Mixture	Gs Slope in densification Zone	Strain at initial minimum Gs	APA rut depth(mm)
GAC1	13.8	2.128	7.0
GAC2	23.05	1.7	5.87
GAC3	24.46	1.61	7.1
GAF1	13.84	1.66	7.375
GAF2	29.95	1.45	5.075
GAF3	22.7	1.604	4.4

Table D-4 Field Projects and HVS Mixtures

Mixture	Gs Slope in densification Zone	Strain at initial minimum Gs	APA rut depth(mm)
P1	19.95	2.11	7.1
P2	20.25	1.585	6.55
P3	24.44	1.485	3.18
P5	22.43	-	3.98
P7	17.79	1.455	7.6
P8	21.68	1.530	5.5
HVS 67-22	21.68	2.06	7.5
HVS 76-22	21.89	1.60	5.3

APPENDIX E
MARSHALL TEST RESULTS

Table D-1 FAA Mixtures

Mixture	Marshall Stability (lbs)	Marshall Flow (x 0.01 in)	Marshall Modulus
WRC	1901	22.4	8,475.3
CGC	2063.8	14.0	14,741.4
RBC	1382.5	18.6	7,432.8
CALC	2087.7	15	13,918
CHC	1496.9	15.3	9,784
WRF	1713.8	16.2	10,598.6
CGF	2481	15.25	16,268.8
RBF	1353	14.17	9,548.3
CALF	1939	14.41	13,455.9
CHF	1590	10.67	14,901.6

Table D-2 Whiterock Mixtures

Mixture	Marshall Stability (lbs)	Marshall Flow (x 0.01 in)	Marshall Modulus
WRC1	1901	22.4	8,475.3
WRC2	1780	20.00	8,900.0
WRC3	1696	16	10,600.0
WRC4	1772	16.3	10,871.2
WRC5	1750	17.5	10,000.0
WRF1	1713.8	16.2	10,598.6
WRF2	1985.9	14.9	13,310.3
WRF4	2361.5	13.3	17,715.7
WRF5	1627.5	22.5	7246.2
WRF6	2257.5	15.4	14,640.1

Table D-3 Granite Mixtures

Mixture	Marshall Stability (lbs)	Marshall Flow (x 0.01 in)	Marshall Modulus
GAC1	1124.4	17.7	6,352.5
GAC2	1155.5	23.1	5013.0
GAC3	1109.9	17.7	6,270.6
GAF1	1274.5	13.33	9,561.1
GAF2	1590	13.0	12,230.8
GAF3	1478	12.1	12,194.7

Table D-2 Field Projects and HVS Mixtures

Mixture	Marshall Stability (lbs)	Marshall Flow (x 0.01 in)	Marshall Modulus
P1	1231.3	14.33	8,592.5
P2	1818.3	14.7	12,832
P3	2140.5	16.5	12,972.7
P7	1690.6	14.5	11,659.3
P8	2032.7	11.5	17,675
HVS 67-22	-	-	-
HVS 76-22	-	-	-

APPENDIX F
COMPLEX MODULUS TEST RESULTS

TableF-1 CGF

Temperature	Frequency	Sample	Modulus			Phase Angle
			Complex	Elastic	Loss	
10°C	16Hz	1	9827	9006.7	3930.8	23.6
		2	13902	12348	6306	27.3
		3	15796	15451	3281	22.0
		Average	13175	12268.57	4505.933	24.3
	10Hz	1	9630.4	9008.4	3404.8	20.7
		2	17152	15187	7971	27.7
		3	8150	7897.6	2012	14.3
		Average	11644.13	10697.67	4462.6	20.9
	4Hz	1	7889.7	7463	2557.9	18.9
		2	12098	11127	4748	23.1
		3	6885.6	6535	2169	18.36
		Average	8957.767	8375	3158.3	20.12
	1Hz	1	6769.3	6436.8	2095.6	18.9
		2	10013	9201	3950	23.2
		3	6617	6409	1647	14.4
		Average	7799.767	7348.933	2564.2	18.5
40°C	16HZ	1	2423.4	2026.9	1328.3	33.2
		2	2673	1986.8	1788.1	42.0
		3	2405	1823	1568	40.5
		Average	2500.467	1945.567	1561.467	38.6
	10Hz	1	2183.4	1880.3	1109.8	30.5
		2	2376.9	1892.2	1438.5	37.2
		3	2097.4	1723.5	1195.2	34.7
		Average	2219.233	1832	1247.833	34.2
	4Hz	1	1828.4	1594.8	894.2	29.3
		2	1820.1	1531.5	983.7	32.7
		3	1683	1444	853.7	30.9
		Average	1777.167	1523.433	910.5333	31.0
	1Hz	1	1264.5	1149.2	527.6	24.7
		2	1250.5	1103	589	26.1
		3	1138.3	1037.1	469.3	24.3
		Average	1217.767	1096.433	528.6333	25.0

Table F-2 RBF

Temperature	Frequency	Sample	Modulus			Phase Angle
			Complex	Elastic	Loss	
10°C	16Hz	1	10962	10431	3370	17.9
		2	8764	7503	4528	31.11
		3	8532	7912	3195	22
		Average	9419.333	8615.333	3697.667	23.67
	10Hz	1	10652	10249	2903	15.8
		2	8532.6	7366	4305	30.3
		3	8549	7982	3062	21
		Average	9244.533	8532.333	3423.333	22.36667
	4Hz	1	8827.4	8513	2335	15.3
		2	7162.5	6347	3319	27.6
		3	8026.3	7431.2	2822.1	21.5
		Average	7994.95	7430	2827	21.45
	1Hz	1	6871	6664	1671	14.1
		2	5613.65	4986.3	2578.8	27.3
		3	9112	8616.8	2964.8	19
		Average	7198.883	6755.7	2404.867	20.13333
40°C	16HZ	1	2294.8	1854.7	1351.5	36.1
		2	2148.55	1364.8	1659.3	50.5
		3	1760.8	1344.6	1136.9	40.2
		Average	2068.05	1521.367	1382.567	42.26667
	10Hz	1	2053	1744	1083	31.8
		2	1922.4	1565.5	1848.6	49.7
		3	1546	1252	907	35.9
		Average	1840.467	1520.5	1279.533	39.13333
	4Hz	1	1682.3	1476.2	806.7	28.65
		2	1434.6	1121.6	893.6	38.5
		3	1149	965.9	622.3	32.8
		Average	1421.967	1187.9	774.2	33.31667
	1Hz	1	1173.1	1055.2	512.3	25.9
		2	834.6	688.7	471.4	34.4
		3	735.2	637.9	365.5	29.8
		Average	914.3	793.9333	449.7333	30.03333

Table F-3 CALF

Temperature	Frequency	Sample	Modulus			Phase Angle
			Complex	Elastic	Loss	
10°C	16Hz	1	14332	13196	5593	23
		2	10285	9494.6	3954.6	22.6
		3	8288.1	7709	3931.9	20.8
		Average	10968.37	10133.2	4493.167	21.9
	10Hz	1	14247	13198	5363	22.1
		2	10363	963.9	3805	21.5
		3	8025.8	7562.6	2686.2	19.6
		Average	10878.6	7241.5	3951.4	21.06667
	4Hz	1	14198	13275	5035	20.8
		2	9069.3	8559.3	2998.4	19.3
		3	7143.5	6822.8	2116.3	17.2
		Average	10136.93	9552.367	3383.233	19.1
	1Hz	1	11289	10635	3784	19.6
		2	7290.5	6895.5	2367	18.9
		3	6012.8	5728.8	1826.3	17.7
		Average	8197.433	7753.1	2659.1	18.73333
40°C	16HZ	1	4011.7	2774	2897.9	46
		2	2682	1917.6	1875	44.4
		3	2339.9	1800.8	1494	39.7
		Average	3011.2	2164.133	2088.967	43.36667
	10Hz	1	3481.6	2608.5	2306	41.5
		2	2413.7	1851.8	1548	39.9
		3	2056.3	1676.2	1191	35.4
		Average	2650.533	2045.5	1681.667	38.93333
	4Hz	1	2627	2178.2	1468	34
		2	1779.3	1476.5	992.9	33.9
		3	1565.1	1356.8	780.3	29.9
		Average	1990.467	1670.5	1080.4	32.6
	1Hz	1	1746	1549.8	804.3	27.4
		2	1184.1	1055.3	537	26.9
		3	1077.5	970.4	468.4	25.8
		Average	1335.867	1191.833	603.2333	26.7

Table F-4 CHF

Temperature	Frequency	Sample	Modulus			Phase Angle
			Complex	Elastic	Loss	
10°C	16Hz	1	20015	15852	12219	37.6
		2	14790.5	12613	7722.5	31.5
		3	17287	15225	8180	28.2
		Average	17364.17	14563.33	9373.833	32.43333
	10Hz	1	15130	11898	9345	38.14
		2	16669	14642	7965	28.5
		3	17030	14981	8102	28.4
		Average	16276.33	13840.33	8470.667	31.68
	4Hz	1	11959	10767	5202	35.7
		2	13794	12051	6711	29.1
		3	12890.2	11402.3	5955	32.4
		Average	12876.5	11409	5956.5	32.4
	1Hz	1	9437.1	7937.6	5105	32.7
		2	8187.9	6927.5	4364.7	32.2
		3	8812	7398.1	4736.4	32.5
		Average	8812.5	7432.55	4734.85	32.45
40°C	16HZ	1	1747.1	1195.8	1273.7	46.8
		2	1803.8	1326.6	1222.2	42.6
		3	2023.2	1271.1	1574.1	51
		Average	1858.033	1264.5	1356.667	46.8
	10Hz	1	1440.2	1073.1	960.5	41.8
		2	1578.1	1250.4	962.8	37.6
		3	1633.3	1166.8	1142.8	44.4
		Average	1550.533	1163.433	1022.033	41.26667
	4Hz	1	1025.7	823	612.2	36.6
		2	1262	1031.7	726.8	35.1
		3	1124	930.5	630.5	34.1
		Average	1137.233	928.4	656.5	35.26667
	1Hz	1	646.8	552.8	335.7	31.3
		2	809.3	711.16	386.2	28.5
		3	704.3	624.6	325.5	27.5
		Average	720.1333	629.52	349.1333	29.1

Table F-5 GAF1

Temperature	Frequency	Sample	Modulus			Phase Angle
			Complex	Elastic	Loss	
10°C	16Hz	1	7590	6620	3402	27.2
		2	8209	7208	3927	28.6
		3	8844	7760	4243	28.7
		Average	8214.333	7196	3857.333	28.16667
	10Hz	1	7128	6782	3059	24.3
		2	7833	6960	3596	27.3
		3	8423	7533	3769	26.6
		Average	7794.667	7091.667	3474.667	26.06667
	4Hz	1	6170	5808	2487	23.2
		2	6462	5850	2746	25.1
		3	7254	6613	2982	24.3
		Average	6628.667	6090.333	2738.333	24.2
	1Hz	1	4926	4537	1918	22.9
		2	4785	4317	2064	25.5
		3	5131	4619	2236	25.8
		Average	4947.333	4491	2072.667	24.73333
40°C	16HZ	1	1400	608	786	45.37
		2	1146	612	666	43.5
		3	1371	551	991	46.36
		Average	1305.667	590.3333	814.3333	45.07667
	10Hz	1	1269	563	644	39
		2	986	591	527	36.7
		3	1215	535	790	38.8
		Average	1156.667	563	653.6667	38.16667
	4Hz	1	989	459	437	32.93
		2	748	465	332	30.8
		3	880.6	487	505	33.34
		Average	872.5333	470.3333	424.6667	32.35667
	1Hz	1	598	323	249	28.3
		2	362	517.5	177	25.9
		3	433	600.5	279	27.5
		Average	464.3333	480.3333	235	27.23333

Table F-6. GAF2

Temperature	Frequency	Sample	Modulus			Phase
			Complex	Elastic	Loss	Angle
		2	16856	15806	5855	20.3
	16Hz	4	16195	13746	8563	31.9
		1	16522.3	14777.3	7300.1	26.2
		Average	16525.5	14776	7209	26.1
		2	16037	15127	5324	19.4
	10Hz	4	12583	11033	6051	28.7
			14300	13008	569.0	24.1
10°C		Average	14310	13080	5687.5	24.05
		2	13405	12741	4165	18.1
	4Hz	4	9151	8270	3918	25.3
		1	11280.0	10505.6	4042	21.6
		Average	11278	10505.5	4041.5	21.7
		2	8790	8179	3220	21.5
	1Hz	4	6186	5723	2349	22.3
		1	7489	6952.1	2765.0	21.85
		Average	7488	6951	2784.5	21.9
		2	1619	1108	1181	46.8
	16HZ	4	1206	917	1223	50.4
		1	1214			43.3
		Average	1346.333	1012.5	1202	46.83333
		2	1358	999	919	42.6
	10Hz	4	1031	834	947	41.04
40°C		1	1041			35.8
		Average	1143.333	916.5	933	39.81333
		2	937	741	573	37.8
	4Hz	4	760	646	590	32.9
		1	850			26.5
		Average	849	693.5	581.5	32.4
		2	561	474	300	32.3
	1Hz	4	529	419	292	27.7
		1	589			24.8
		Average	559.6667	446.5	296	28.26667

Table F-7 GAF3

Temperature	Frequency	Sample	Modulus			Phase
			Complex	Elastic	Loss	Angle
		1	8216	7575	3179	22.8
	16Hz	2	9999	9100	4145	24.5
		3	8436	7293	4239	30.2
		Average	8883.667	7989.333	3854.333	25.83333
		1	7704	7215	2702	20.5
	10Hz	2	8635	7993	3268	22.2
		3	7530	6641	3551	28.1
10°C		Average	7956.333	7283	3173.667	23.6
		1	6514	6173	2080	1.6
	4Hz	2	7233	6755	2585	20.9
		3	6924	6283	2911	24.8
		Average	6890.333	6403.667	2525.333	15.76667
		1	4870	4603	1588	19
	1Hz	2	5623	5187	2172	22.7
		3	5618	5075	2408	25.4
		Average	5370.333	4955	2056	22.36667
		1	1172.5	674	647	42.6
	16HZ	2	1499.4	654	881	48.4
		3	1349.2	699	756	47.1
		Average	1340.367	675.6667	761.3333	46.03333
		1	1021	627	584	37.9
	10Hz	2	1387	448	697	46
40°C		3	1233	624	578	41.2
		Average	1213.667	566.3333	619.6667	41.7
		1	792	468	370	30.2
	4Hz	2	1010	504	431	38.8
		3	958	463	358	36.7
		Average	920	478.3333	386.3333	35.23333
		1	591	317	197	24.6
	1Hz	2	400	328	229	30.8
		3	670	306	190	31.9
		Average	553.6667	317	205.3333	29.1

Table F-8 HVS67-22

Temperature	Frequency	Sample	Modulus			Phase Angle
			Complex	Elastic	Loss	
10°C	16Hz	1	8064.5	6213	2408	21.2
		2	8572.5	7793	3715	24.3
		3	8097	6746	2598	19.79
		Average	8244.667	6917.333	2907	21.76333
	10Hz	1	7467.4	5854	2020	18.71
		2	8272.3	7415	3188	22.97
		3	7465.3	5481	2493	17.6
		Average	7735	6250	2567	19.76
	4Hz	1	6856.5	5267	1641	17.22
		2	7070.9	6547	2505.5	21.26
		3	6706	3791	1936	15
		Average	6877.8	5201.667	2027.5	17.82667
	1Hz	1	5575.9	4372	1442	18.46
		2	6010.4	5311	2048	22.44
		3	5398.6	2840	1535	15.94
		Average	5661.633	4174.333	1675	18.94667
40°C	16HZ	1	1282.2	1229	917	38.27
		2	1198.2	1024.5	764	43.7
		3	1358.5	946	822	39.4
		Average	1279.633	1066.5	834.3333	40.45667
	10Hz	1	1113.4	1129	712	35.07
		2	1089.8	917	618	37.74
		3	1173.85	913	614	35.34
		Average	1125.683	986.3333	648	36.05
	4Hz	1	851	910	476	29.55
		2	820.7	761	421	34.26
		3	900.55	753	416	30.55
		Average	857.4167	808	437.6667	31.45333
	1Hz	1	569.15	639	275	25.04
		2	549.57	565	249	29.2
		3	608.6	547	249	27.3
		Average	575.7733	583.6667	257.6667	27.18

Table F-9 Project #1

Temperature	Frequency	Sample	Modulus			Phase
			Complex	Elastic	Loss	Angle
		1	11678	9611	6633	34.6
	16Hz	2	9439	8518	4066	25.5
		3	8175	7425	3420	24.7
		Average	9764	8518	4706.333	28.26667
		1	10407	8621	5829	34.1
	10Hz	2	8453	7839	3165	22
		3	8392	7656	3437	24.1
10°C		Average	9084	8038.667	4143.667	26.73333
		1	8321	7171	4222	30.5
	4Hz	2	7107	6750	2226	18.25
		3	6936	6385	2708	23
		Average	7454.667	6768.667	3052	23.91667
		1	6149	5419	2904	28.2
	1Hz	2	5138	4800	183	20.9
		3	5264	4823	2108	23.6
		Average	5517	5014	1731.667	24.23333
		1	2880	1380	2527	61
	16HZ	2	1073.9	741	777	46.4
		3	1448	1059	988	43
		Average	1800.633	1060	1430.667	50.13333
		1	1786	1176	1345	48.8
	10Hz	2	1030.3	796.2	653.8	39.4
40°C		3	1161.5	909.5	722.3	38.4
		Average	1325.933	960.5667	907.0333	42.2
		1	988.7	853	500	30.4
	4Hz	2	779.6	652.1	427.2	33.2
		3	808	673	447	33.6
		Average	858.7667	726.0333	458.0667	32.4
		1	726.4	620.9	377	31.3
	1Hz	2	492.4	436	228.4	27.6
		3	523.7	464	243	27.7
		Average	580.8333	506.9667	282.8	28.86667

Table F-10 Project #2

Temperature	Frequency	Sample	Modulus			Phase
			Complex	Elastic	Loss	Angle
		1	6709	5894	3204	28.5
	16Hz	2	6747	5874	3312	29.4
		3	6728	5884	3258	29
		Average	6728	5884	3258	28.95
		1	6676	5968	2990	26.6
	10Hz	2	6660	5973	2947	26.3
		3	6668	5970	2968.5	26.4
10°C		Average	6668	5970.5	2968.5	26.45
		1	5658	5184	2268	23.6
	4Hz	2	5575	5105	2241	23.7
		3	5616.5	5144.5	2254.5	23.7
		Average	5616.5	5144.5	2254.5	23.65
		1	4468	4082	1817	24
	1Hz	2	4450	4078	1781	23.6
		3	4459	4080	1799	23.65
		Average	4459	4080	1799	23.8
		1	1646.2	1077	1245	49.1
	16HZ	2	1582	1092	1146	46.4
		3	1613.9	1085	1195.8	47.8
		Average	1614.1	1084.5	1195.5	47.75
		1	1369.1	1056	870	39.5
	10Hz	2	1343.8	1052.9	835	38.4
40°C		3	1356.4	1054.5	852.6	38.9
		Average	1356.45	1054.45	852.5	38.95
		1	957.7	810.5	510	32.2
	4Hz	2	932.8	760.5	532.3	28.9
		3	945.3	785.4	521.2	30.6
		Average	945.25	785.5	521.15	30.55
		1	492.4	436.2	228.4	27.6
	1Hz	2	595.7	522.7	285.8	28.6
		3	544	479.8	257.3	28.15
		Average	544.05	479.45	257.1	28.1

Table F-11 Project # 3

Temperature	Frequency	Sample	Modulus			Phase
			Dynamic	Elastic	Loss	Angle
		1	5313	4816	2243	25
	16Hz	2	5483	4662	2885	31.7
		3	5340	4740	2564	28.4
		Average	5398	4739	2564	28.35
		1	5022	4645	1910	22.4
	10Hz	2	5483	4662	2885	31.7
		3	5253	4654	2398	27.1
10°C		Average	5252.5	4653.5	2397.5	27.05
		1	4180	3888.5	1534	21.5
	4Hz	2	4776	4093	2461	31
		3	4480	3991	1998	26.3
		Average	4478	3990.75	1997.5	26.25
		1	3278	3022	1269	22.8
	1Hz	2	3369	29.21	1680	29.9
		3	3324	1526	1474.5	26.4
		Average	3323.5	1525.605	1474.5	26.35
		1	992.7	771.6	624.6	39
	16HZ	2	824.7	573.7	617.3	47.1
		3	909	673	621.0	43.1
		Average	908.7	672.65	620.95	43.05
		1	871.4	701.9	516.5	36.3
	10Hz	2	710.7	532.4	470.6	41.5
40°C		3	791.0	617.2	493.6	39.0
		Average	791.05	617.15	493.55	38.9
		1	665.6	590.8	306.4	27.4
	4Hz	2	525.7	420	316	26.9
		3	595.7	505.4	311.3	27.2
		Average	595.65	505.4	311.2	27.15
		1	469.7	438.3	168.9	21.1
	1Hz	2	349.6	310.3	160.9	27.4
		3	410.0	374.4	165.0	24.3
		Average	409.65	374.3	164.9	24.25

Table F-12 Project #5

Temperature	Frequency	Sample	Modulus			Phase
			Complex	Elastic	Loss	Angle
		1	6664	6213	2408	21.2
	16Hz	2	6946.5	6480.0	2503	21.1
		3	7229	6746	2598	21
		Average	6946.5	6479.5	2503	21.1
		1	6193	5854	2020	19
	10Hz	2	8071	7415	3188	23.3
		3	6021	5481	2493	24.4
10°C		Average	6761.667	6250	2567	22.23333
		1	5517	5267	1641	17.3
	4Hz	2	4887	4529	1789	22.2
		3	4257	3791	1936	27
		Average	4887	4529	1788.5	22.15
		1	4604	4372	1442	18.25
	1Hz	2	3916.5	3606	1488.5	23.35
		3	3229	2840	1535	28.4
		Average	3916.5	3606	1488.5	23.325
		1				
	16HZ	2	1277.9	1024.5	764	36.7
		3	1253	946	822	41
		Average	1265.45	985.25	793	38.85
		1	1335	1129	712	32.2
	10Hz	2	1106	917	618	34
40°C		3	1100	913	614	33.9
		Average	1180.333	986.3333	648	33.36667
		1				
	4Hz	2	869	761	421	29
		3	861	753	416	29
		Average	865	757	418.5	29
		1				
	1Hz	2	618	565	249	23.8
		3	601	547	249	24.4
		Average	609.5	556	249	24.1

Table F-13 Project# 7

Temperature	Frequency	Sample	Complex Modulus	Phase Angle
		1	6592	25.7
	16Hz	2	6736	24.8
		3	4838	28
		Average	6055.333	26.16667
		1	6248	23.3
	10Hz	2	6246.5	22.8
		3	4192	27.7
10°C		Average	5562.167	24.6
		1	5128	22.7
	4Hz	2	5052	21.7
		3	5090.1	27.5
		Average	5090	23.96667
		1	3826	24.1
	1Hz	2	4269	22.6
		3	2343	27
		Average	3479.333	24.56667
		1	1124.5	39.1
	16HZ	2	1342.9	48.7
		3	1253	41
		Average	1240.133	42.93333
		1	982.3	36.1
	10Hz	2	1191.3	44.5
40°C		3	1100	37.8
		Average	1091.2	39.46667
		1	747.2	29.8
	4Hz	2	885.3	36.4
		3	861	30.4
		Average	831.1667	32.2
		1	526.8	24.9
	1Hz	2	595.3	30.2
		3	561.5	24.4
		Average	561.2	26.5

Table F-14 CGC

Temperature	Frequency	Sample	Complex Modulus	Phase Angle
		1	9623.4	28.4
	16Hz	2	10100	34.1
		3	9130.9	22.8
		Average	9618.1	28.43333
		1	8713	20.07
	10Hz	2	9403	19.3
		3	8325	21.25
10°C		Average	8813.667	20.20667
		1	7729.1	17.47
	4Hz	2	8595	16.1
		3	7062.7	19.02
		Average	7795.6	17.53
		1	6653	19.25
	1Hz	2	7588	19.9
		3	5728	19.6
		Average	6656.333	19.58333
		1	2864.4	40.8
	16HZ	2	2795	38.9
		3	1864	39.43
		Average	2507.8	39.71
		1	2702.25	37
	10Hz	2	2512.5	31.9
40°C		3	1633.9	36
		Average	2282.883	34.96667
		1	2043.8	31.3
	4Hz	2	1879	29.4
		3	1241.9	31.9
		Average	1721.567	30.86667
		1	1446.5	25.3
	1Hz	2	1272	26.5
		3	838.5	25.8
		Average	1185.667	25.86667

Table F-15 RBC

Temperature	Frequency	Sample	Complex Modulus	Phase Angle
		1	8711	24.95
	16Hz	2	8325	28.85
		3	7945	26.27
		Average	8327	26.69
		1	8190	22
	10Hz	2	7677	24.64
		3	7198	22.95
10°C		Average	7688.333	23.19667
		1	7256	19
	4Hz	2	6855	23.95
		3	6599	19.76
		Average	6903.333	20.90333
		1	5982	18.4
	1Hz	2	5523	30.19
		3	5062	19.68
		Average	5522.333	22.75667
		1	1341.8	41.66
	16HZ	2	1827	40.32
		3	2303.9	36.7
		Average	1824.233	39.56
		1	1187	37.2
	10Hz	2	1642.8	37.3
40°C		3	2105.1	32.5
		Average	1644.967	35.66667
		1	893	32.4
	4Hz	2	1376	32.3
		3	1740	28.5
		Average	1336.333	31.06667
		1	537.92	28.3
	1Hz	2	857.2	28.3
		3	1164.4	25.4
		Average	853.1733	27.33333

Table F-16 CALC

Temperature	Frequency	Sample	Complex Modulus	Phase Angle
		3	17196	36.7
	16Hz	4	17332	34.1
		5	8248	20.8
		Average	14258.67	30.53333
		2	16213	35.4
	10Hz	4	11034	24.6
		5	8025.8	19.6
10°C		Average	11757.6	26.53333
		3	16066	31.2
	4Hz	4	11574	22
		5	7144	17.2
		Average	11594.67	23.46667
		3	11775	33.3
	1Hz	4	9718	21.7
		5	6638	16.9
		Average	9377	23.96667
		3	2611.1	47.2
	16HZ	4	3240.2	42.6
		5	2339.9	39.7
		Average	2730.4	43.16667
		3	2273.6	43.1
	10Hz	4	2742.1	38.1
40°C		5	2056.3	35.4
		Average	2357.333	38.86667
		3	1756.5	39.4
	4Hz	4	2056.9	33.4
		5	1565.1	29.9
		Average	1792.833	34.23333
		3	1122.6	36.6
	1Hz	4	1347.9	29.2
		5	1077.5	25.8
		Average	1182.667	30.53333

Table F-17 CHC

Temperature	Frequency	Sample	Modulus			Phase
			Complex	Elastic	Loss	Angle
		1	30146	24203	17972	36.6
	16Hz	2	30142	24203	17972	36.6
		3	6491	5509	3432	31.9
		Average	22259.67	17971.67	13125.33	35.03333
		1	27192	23364	13911	30.8
	10Hz	2	11066	10040	4653	24.9
		3	6108	5374	2903	28.4
10°C		Average	14788.67	12926	7155.667	28.03333
		1	19878	16665	10836	33
	4Hz	2	9925	9173	3789	22.4
		3	5192	4667	2277	26
		Average	11665	10168.33	5634	27.13333
		1	13731	11465	7557	33.4
	1Hz	2	8038	7424	3079	22.5
		3	4221	3853	1724	24.1
		Average	8663.333	7580.667	4120	26.66667
		1	1546.3	1416	621	23.7
	16HZ	2	1681	1168	1209	46
		3	1297	858	972	48.5
		Average	1508.1	1147.333	934	39.4
		1	1327	1258	422	40
	10Hz	2	1422	1092	911	39.8
40°C		3	1116	793	785	44.7
		Average	1288.333	1047.667	706	41.5
		1	1042	870	573	33.4
	4Hz	2	1042	870	573	33.4
		3	713	532	474	41.7
		Average	932.3333	757.3333	540	36.16667
		1	658.4	570	329	30
	1Hz	2	684.65			30.9
		3	456	377	257	34.2
		Average	599.6833	473.5	293	31.7

Table F-18 GAC1

Temperature	Frequency	Sample	Modulus			Phase
			Complex	Elastic	Loss	Angle
10°C	16Hz	1	6934	5411	4336	38.7
		2	6008	558	2353	23.1
		3	7501	6718	3337	26.2
		Average	6814.333	4229	3342	29.33333
	10Hz	1	6436	5054	3980	38.1
		2	5376	4699	2611	29
		3	6652	6070	2720	14.1
		Average	6154.667	5274.333	3103.667	27.06667
	4Hz	1	5483	4775	2695	29.4
		2	4922	4515	1961	27.4
		3	5945	5487	2288	22.6
		Average	5450	4925.667	2314.667	26.46667
	1Hz	1	3895	2104	2003	32.8
		2	3748	3410	1555	27.75
		3	4274	3881	1790	24.8
		Average	3972.333	3131.667	1782.667	28.45
40°C	16HZ	1	1360	963	961	44.9
		2	984	768	616	38.8
		3	854	551	652	49.8
		Average	1066	760.6667	743	44.5
	10Hz	1	1098	864	678	38.1
		2	853	673	524	37.9
		3	583	444	378	40.4
		Average	844.6667	660.3333	526.6667	38.8
	4Hz	1	807	690	418	31.2
		2	621	528	327	31.8
		3	425	349	244	34.9
		Average	617.6667	522.3333	329.6667	32.63333
	1Hz	1	571	521	232	24
		2	422	379	186	26.2
		3	281	250	129	27.3
		Average	424.6667	383.3333	182.3333	25.83333

Table F-19 GAC2

Temperature	Frequency	Sample	Modulus			Phase
			Complex	Elastic	Loss	Angle
10°C	16Hz	4	9682	8750	4145	32.3
		5	10790	8232	6976	37.2
		6	6268	4844	3978	39.4
		Average	8913.333	7275.333	5033	36.3
	10Hz	4	8086	6638	4618	34.8
		5	9594	7727	5686	32.1
		6	4992	4261	2601	31.4
		Average	7557.333	6208.667	4301.667	32.76667
	4Hz	4	7894	7075	3502	26.3
		5	8541	7238	4535	32.1
		6	4992	4261	2601	31.4
		Average	7142.333	6191.333	3546	29.93333
	1Hz	4	5925	5233	2779	28
		5	6062	5083	3303	25
		6	3881	3315	2018	31.3
		Average	5289.333	4543.667	2700	28.1
40°C	16HZ	4	1347	962	1335	40.7
		5	1525	610	1237	34.5
		6	1435.8	786	1286.1	37.5
		Average	1436	786	1286	37.6
	10Hz	4	1148	936	1014	35.8
		5	1215	569	1105	35.4
		6	1182	753	1060	35.7
		Average	1181.5	752.5	1059.5	35.6
	4Hz	4	874	732	673	30.6
		5	904	535	611	31.5
		6	888.8	633.6	642	31.1
		Average	889	633.5	642	31.05
	1Hz	4	598	535	405	25.95
		5	606	400	420	25.8
		6	602.3	467.6	412	25.9
		Average	602	467.5	412.5	25.875

Table F-20 GAC3

Temperature	Frequency	Sample	Modulus			Phase
			Complex	Elastic	Loss	Angle
		6	7904	7219	3217	32.7
	16Hz	8	6733	5511	3867	35
		9	7319	6364.6	3541.8	33.9
		Average	7318.5	6365	3542	33.85
		6	7984	7213	3426	26.9
	10Hz	8	5819	5361	2261	29.7
		9	6902	6287.2	2843.5	28.2
10°C		Average	6901.5	6287	2843.5	28.3
		6	6889	6408	2529	26.4
	4Hz	8	6243	5382	3163	30.4
		9	6565.8	5695.2	2845.9	28.4
		Average	6566	5895	2846	28.4
		6	5103	4700	1986	22.9
	1Hz	8	4662	4007	2383	30.7
		9	4882.6	4353.5	2185	27.0
		Average	4882.5	4353.5	2184.5	26.8
		6	1252	908	862	43.5
	16HZ	8	1247	662	1057	57.9
		9	1250.0	764.8	959.2	50.65
		Average	1249.5	785	959.5	50.7
		6	983	751	634	40.2
	10Hz	8	1154	745	881	49.8
40°C		9	1069.1	748.1	757.5	45.1
		Average	1068.5	748	757.5	45
		6	715	586	410	35
	4Hz	8	782	581	524	42
		9	748.6	583.7	467.1	38.5
		Average	748.5	583.5	467	38.5
		6	476	415	231	29.1
	1Hz	8	551	440	332	37
		9	513.6	427.5	281.6	33.06
		Average	513.5	427.5	281.5	33.05

LIST OF REFERENCES

Ahlrich RC. Marginal aggregates in flexible pavements. Federal Aviation Report No. DOT/FAA/AR-97/5. U. S. Department of Transportation. April, 1998.

Akhtahusein TA, Khosa, PN, Malpass GA. Impact of fines on asphalt mix design. Final Report, Transportation Materials Research Center, Department of Civil Engineering, North Carolina State University, 1996.

Al- Suhaibani A, Al-Mudaiheem J, Al-Fozan F. Effect of filler type and content on properties of asphalt concrete mixes. In: Meininger RC, editor. Efects of aggregates and mineral fillers on asphalt mixture performance. ASTM STP 1147, American Society for Testing and Materials, Philadelphia, 1992.

Anderson RM. Relationship between Superpave gyratory compaction properties and the rutting potential of asphalt mixtures. Proceedings of Association of Asphalt Paving Technologists 2002.

Anderson RM, Bahia HU. Evaluation and selection of aggregate gradations for asphalt mixtures using Superpave. Transportation Research Record No. 1583, Transportation Research Board, Washington, D.C, 1997.

Anderson RM, Bukowski JR,Turner PA. Evaluating asphalt mixtures using Superpave performance tests. Paper presented at Transportation Research Board Meeting, Washington D. C., 1999.

Bahia HU, Friemel T, Peterson P, Russell J, Optimization of constructability and resistance to Traffic: A new design approach for HMA using the Superpave Gyratory Compactor. Proceedings of Association of Asphalt Paving Technologists, Vol. 67. Association of Asphalt Paving Technologists, 1998.

Berthelot C, Crackford B, White S, Sparks G. Mechanistic quality control/quality assurance evaluation of Saskatchewan specific pavement studies – 9A Asphalt Mixes. Proceedings of the 42nd Annual Conference of Canadian Technical Asphalt Association –1996.

Bouchard GP. Effects of aggregate absorption and crush percentage on bituminous concrete. In: Meininger RC, editor. Effects of Aggregates and Mineral Fillers on Asphalt Mixture Performance. ASTM STP 1147. American Society for Testing and Materials, Philadelphia, 1992.

Brown ER, Cross SA. A national study of rutting in Hot Mix Asphalt (HMA) pavements. Proceedings of Association of Asphalt Paving Technologists, 1993 pp 535-581

Brown ER, Kandhal PS and Zhang J. Performance Testing for Hot Mix Asphalt. National Center for Asphalt Technology report number NCAT 2001-05 Auburn, Alabama, November 2001.

Brown SF Practical test procedures for mechanical properties of bituminous materials. Proceedings of Institution of Civil Engineers (Transportation) 1995 Vo11 1Nov.Pp289-297.

Brown SF, Cooper KE. The mechanical properties of bituminous materials for road bases and base courses. Proceedings of Association of Asphalt Paving Technologists, 1984,pp415-437.

Butcher M. Determining gyratory compaction characteristics Uusing Servopac gyratory compactor. Transportation Research Record, vol.1630, 1998. pp. 89-97. Transportation Research Board, Washington, D.C, 1998.

Butler WG, Roque R, Development and evaluation of the Strategic Highway Research Program measurement and analysis system for indirect tensile testing at low temperatures. Transportation Research Record, vol.1454, 1994. pp. 163-171. Transportation Research Board, Washington, D.C, 1994.

Collins R, Shami H, Lai JS. Use of Georgia loaded wheel tester to evaluate rutting of asphalt samples prepared by Superpave gyratory compactor. Transportation Research Record No. 1545 1996pp 161-168.

Collins R, Watson DE, Campbell B. Development and use of the Georgia loaded wheel tester. Transportation Research Record No. 1942 1995pp 202-207, National Research Council, Washington DC.

Corte J, Serfass J. The French approach to asphalt mixture design: A performance-related system of specification. Proceedings of the Association of Asphalt Paving Technologists, Vol 69. 2000.

Cross SA, Brown ER. Selection of aggregate properties to minimize rutting of heavy duty pavements. In: Meininger RC, editor. Effects of Aggregates and Mineral Fillers onAsphalt Mixture Performance. ASTM STP 1147. American Society for Testing and Materials, Philadelphia, 1992.

Dawley CB, Hogenwiede BL, Anderson KO. Mitigation of instability rutting of asphalt concrete pavements in Lethbridge, Alberta, Canada. Journal of the Association of Asphalt Paving Technologists,Vol.59,pp A91-508.1990.

Daniel JS, Kim YR. Relationship among rate dependent stiffness of asphalt concrete using laboratory and field test methods. Presented at the 77th Annuat Transportation Research Board Meeting, Washington D.C., 1998.

De Sousa J, Manuel B. (1989). Dynamic properties of pavement materials. Dissertation Report – University of California at Berkeley. 1989.

Findley WN, Lai JS, Onaran K. Creep and relaxation of non-linear viscoelastic materials. Dover Publications Inc. New York. 1989.

Florida Department of Transportation. Slicing more than oranges. Roads and Bridges, December, 1998 pp. 22-23.

Ford MC. Pavement densification related to asphalt mix characteristics. Transportation Research Record, vol. 1178, 1988 pp. 9-15. Transportation Research Board, Washington, D.C, 1988.

Ford MC. Development of a rational mix design method for asphalt bases and characterization of Arkansas asphalt mixtures. Report FHWA/AR/004, FHWA/Arkansas Department of Transportation, July 1985.

Guler M. Device for measuring the shear resistance of Hot-Mix Asphalt in gyratory compactor. Transportation Research record Vo1 1723 00-1318, 2000 pp 116 -124.

Moseley H. An evaluation of Superpave™ compaction and asphalt mixture properties. Master of Engineering Thesis. University of Florida, 1999.

Hanson ID. Evaluation of Servopac Superpave gyratory compactor. Report of National Center for Asphalt Technology, Auburn, Alabama, 1998, pp 1-16.

Hills JF, Brien D, Van de loo, PJ. The correlation of rutting and creep tests of asphalt mixes. Journal of the Institute of Petroleum, London, England, 1974.

Huber GA, Schuler TS. Providing sufficient void space for asphalt cement: Relationship of mineral aggregates voids and aggregate gradation. In: Meininger RC, editor. Effects of Aggregates and Mineral Fillers on Asphalt Mixture Performance. ASTM STP 1147, American Society for Testing and Materials, Philadelphia, 1992.

Kandhal PS, Cooley LA. Evaluation of permanent deformation of asphalt mixtures using loaded wheel tester. National Center for Asphalt Technology (NCAT) Report No. 2002-08, Octobr, 2002, Auburn Alabama.

Kandhal PS, Mallick RB. Evaluation of Asphalt Pavement Analyzer for HMA mix design. National Center for Asphalt Technology (NCAT) Report No. 99-4, 1999, Auburn Alabama.

Khedar SA. Deformation mechanism in asphalt concrete . Journal of Transportation Engineering, American Society of Civil Engineers. Vol. 112(1) pp29-45. 1986.

Kim YR, Drescher A, Newcomb DE. Rate sensitivity of asphalt concrete in triaxial testing. Journal of Materials in Civil Engineering Vol. 9(2) May, 1997.

Kim YR, Little DN. One dimensional constitutive modeling of asphalt concrete. Journal of Engineering Mechanics, ASCE, vol. 116(4) pp 751-772 , 1990.

Lai JS. Evaluation of Rutting Characteristics of Asphalt Mixes Using Loaded-Wheel Tester. Final Report, Georgia Department of Transportation Project No. 8609, August 1986.

Lai JS. Evaluation of the Effect of Gradation on Rutting Characteristics of Asphalt Mixtures. Final Report, Georgia Department of Transportation Project No. 8706, August 1988.

Langlois P, Beaudoin M. The correlation between rutting resistance and Hot-Mix design with a gyratory compactor. Proceedings of Canadian Technical Asphalt Association, 1998.

Learhy RB, Monismith CL, Finn FN, and Hicks RG. Recommended mix testing and analysis system resulting from SHRP Contract A – 003A . Proceedings of Association of Asphalt Paving Technologists 1995.

Mahboud K, Little DN. Improved asphalt concrete design procedure. Reseach Report No. 474-1f Texas Transportation Institute. College Station Texas, 1988.

Mallick RB. Use of Superpave gyratory compactor to characterize Hot Mix Asphalt (HMA), Transportation Research Record No. 1681. Transportation Research Board, Washington, DC, 1999.

Marks VJ, Monroe RW. Adam JF. Relating creep testing to rutting of asphalt concrete mixes. Transportation Research Record . Vo1 1307.1991. Transportation Research Board, Washington, DC, 1991.

McGennis RB. Evaluation of materials from Northeast Texas using Superpave mix design technology. Transportation Research Record No. 1583, Transportation Research Board, Washington, D.C, 1997.

Mohammed EHH, Yue Z. Criteria for evaluation of rutting potential based on repetitive uniaxial compressive test. Transportation Research record Vo1. 1492 pp 74-81. Transportation Research Board, Washington, D.C, 1995.

Miller TK. Ksaibati, Farrar M. Utilizing the Gerogia Loaded-Wheel tester to predict rutting. Paper Presented at the 73rd Annual Meeting of the Transportation Research Board, 1995.

Myers LA, Roque R, Ruth BE, Drakos C. Measurement of contact stresses for different truck tire types to evaluate their influence on near surface cracking and rutting. Paper presented at the Transportation Research Board Meeting Washington D. C. – 1999.

Nukunya B. Evaluation of aggregate type, gradation and volumetric properties for design and acceptance of durable Superpave mixtures. Ph. D Dissertation, University of Florida, August 2001.

Nukunya B, Roque R, Tia M, Metha Y. Effect of aggregate structure on rutting potential of dense-graded asphalt mixtures. Transportation Research record, 2002., Vol 1789 pp 136 – 145.

Park DW, Chowdhury A, Button J. Effects of aggregate gradations and angularity on VMA and rutting Resistance. International Center for Aggregate Research, Texas Transportation Institute, University of Texas at Austin, College Station. 2001. Report # ICAR/201-3F.

Pellinen TK, Witczak MW. Linear and non-linear (Stress dependent) master curve construction for dynamic (Complex) modulus, Journal of the Association of Asphalt Paving Technologists. Volume 71, Preprint (2002).

Roberts FL, Kandhal PS, Brown ER, Lee D, Kennedy TW. Hot mix asphalt materials, mixture design, and construction. NAPA Education Foundation, Lanham, Maryland. 1996.

Roque R, Butler WG. Development of a measurement and analysis system to accurately determine asphalt concrete properties using the indirect tensile mode. Journal of the Association of Asphalt Paving Technologists. Volume 61,(1994) pp 304-332.

Roque R, Butler WG, Ruth BE, Tia M, Dickson SW, Reid B. Evaluation of SHRP indirect tension tester to mitigate cracking in asphalt pavement overlays. Final Project Report, Florida Department of Transportation/University of Florida, Gainesville, August 1997.

Rowe M, Brown SF, Sharrock MJ, Bouldin MG. Visco-elastic analysis of Hot Mix Asphalt pavement structures. Proceedings of Association of Asphalt Paving Technologists, 1995.

Ruth BE, Shaub JH. Gyratory testing machine simulation of field compaction of asphalt concrete. Proceedings of Association of Asphalt Paving Technologists. Vol 35, 1966, pp.451-480.

Ruth BE., Scherocman JA, Carroll JJ. Evaluation of FDOT specifications and procedures for asphalt mixtures in relation to pavement rutting under heavy traffic conditions. University of Florida Project # 4910450421412, Department of Civil Engineering, University of Florida, Gainesville, 1989. Sponsored by the Florida Department of Transportation.

Sanders CA, Dukatz EL. Evaluation of percent fracture on Hot Mix Asphalt gravels in Indiana. In: Meininger RC, editor. Effects of Aggregates and Mineral Fillers onAsphalt Mixture Performance. ASTM STP 1147, Richard C. Meininger, editor, American Society for Testing and Materials, Philadelphia, 1992.

Shami HI, Lai JS, D'Angelo JA and Harmon Tp. Development of temperature effect model for predicting rutting of asphalt mixtures using Georgia Loaded Wheel Tester. Transportation Research Record No. 1590. Transportation Research Board, Washington, DC, 1997, pp. 17-22.

Sigurjon S, Ruth BE. Use of gyratory testing machine to evaluate shear resistance of asphalt paving mixtures. Transportation Research Record No. 1259,1990.

Stakston AD. Effect of fine aggregate angularity on compaction and shearing resistance of asphalt mixtures. Transportation Research record Vo1 1789, 2002 pp 14 – 24.

Stuart KD, Mogawer W. Validation of asphalt binder and mixture tests that predict rutting susceptibility using the FHWA ALF. Proceedings of Association of Asphalt Paving Technologists March, 1997.

Swan DJ. Evaluation of the testing procedure and data analysis for the uniaxial complex modulus test on hot mix asphalt. Master of Engineering Thesis Sumbitted to the University of Florida. May, 2002.

Tarn JC, Lin JD, Chang JR. The study on asphalt concrete performance with different gradations using SGC in SHRP. Proceedings of the 9th REAAA Conference, Wellington, New Zealand 1999.

Tayebali AA, Malpass GA, Walker FH. Evaluation of Superpave repeated shear at constant height test to predict rutting potential of mixes based on field performance of three pavement sections in North Carolina. Paper presented at Transportation Research Board Meeting, Washington D. C., 1999.

Ullidtz P. Pavement analysis. Elsevier Science Publishers B.V. Amsterdam, The Netherlands, 1987.

University of Maryland Department of Civil Engineering. Model Evaluation Volume 1 – FHWA Contract DTFH61-95-C-00100, Superpave Support and Performance Management, 1996.

West RD, Page GC, and Murphy KH. Evaluation of the wheel tester. Research Report No. FL/DOT/SMO/91-391. State of Florida Department of Transportation, December 1991.

Williams CR, Powell BD. Comparison f laboratory wheel-tracking test results to Westrack performance. – Paper presented at the Transportation Research Board meeting Washington D. C. –1999.

Witczak MW, Kaloush K, Pellinen T, El-Basyouny M, Von Qintus H. Simple performance test for Suprpave mix design. NCHRP Report 465. Transportation Research Board-National Reasearch Council, Washington D.C. 2002.

Xishun Z. Evaluating Superpave performance prediction models using a controlled laboratory equipment. Proceedings of Association of Asphalt Paving Technologists VOL66 1997.

Zhang W, Drescher A, Newcomb DE. Viscoelastic behavior of asphalt concrete in diametral compression. Journal of Transportation Engineering ASCE 123(6) 1997 pp. 495-501.

BIOGRAPHICAL SKETCH

Daniel Duaguaye Darku was born in Accra, Ghana on December 9th 1956 to Mr. Darku Boctway and Madam Yarkor Mensah of Accra, Ghana. After 8 years of primary schooling through the public school system in Accra, he attended the Saint Thomas Aquinas Secondary School in Accra from 1971 to 1976 after which he received the GCE "O" level certificate in June 1976. Daniel continued his secondary education at the Saint Augustine's College, Cape Coast, the premier Catholic secondary school in the country from 1976 to 1978 and obtained the GCE "A" level in 1978. Not satisfied with this level of education, Daniel proceeded to the University of Science and Technology in 1979, graduating with a Bachelor of Science with honors (B.Sc Hons) degree in Civil Engineering in 1982.

Daniel worked with the Department of Feeder Roads, Ghana as regional engineer in various regions of Ghana between 1982 and 1996. He then proceeded to the University of Florida to further his education in January 1997. He obtained the Master of Engineering degree in May 1999. His quest for greater knowledge in his field, coupled with the desire to learn new technology to help in building his country, led Daniel to accept a research assistantship at the University of Florida in May 1999 to enable him to study for the doctorate degree.

I certify that I have read this study and that in my opinion it conforms to acceptable standards of scholarly presentation and is fully adequate, in scope and quality, as a thesis for the degree of Doctor of Philosophy.

Bjorn Birgisson

Bjorn Birgisson, Chair
Assistant Professor of Civil and Coastal Engineering

I certify that I have read this study and that in my opinion it conforms to acceptable standards of scholarly presentation and is fully adequate, in scope and quality, as a thesis for the degree of Doctor of Philosophy.

Reynaldo Roque

Reynaldo Roque, Cochair
Professor of Civil and Coastal Engineering

I certify that I have read this study and that in my opinion it conforms to acceptable standards of scholarly presentation and is fully adequate, in scope and quality, as a thesis for the degree of Doctor of Philosophy.

Byron E. Ruth

Byron E. Ruth
Professor Emeritus of Civil and Coastal Engineering

I certify that I have read this study and that in my opinion it conforms to acceptable standards of scholarly presentation and is fully adequate, in scope and quality, as a thesis for the degree of Doctor of Philosophy.

Mang Tia

Mang Tia
Professor of Civil and Coastal Engineering

I certify that I have read this study and that in my opinion it conforms to acceptable standards of scholarly presentation and is fully adequate, in scope and quality, as a thesis for the degree of Doctor of Philosophy.

Randolph L. Carter

Randolph L. Carter
Professor of Statistics

This thesis was submitted to the Graduate Faculty of the College of Engineering and to the Graduate School and was accepted as partial fulfillment of the requirements for the degree of Doctor of Philosophy.

May 2003

Pramod P. Khargonekar
Dean, College of Engineering

Winfred M. Phillips
Dean, Graduate School